



**The Study of the Measurement of Internal Gumming and Translucent
Fruit in Mangosteen (*Garcinia mangostana* Linn.)**

Rittisak Jaritngam

T

เลขที่	SB399.M25 R57 2014
Bib Key	3015A6
	/ /

**A Thesis Submitted in Fulfillment of the Requirements for the Degree of
Doctor of Philosophy in Electrical Engineering
Prince of Songkla University
2014
Copyright of Prince of Songkla University**

Thesis Title The Study of the Measurement of Internal Gummy and Translucent Fruit in Mangosteen (*Garcinia mangostana* Linn.)
Author Rittisak Jaritngam
Major Program Electrical Engineering

Major Advisor:

Ch. Limsakul

 (Assoc.Prof.Dr.Chusak Limsakul)

Co-advisor:

B.wongkittisuksa

 (Assoc.Prof.Booncharoen Wongkittisuksa)

Examining Committee:

Mitchai Chairperson
 (Assoc.Prof.Dr.Mitchai Chongcheawchamnan)

S. Sdoodee

 (Assoc.Prof.Dr.Sayan Sdoodee)

Chairat

 (Asst.Prof.Dr.Chairat Siripatana)

Ch. Limsakul

 (Assoc.Prof.Dr.Chusak Limsakul)

B.wongkittisuksa

 (Assoc.Prof.Booncharoen Wongkittisuksa)

The Graduate school, Prince of Songkla University, has approved this thesis as fulfillment of the requirement for the Doctor of Philosophy degree in Electrical Engineering

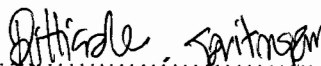
Teerapol Srichana

 (Assoc.Prof.Dr.Teerapol Srichana)
 (Dean of Graduate School)

This is to certify that the work here submitted is the result of the candidate's own investigations. Due acknowledgement has been made of any assistance received.

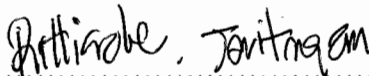


.....Signature
(Assoc.Prof.Dr.Chusak Limsakul)
Major Advisor



.....Signature
(Mr Rittisak Jaritngam)
Candidate

I hereby certify that this work has not already been accepted in substance for any degree, and is not being concurrently submitted in candidature for any degree.


.....Signature
(Mr Rittisak Jaritngam)
Candidate

ชื่อวิทยานิพนธ์	การศึกษาวิธีการวัดอาการเนื้อแก้วและยางไหลในผลมังคุด
ผู้เขียน	นายฤทธิศักดิ์ จริตงาม
สาขาวิชา	วิศวกรรมไฟฟ้า
ปีการศึกษา	2556

บทคัดย่อ

มังคุด (*Garcinia mangostana* L.) ได้รับการยกย่องว่าเป็นราชินีของผลไม้ เพราะมีรสชาติที่ดีและน่าประทับใจ โดยทั่วไปมังคุดที่มีคุณภาพเป็นที่ยอมรับของผู้บริโภคจะพิจารณาจากลักษณะภายนอก ได้แก่ สี ขนาด การแตก ความมันของผิว และยางไหล รวมถึงความเสียหายที่ผิวอันเกิดจากแมลง นอกจากนี้จะพิจารณาจากลักษณะภายในด้วยเช่นกัน ได้แก่ ต้องไม่มีอาการเนื้อแก้ว ไม่มีอาการยางไหล และไม่มีอาการเปลือกแข็ง ซึ่งปัญหาที่สำคัญในการส่งออกของมังคุดคือ คุณภาพของผลไม้สม่ำเสมอ โดยเฉพาะอย่างยิ่งคุณภาพภายในคือ อาการเนื้อแก้ว อาการยางไหลซึ่งพบปะปนอยู่กับผลดีเป็นปริมาณมาก ดังนั้นวิธีการส่งออกมังคุดในปัจจุบันทำได้โดยการผ่าผลและทำการแช่แข็งซึ่งวิธีการดังกล่าวทำให้มูลค่าและรสชาติหายไป ปัจจุบันวิธีการตรวจสอบอาการผิดปกติโดยการลายนํ้าเป็นวิธีการดั้งเดิมแบบชาวบ้านแต่พบว่าวิธีการลายนํ้ายังไม่สามารถนำมาใช้ในการคัดแยกได้จริงเนื่องจากมักเจอปัญหาในฤดูที่มีฝนตกชุกมังคุดได้รับนํ้ามากกว่าปกติทำให้ผลการทดลองคลาดเคลื่อนไปมาก ดังนั้นวิธีการทางไฟฟ้าจึงได้ถูกนำมาเพื่อแก้ปัญหาที่เกิดขึ้น ซึ่งวิธีการทางไฟฟ้าที่น่าสนใจ อาทิเช่น วิธีการวัดคลื่นเสียงได้ถูกนำมาประยุกต์ใช้วัดคุณสมบัติของผลไม้เช่น อายุ ความสุก ความแน่นเนื้อ ซึ่งให้ผลเป็นที่น่าสนใจ วิธีการวัดคลื่นอัลตราโซนิกได้ถูกนำมาประยุกต์ใช้ในการวัดโพรงในผลกีวี ความสุก ความแน่นเนื้อของผลทุเรียน วิธีการวัดคลื่นไมโครเวฟถูกนำมาประยุกต์ใช้ในการวัดความเป็นเนื้อแก้วในมังคุดพบว่าสามารถคัดอาการเนื้อแก้วได้ถูกต้องประมาณ 79 % วิธีการวัดคลื่นย่านอินฟราเรดสามารถนำมาประยุกต์ใช้ในการคัดอาการเนื้อแก้วพบว่าสามารถคัดได้ถูกต้อง 80 %

ที่ผ่านมาพบว่าวิธีการตรวจวัดคุณภาพของผลไม้สามารถวิเคราะห์ด้วยวิธีการทางไฟฟ้าได้หลายวิธีขึ้นอยู่กับตัวแปรหรือคุณสมบัติของผลไม้ตัวอย่างและมีแนวโน้มในการประยุกต์ใช้กับการคัดอาการเนื้อแก้วและยางไหลในผลมังคุดก่อนหน้านี้วิธีการวัดความถี่รีโซแนนซ์ได้นำมาประยุกต์ใช้กับผลไม้หลายชนิดเช่น การวัดความสุกของผลทุเรียน, การตรวจสอบช่องว่างในผลแตงโมและอาการเนื้อแก้วและยางไหลในผลมังคุดโดยวิธีการเคาะผลมังคุด

ดังนั้นในงานวิจัยนี้จึงได้ประยุกต์ใช้วิธีการวิเคราะห์ความถี่รีโซแนนซ์ในผลมังคุด โดยทำการสั่นผลมังคุดซึ่งวางอยู่บนฐานและทำการสั่นผลมังคุดที่ความถี่ 25,30,35 และ 40Hz ตามลำดับและจับสัญญาณด้วย strain gauge sensors ทำการเก็บสัญญาณที่วัดได้ด้วยโปรแกรม LabVIEW® และวิเคราะห์สัญญาณด้วยโปรแกรม MATLAB® โดยวิเคราะห์สัญญาณในแกนเวลา และแกนความถี่จาก 10 สมการคือ FFT,AR,HIST,MAV,MAVSLP,RMS,SSC,WAMP,WL and ZC และแบ่งผลมังคุดออกเป็น 3 กลุ่ม จากผลการทดลองพบว่าในกรณีที่น่าผลมังคุดมาแยกด้วย วันที่ทำการทดลองและใช้วิธีการตัดแยกด้วยการสังเกตจากกราฟให้ผลการทดลองดีที่สุด โดยสามารถตัดแยกผลมังคุดได้ถูกต้อง 90.36% และเมื่อนำมังคุดมาตัดแยกโดยการสังเกตและตัดแยกผล มังคุดโดยไม่ระบุวันที่ทำการทดลองให้ผลการตัดแยกได้ถูกต้อง 85.54% และเมื่อวิเคราะห์ด้วย วิธีการวัดความถี่รีโซแนนซ์และออโตเรเกรสซีฟโมเดล นอกจากนี้วิธีการวิเคราะห์สัมประสิทธิ์ออโตเรเกรสซีฟสามารถตัดแยกผลดีได้ 15 ผล จากผลดีทั้งหมด 50 ผล เมื่อวิเคราะห์ด้วยวิธีฟูเรียร์ ทรานสฟอร์มที่ความถี่ของกระสั่นผลมังคุดที่ 35 และ 40Hz พบว่ากลุ่มมังคุดที่มีอาการยางไหลมีค่า แอมพลิจูดสเปคตรัมต่ำกว่ามังคุดกลุ่มอื่นอย่างชัดเจน

ดังนั้นในงานวิจัยนี้จึงเป็นการประยุกต์ใช้การคัดอาการเนื้อแก้วและยางไหลในผล มังคุดโดยไม่ทำการผ่าผล โดยวิธีการวิเคราะห์ความถี่รีโซแนนซ์จากการสั่นผลมังคุดซึ่งเป็นการคัด แบบไม่ทำลายและผลการทดลองที่ได้มีแนวโน้มและให้ผลที่น่าสนใจเพื่อนำไปประยุกต์ใช้ในการ ตรวจจับอาการผิดปกติดังกล่าวเพื่อนำไปประยุกต์และเป็นแนวทางในการคัดอาการอาการเนื้อแก้ว และยางไหลในผลมังคุดต่อไป

Thesis Title	The Study of the Measurement of Internal Gumming and Translucent Fruit in Mangosteen (<i>Garcinia mangostana</i> Linn.)
Author	Rittisak Jaritngam
Major Program	Electrical Engineering
Academic Year	2013

Abstract

Mangosteen (*Garcinia mangostana* L.) is well known as the queen of fruits, since its taste is very delicious and impressive. Normally, the quality of mangosteen is observed using physical visual inspection such as color, size and peel damages caused by bugs. Moreover, the defect of mangosteen can also be inspected from the fruit internal for example, translucent flesh disorder, yellow gummy latex and hard shell. The main issue in mangosteen export is quality consistency. There are a lot of internal defects which were mixing with good quality mangosteen. To avoid those defects in export, the mangosteen should be peeled and then frozen. However, the taste of mangosteen can be degraded by the frozen and de-frozen processes. Conventionally, the water floating technique has been applied for classifying translucent flesh disorder and yellow gummy latex. The weakness of this technique is inability to classify the mangosteen in rainy season because the mangosteen absorbs much water. The electrical method is very interesting for example acoustic wave technique that can apply for fruit quality measuring such as aging, ripeness and density. The ultrasonic wave was applied for detecting air gap in kiwi, ripeness and density of durian. The microwave technique was applied for detecting translucent flesh disorder in mangosteen with accuracy of 79%. The infrared was also applied for classified the translucent flesh disorder in mangosteen with accuracy of 80%.

From the past, the electric methods can be use for measuring fruit quality. Some proper control parameters are required. As well as the resonance frequency technique that applied for measuring fruits such as ripeness of durian, air gap in water melon and glass tissue and mucilage in mangosteen by using percussion technique. This technique is very attractive to classify translucent flesh disorder and yellow gummy latex in mangosteen.

In this research the resonance frequency technique is applied for measuring translucent flesh disorder and yellow gummy latex in mangosteen. The mangosteen is placed on a vibration plate at various frequencies 25, 30, 35 and 40 Hz, respectively. The strain gauge sensors are mounted on the mangosteen for sensing vibration signals. The vibration signals are amplified and captured by LabVIEW® card sent to PC. The signals are analyzed on MATLAB® in time and frequency domain using 10 features, FFT; AR, HIST, MAV, MAVSLP, RMS, SSC, WAMP, WL and ZC. The mangosteen is separated into 3 groups to form a prediction model. The best accuracy of translucent flesh disorder and yellow gummy latex classification was found 90.36% when separated by date and 85.54% when applying f_R and AR, respectively. Fifteen good quality mangosteens can be classify from 50 mangosteens by using AR technique. Moreover, from the FFT technique the yellow gummy latex produce lower amplitude compare to good quality mangosteen.

From the experiment results, it is concluded that the proposed non-invasive mangosteen by using frequency resonant is very suit for detecting translucent flesh disorder and yellow gummy latex.

Acknowledgements

The work of this thesis was carried out at Electrical Engineering Department Research, Faculty of Engineer, Prince of Songkla University.

I would like to express my sincerest gratitude to everyone who has helped and supported me in various ways through the years. I especially want to thank you:

My advisor Assoc. Prof. Dr. Chusak Limsakul, for his help and support over the past several years, for advice, encouragement and patience of correcting my writing, for project discussions that make the work so much easier to keep going. His is the most essential activator which induces me to be a researcher instead of a student.

My co-advisor Assoc. Prof. Dr. Booncharern Wongkittiserksa, for his supervision, which help me a lot for correcting my writing and interesting discussion.

Assoc. Prof. Dr. Mitchai Chongcheawchamnan, for teaching me as scientific thinking and for interesting discussions at project reports and patience of correcting my writing.

Dr. Kittinan Maliwon, Lecturer of Mechanical Engineering, faculty of engineer, Prince of Songkla University. for his supervision and assisting me in the vibration measurement.

All friend, for often interesting discussion, for their helpful suggestion in the laboratory, it was very nice to work with them.

For this dissertation I would like to thank my oral defense committee, for their time and insightful questions.

Lastly, My parents, for endless love and being supportive all the time. Without them I could not finish.

Rittisak Jaritngam

Contents

	Page
1 Introduction	1
1.1 Mangosteen Defect	1
1.1.1 Translucent fresh disorder (TFD)	2
1.1.2 Yellow gummy latex (YGL)	3
1.2 Objectives	3
2 Literature Reviews and Research Methodology	4
2.1 Introduction	4
2.2 Principles of non-destructive testing	5
2.3 Materials and methods	6
2.3.1 Fruit sample and experiment set-up	6
2.3.2 Data analysis	9
2.3.3 Feature extraction	13
2.3.4 Feature selection stage	15
2.3.5 Artificial Neuron Network (ANN)	15
3 Results and Discussion	18
3.1 TFD and YGL detection	18
3.1.1 Frequency-domain features	18
3.1.2 AR feature	21
3.1.3 Resonance frequency feature based on f_v at 40 Hz	21
3.2 Case study	24
3.2.1 Case study 1: Pre-classification using AR and f_R	24
3.2.2 Case study 2: All VFSS samples	32
3.2.3 Case study 3: Classification by date	41
3.3 Research Syntheses and Discussion	66
3.3.1 Background	66
3.3.2 Summary of Accuracy Performances	66
3.3.2.1 Pre-classification using AR and f_R	66
3.3.2.2 All VFSS samples	68
3.3.2.3 Classification based on experiment day	69
3.3.2.4 Performance comparison	71
4 Conclusion and Future Works	72
4.1 Conclusion	72
4.2 Future Works	74
References	75
A Conferences/Journals	79
A.1 International conference	79
A.2 International journals	79

List of Tables

		Page
Table 1.	Pericarp color index and its character.....	1
Table 2.	Color change of a mangosteen at room temperature.....	2
Table 3.	VFSS spectrum (mV).....	20
Table 4.	Normalized VFSS spectrum with weight (mV/g).....	20
Table 5.	Normalized VFSS spectrum with diameter (mV/cm).....	20
Table 6.	Normalized VFSS spectrum with peel thickness (mV/cm).....	20
Table 7.	Number of samples which have f_R at 77 and 187 Hz for different f_v	21
Table 8.	Techniques for feature selection and good/defected detection.....	24
Table 9.	Summary of classification performances ($[-a_4, 77 \text{ Hz}]$).....	26
Table 10.	Summary of classification performances ($[-a_4, 187 \text{ Hz}]$).....	28
Table 11.	Summary of classification performances ($[+a_4, 77 \text{ Hz}]$).....	30
Table 12.	Summary of performances ($[+a_4, 187 \text{ Hz}]$).....	31
Table 13.	Summary of applied techniques.....	32
Table 14.	Performances of techniques applied to all VFSS samples.....	40
Table 15.	Performances of combined techniques applied to all VFSS samples	40
Table 16.	Summary of performances obtained from Technique I.....	42
Table 17.	Summary of performances obtained from Technique II.....	45
Table 18.	Summary of performances obtained from Technique III.....	45
Table 19.	Summary of performance obtained from Technique IV.....	47
Table 20.	Summary of performances Day#1-Day#3) using technique VI.....	52
Table 21.	Summary of performances (Day#1-Day#3) using technique VII.....	55
Table 22.	Summary of performances (Day#1-Day#3) using Technique VIII	55
Table 23.	Summary of performances ($[187\text{Hz}]$, Day#1-Day#3) using Technique IX.....	56
Table 24.	Summary of performances (Day#1-Day#3) using technique X.....	56
Table 25.	Summary of performances (Day#1-Day#3) using technique XI.....	59
Table 26.	Summary of performances (Day#1-Day#3) using technique XII.....	62
Table 27.	Summary of performances (Day#1-Day#3) using technique XIII.....	65
Table 28.	Summary of performances (Day#1-Day#3) using technique XIV.....	65
Table 29.	Summary of performances (Day#1-Day#3) using technique XV.....	66
Table 30.	Performances of techniques obtained by applying pre-classification methods.....	66
Table 31.	Performances of techniques obtained by applying a combination of pre-classification methods.....	67
Table 32.	Performances of applied techniques based on pre-classification method.....	67
Table 33.	Performances of techniques applied to all VFSS samples.....	68
Table 34.	Performances of combined techniques applied to all VFSS samples	68
Table 35.	Performances of techniques applied to Day#1 VFSS samples.....	69
Table 36.	Performances of techniques applied to Day#2 VFSS samples.....	69
Table 37.	Performances of techniques applied to Day#3 VFSS samples.....	70

List of Tables (cont.)

	Page
Table 38	Performances of combined techniques applied to Day#1-Day#3 VFSS samples..... 70
Table 39	Performances of combined techniques applied to three different sample groups..... 70
Table 40	Comparison performances of techniques without and with pre- classification (by day)..... 71
Table 41	Comparison performances of the techniques applied to combined samples 71
Table 42	Performances of the proposed and three previously proposed techniques..... 73

List of Figures

	Page
Figure 1.	Translucent flesh disorder..... 2
Figure 2.	Desecrated yellow gummy latex in the aril..... 3
Figure 3.	Experiment set-up..... 7
Figure 4.	Vibro-motor:TYPE BM 50/3, 2 pole : 3000 rpm, 50Hz)..... 7
Figure 5.	Rotating unbalance..... 7
Figure 6.	Accelerometer sensor..... 8
Figure 7.	Amplifier circuit..... 8
Figure 8.	Images of test samples..... 9
Figure 9.	VFSS responses at f_v of a 25Hz..... 11
Figure 10.	VFSS responses at f_v of a 30Hz..... 11
Figure 11.	VFSS responses at f_v of a 35Hz..... 12
Figure 12.	VFSS responses at f_v of a 40Hz..... 12
Figure 13.	Structure of NN..... 16
Figure 14.	Proposed ANN..... 17
Figure 15.	VFSS spectrum at f_v 18
Figure 16.	Normalized spectrum 19
Figure 17.	AR coefficients computed from VFSS response signals for 25 Hz f_v 21
Figure 18.	f_R at 77 and 187 Hz 22
Figure 19.	Methodology used in the research 23
Figure 20.	MAV-ZC plot ($[-a_4, 77 \text{ Hz}]$)..... 24
Figure 21.	RES indexes of features ($[-a_4, 77 \text{ Hz}]$)..... 25
Figure 22.	MAVSLP-ZC plot ($[-a_4, 77 \text{ Hz}]$)..... 25
Figure 23.	HIST-RMS plot ($[-a_4, 187 \text{ Hz}]$)..... 26
Figure 24.	RES indexes of features ($[-a_4, 187 \text{ Hz}]$)..... 27
Figure 25.	HIST-SSC plot ($[-a_4, 187 \text{ Hz}]$)..... 27
Figure 26.	HIST-MAV plot ($[+a_4, 77 \text{ Hz}]$)..... 28
Figure 27.	RES indexes of features ($[+a_4, 77 \text{ Hz}]$)..... 29
Figure 28.	HIST-SSC plot ($[+a_4, 77 \text{ Hz}]$)..... 29
Figure 29.	HIST-MAVSLP plot ($[+a_4, 187 \text{ Hz}]$)..... 30
Figure 30.	RES indexes of features ($[+a_4, 187 \text{ Hz}]$)..... 31
Figure 31.	ZC-WAMP plot ($[+a_4, 187 \text{ Hz}]$)..... 31
Figure 32.	HIST-MAVSLP plot (All VFSS samples)..... 33
Figure 33.	Figure 29 RES indexes of features (All VFSS samples)..... 33
Figure 34.	WAMP-WL plot All VFSS samples)..... 34
Figure 35.	MAVSLP-HIST plot (All VFSS samples)..... 34
Figure 36.	RES indexes of features (All VFSS samples)..... 35
Figure 37.	MAVSLP-ZC plot (All samples)..... 35
Figure 38.	RES indexes of features (All samples)..... 36
Figure 39.	MAV-MAVSLP plot All VFSS samples)..... 37
Figure 40.	SSC-ZC plot (All VFSS samples)..... 37
Figure 41.	RES indexes of features (All samples)..... 38

List of Figures(cont.)

		Page
Figure 42.	HIST-WL plot ($[-a_4]$, All samples).....	38
Figure 43.	RES indexes of features (All VFSS samples).....	39
Figure 44.	MAV-SSC plot (All VFSS samples).....	39
Figure 45.	Optimum feature pairs based on (a) Day#1, (b) Day#2 and (c) Day#3.....	42
Figure 46.	RES indexes of features based on (a) Day#1 (b) Day#2 and (c) Day#3.....	43
Figure 47.	Optimum feature pairs based on (a) Day#1, (b) Day#2 and (c) Day#3.....	45
Figure 48.	Optimum feature pairs based on (a)-(b) Day#1 and (c)-(d) Day#2 samples obtained from Technique III.....	47
Figure 49.	Optimum feature pairs based on (a)-(b) Day#1, and (c) Day#2 and (d) Day#3 samples obtained from technique V.....	49
Figure 50.	RES indexes of features based on (a) Day#1 (b) Day#2 and (c) Day#3 obtained from Technique VI.....	50
Figure 51.	Optimum feature pairs based on (a) Day#1, (b) Day#2 and (c) Day#3 samples obtained from Technique VI.....	52
Figure 52.	RES indexes of features based on (a) Day#1 (b) Day#2 and (c) Day#3 obtained from Technique VII.....	53
Figure 53.	Optimum feature pairs based on (a) Day#1, (b) Day#2 and (c) Day#3 samples obtained from technique VII.....	55
Figure 54.	Optimum feature pairs based on (a) Day#1, (b) Day#2 and (c) Day#3 groups obtained from technique X.....	57
Figure 55.	Optimum feature pairs based on (a) Day#1, (b) Day#2 and (c) Day#3 obtained from technique XI.....	59
Figure 56.	RES indexes of features based on (a) Day#1 (b) Day#2 and (c) Day#3 obtained from technique XII.....	60
Figure 57.	Optimum feature pairs based on (a) Day#1, (b) Day#2 and (c) Day#3 group obtained from technique XII.....	62
Figure 58.	RES indexes of features based on (a) Day#1 (b) Day#2 and (c) Day#3 obtained from technique XIII.....	63
Figure 59.	Optimum feature pairs based on (a) Day#1, (b) Day#2 and (c) Day#3 groups obtained from technique XIII.....	65
Figure 60.	Summary of the accuracy performances.....	73

ABBREVIATIONS

ANN	Artificial neural network
AR	Auto-regressive (AR) coefficients
FFBP	Feed-forward back propagation algorithm
f_R	Resonance frequency
f_V	Vibration frequency
HIST	Histogram
MAV	Mean Absolute Value
MAVSLP	Mean Absolute Value Slope
RMS	Root Mean Square
SG	Specific Gravity
TFD	Translucent flesh disorder
VFSS	Vibration force base on strain gage sensor
WAMP	Willison amplitude
WL	Waveform length
YGL	Yellow gummy latex
ZC	Zero crossing

Chapter 1

Introduction

1.1 Mangosteen Defect

Mangosteen (*Garcinia mangostana* Linn.) is classified in the family of *Guttiferae*. A mangosteen is found to be popular. Its pulp has sweet smell and very attractive to eat. Each fruit has four to seven petals with not more than three seeds. Generally, a mangosteen can be harvested once a year. Because of weather difference in different crop areas, its harvest season is different in several regions of Thailand. For example, the harvest season in the Eastern region is from May to July while it is during August–October in the Southern region. As a mangosteen is unripe, its peel is thick and green. Color of the peel gradually turns red and finally black violet when overripe. At this stage, mangosteen pulp is white, soft and juicy.

Table 1 shows the color characteristics of mangosteen pericarp. There are seven color indexes relating to seven characteristics. As shown in Table 1, the peel color changes to violet-red. Several dots on the peel can be found. These dots increase continuously until ripe. This occurs after the mangosteen was produced around 12 months. At the ripe stage, color of the peel becomes black-violet and the color incenses continuously. From Table 1, pericarp color appears as either color index 3 or 4, which is suitable for export. Yellow gummy latex (YGL) is developed in a mangosteen at the initial stage as shown in Table I. The appearance of YGL will not change much from the stage of color index 3 onward.

Table 1 Pericarp color index and its characteristic

Color index	Color characteristic	YGL appearance	Easy to peel	Note
0	white-yellow or green	much	difficult	not easy to peel
1	yellow, pink dot spreading	much	difficult	easy to peel
2	yellow and pink, dots spreading	moderate	difficult	young sporadically for good harvest quality
3	pink regularly	little	moderate	suitable for export
4	brown-red	little	easy	suitable for export
5	violet	unchanged	easy	edible
6	black violet	unchanged	very easy	edible

The harvesting time for mangosteen which plans for exporting should be designed appropriately. Exporters carefully plan the harvest time by taking the transportation time into account so that the fruit color, when arriving to their customers, should be black-violet. It was reported that (Tanachai, 1996) color of a mangosteen changes from red-violet to black-violet within seven days. A black-violet mangosteen can be preserved for more than 15 days at room temperature (25°C).

Table 2 shows the color characteristic of mangosteen pericarp in postharvest. The color information given in Table 2 can be used as the indicator for harvest planning.

Table 2 Characteristic of mangosteen pericarp at room temperature

Day	Color
1	pink
2	pink
3	pink
4	red
5	red
6	red-violet
7	black-violet
8	black-violet
9	black
10	black
11	black
12	black
13	black
14	black
15	black

1.1.1 Translucent flesh disorder (TFD)

There are several physiological disorders of mangosteens caused by excess water prior to pre-harvest season (Sdoodee and Limpun-Udom, 2002). Translucent flesh disorder (TFD) appears as a water soaking flesh. TFD is caused by excess water during the pre-harvest stage of fruit development, where water uptake is driven by the difference in osmotic potential between that of rain water and the affected fruits. When water content in fruit is high, a breakdown of apoplast or symplast compartmentation which exhibits as the occurrence of TFD (Voraphat, 1996) occurs. It is usually found as a large segment in fruit carpels. TFD is a major cause to degrade the fruit quality. This defect changes white pulp to translucent while the pulp texture turns from soft to firm and finally crisp (Tanachai, 1996). Voraphat (1996) studied the effect of water on TFD using a chemical technique to determine the internal quality of a mangosteen.

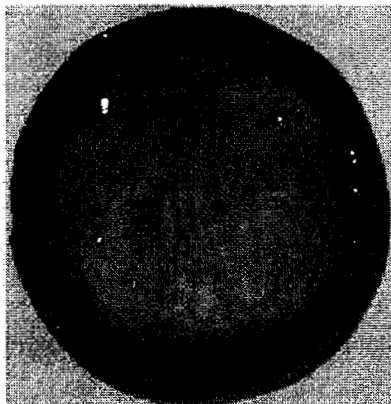


Figure 1 Translucent flesh disorder (Osman, 2006)

1.1.2 Yellow gummy latex (YGL)

In a yellow gummy latex (YGL) mangosteen, its pericarp and pulp are discolored by yellowish resin. This yellow resin becomes red-brown and hardened laterally. The defected fruit exudes yellow latex which discolors and changes the fruit taste. Naturally this yellow resin is produced by several organs consisting of branched canal-liked secretory ducts (Osman, 2006). These ducts are commonly found in the pericarp, mesocarp, endocarp and aril of the fruit (flower, stem and leaf). The biggest secretory ducts locate in the endocarp from the stalk to the fruit internal (Osman, 2006). The bitter yellow resin permeates into the aril as a result of broken latex secretory ducts caused by excessive rain, wind, careless fruit handling (Sdoodee and Limpun-Udom, 2002). According to Poerwanto *et. al* (2009), latex secretory ducts are usually broken during the rapid fruit growth period (week 5-15) after anthesis. The seed and aril growth rates were reported to be faster than the pericarp, causing a build-up of internal pressure to the endocarp. When the epithelial cells of the secretory ducts are weak, this pressure would break the ducts, (Osman, 2006).

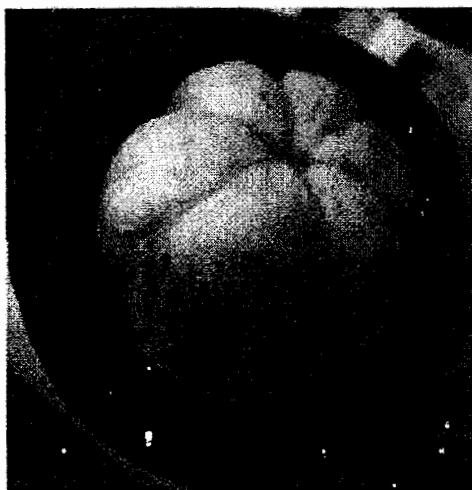


Figure 2 Desecrated YGL in the aril (Osman, 2006)

1.2 Objectives and Contributions

The research aims to detect a defected mangosteen suffering from TFD and YGL. The detection technique is nondestructive. The technique is applied with several mangosteens harvested in Thailand. The fruit samples were obtained from Nakornsritummarat province. The scopes of this Thesis are summarized as follows:

1.2.1 To investigate and apply several techniques based on resonance frequency for detecting a defected mangosteen suffering from TFD and YGL.

1.2.2 To develop a technique for detecting TFD and YGL in a mangosteen.

Chapter 2

Literature Reviews and Research Methodology

2.1 Introduction

A mangosteen is the queen of fruits and one of the high economical fruits in Thailand. The quality of mangosteen is determined not only from several external characteristics (color, shape, size, skin blemishes, skin latex and insect damage) but also from the internal quality. This means that the pulp of qualified fruit must have no internal defect (TFD and YGL). Currently, detecting these internal defects can be achieved by peeling the pericarp. This is not preferable since the taste of mangosteen will be degraded. The quality determination for mangosteen using a destructive technique was first reported by Sriyon (1986). Laterally Voraphat (1996) studied the relation between water supplied to the fruit and the TFD. The study approach is based on a chemical technique. Both techniques are not suitable since they are destructive which is not suitable for exporting.

Several non-destructive testing methods for detecting a defected mangosteen were proposed. A floating technique using specific gravity difference is used to detect TFD in a mangosteen (Tanachai, 1996). Tawatchai (2004) proposed the microwave technique to classify the TFD fruit. The magnitude of reflected signal from the fruit was investigated. Unfortunately the technique is based on the dielectric properties of the fruit, which is sensitive to moisture content. The short-wavelength infrared-spectroscopy technique was proposed to detect a TFD mangosteen based on the absorption parameter (Sontisuk, 2007). Somchai (1999) proposed the two-dimensional cross-sectional visualization for a mangosteen. Later on, the X-ray and Nuclear Magnetic Resonance (NMR) were applied to evaluate the qualities of durian and mangosteen (Yantarasi, 1996). In 2001, the resonance technique was first proposed to detect the TFD as well as YGL (Rittisak, 2001) in a mangosteen. The technique is simple, low-cost, and easy to apply. This inspires our work to aim on investigating the resonance technique to detect the defected mangosteen.

F.J. Garcio-Romus (2005) studied the frequency resonance of a fruit when it is vibrated. It was found that frequency resonance of the vibrated fruit depends on its mass and shape. De Belie *et al.* (2000) applied this technique to measure the firmness of pre-harvested pears. The pear firmness is estimated from the vibration response measured from an accelerometer which is attached to the pear. The vibration response is recorded, analyzed and modeled. Another vibration based technique was proposed to determine maturity stage of a durian (Kongrattanaprasert, 2001), Acoustic technique was proposed to assess tissue firmness of a kiwifruit. The technique performance was compared with a destructive method (Maramatsu, 1997). Similarly, techniques for determining firmness of muskmelons based on acoustic impulse transmission (Junichi, 2005) and vibration element analysis (Nourain, 2005) were proposed. The acoustic impulse based technique was proposed to detect a hollow in a watermelon (B. Diezma, 2002). The acoustic response evaluation of the storability of *Piel de Sapo* melons (L

Lleó, 2005) was studied. In 2006, a laser doppler vibrometer technique was applied to determine ripeness degree for a pear (Shoji, 2006).

This research first proposes a nondestructive testing method by using vibration force based on strain gage sensor (VFSS) measurement. Several spectral estimation and time-domain techniques are proposed to detect a defected mangosteen suffering from TFD and YGL.

2.2 Principle of Non-Destructive Testing

Determining the internal quality of fruit is one of the challenging topics which are highly demanded for post-harvest applications. There are several research works on developing sensors for determining some internal qualities of a fruit. Various internal qualities for example sugar content, acid content, firmness and internal defects (F. J. Garcia-Ramos, 2003) using NDT methods were investigated. Several approaches such as applying impact force, acoustic response to vibration, and optical signal were studied. In addition rebound and NMR techniques were investigated either. Many Non-Destructive Testing (NDT) methods have been applied to determine qualities of fruit. These methods are based on acoustic, ultrasound, infrared spectrometry, microwave and laser techniques. Various NDT methods have been applied for fruit testing applications with different accuracy degrees. Delwiche *et al.* [1987] proposed an impact testing method to implement an automatic machine for sorting fruit firmness. The acoustic testing method relies on the natural resonance frequency of a fruit where the resonance frequency (f_R) of a fruit depends on the quality and physical properties. Physically, measuring fruit firmness based on an impact force can be described using Hertz's and the elastic impact theories (Timoshenko and Goodier, 1951). Chen and Ruiz-Altisent (1996) applied a low-energy elastic impact to a fruit placed on a hard surface sphere. The mechanical response of the impact fruit was studied. Mohsenin (1970) proposed a technique for determining fruit firmness. Similar technique was applied using a pendulum to impact tomatoes to detect fruit defects (Desmet *et al.*, 2002). Chen *et al.* (1996) developed an instrument to measure the impact response of a fruit. The sensor consists of a small semi-spherical mass with an accelerometer. The response was measured by dropping the sensor on a fruit under test from different heights. The same technique was also used laterally to determine the firmness of apples and pears (Jarén *et al.*, 1992; Jarén and García-Pardo, 2002). Ortiz (1999) used this technique to distinguish woolly peaches by combining it with infrared spectroscopy. Moreover, a piezoelectric accelerometer locating on a fruit tip was applied to estimate fruit firmness. The results were in good agreement with previous work performed by Timoshenko and Goodier (1951).

A resonance based method is based on the theory of vibration. Peleg [1993] proposed an automatic fruit classifier based on a method. In this technique, a fruit under investigation is hit with a soft hammer or a similar tool. The fruit vibrates and its vibration signal will be recorded, analyzed. The acoustic response was applied to estimate fruit texture (Studman, 1999). The technique assumes that an object under test is spherical and elastic with small deformation. This assumption was applied for several works (Abbot and Masie, 1998). Piezoelectric film was first proposed to collect the signal response from the impact (Shmulevich *et al.*, 1996). Muramatsu *et al.* (1997) applied the technique to a kiwi fruit. There is a simple and low-cost acoustic

based technique proposed by De Belie *et al.* 2000 for measuring fruit firmness. The details of the test set-up are as follows: An acoustic impulse signal is generated from a small loudspeaker where the impact response was collected from a small microphone nearby the other side of the fruit. This equipment detects the vibration responses of the applied acoustic wave which travels across the fruit. The impact is generated mechanically at the top of the fruit. Based on the study performed by De Baerdemaeker *et al.* (cited by De Belie *et al.*, 2000), the mechanical vibration can also be measured by analyzing the response of the mechanical vibration. In this case, the fruit is placed on a tray vibrating at a certain frequency. The response was measured by an accelerometer. Abbott and Massie (1988) suggested that the vibration frequency (f_v) should be around 0 to 200 Hz. A sonic stiffness coefficient, a relation between fruit mass and f_R , is then calculated. The technique can classify kiwi fruits into two or three firmness levels. Peleg (1993) developed a firmness sensor based on the vibration response obtained by vibrating with an electro-mechanic vibrator installing at the tray. The response signal was measured by the accelerometer attached to the upper part of the fruit. It was found that soft fruits provide lower amplitude response than firm fruits.

2.3 Materials and Methods

2.3.1 Fruit samples and experiment set-up

Mangosteens were purchased from garden in Nakornsritummarat province, Thailand. The samples were brought to the laboratory at Department of Electrical Engineering, Prince of Songkla University, at the purchase day. These samples were kept at the controlled temperature. One hundred mangosteens were randomly chosen for the experiment. Twenty-six out of one hundred mangosteens were used for evaluating the accuracy performance of the proposed techniques. Figure 3 shows the experiment set-up. A test mangosteen is placed on the vibration base where two motors installed under the base control the amplitude and speed of vibration, giving the vibration speed at a frequency range of 0 – 50 Hz. The strain gauge sensor attached to the mangosteen pericarp and converts the vibration response to an electrical signal. This signal is amplified by the instrumental amplifiers and then digitized using LABVIEW™ card. The instrumental amplifiers are differential topology with a differential gain of 500. A 16-bit analog-to-digital converter board (NI, DAQCard-6024E) with 1000 Hz sampling frequency was chosen. In this Thesis, the digitized signal is named Vibration Force based on Strain gauge Sensor signal (VFSS).

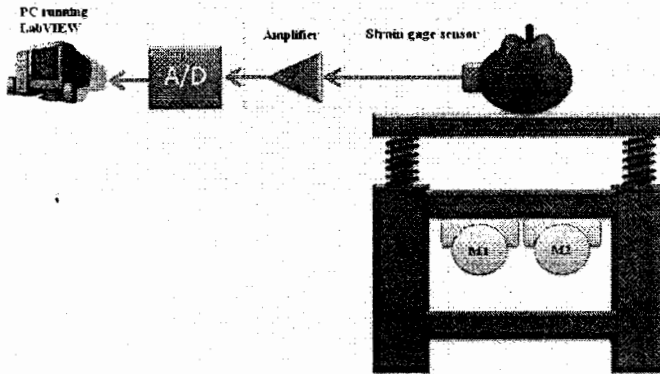


Figure 3 Experiment set-up

2.3.1.1 Vibration base

The vibration base is created by Dr. Kittinan Maliwan, a lecturer at Mechanical Engineering, PSU, Thailand. It is designed with a OMB Vibro-motor: (TYPE BM 50/3, 2 pole, 3000 rpm, 50Hz) as shown in Figure 4. The control frequency is from 0 – 50 Hz. The operation of the vibration can be described by (1).

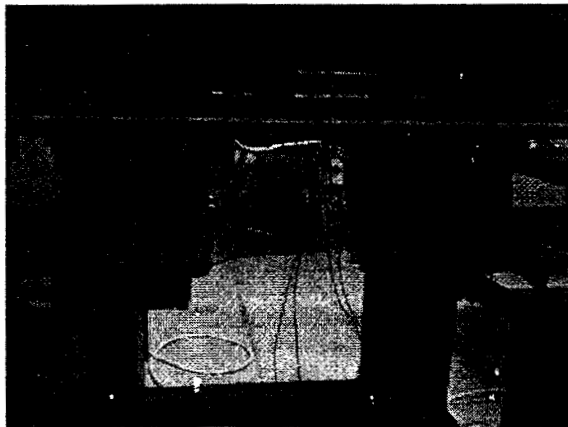


Figure 4. Vibro-motor:TYPE BM 50/3, 2 pole : 3000 rpm, 50Hz)

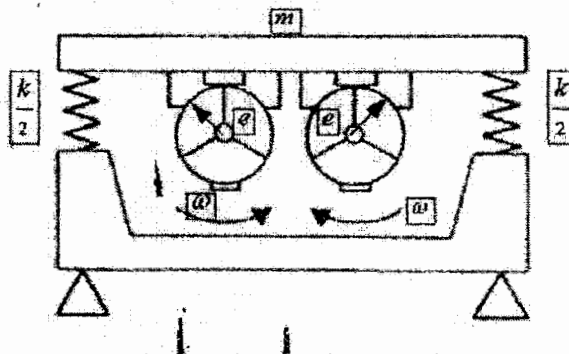


Figure 5 Rotating unbalance

$$m \frac{d^2 x}{dt^2} + kx = (m \cdot e \cdot \omega^2) \sin \omega t \quad (1),$$

where

- m is total masses of a sample and the base ,
 e is eccentric of the vibration motor,
 ω is vibration speed and
 k is stiffness of the spring.

The diagram of the vibration base controlled by the motors is depicted in Figure 5. The vibrator motor rotates in the opposite direction at the frequency of oscillation hence the vibration is resulted from unbalance rotation from two motors. With the assumption that two motors are identical, the vibration forces in the horizon axis from two motors are cancelled out while only vibration force in the vertical axis exists. Therefore, the VFSS signal collected from the samples are theoretically produced from the mechanical vibration in the vertical direction only.

The system of vibration is measured by the accelerometer sensor (analog devices ADXL210 +10 g). As shown in Figure 6, this sensor is installed at the vibration base.

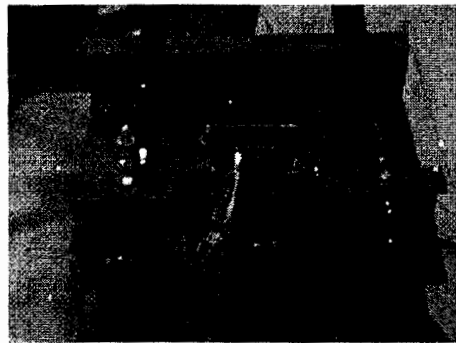


Figure 6 Accelerometer sensor

2.3.1.2 Amplifier circuit

Figure 7 shows the differential amplifier (IC = INA114, gain = 500) designed for amplifying a VFSS signal collected from the bridge circuit. The bridge resistance is 120Ω . The VFSS sensed by the strain gauge sensor increases the VFSS current and hence was amplified by the differential amplifier.

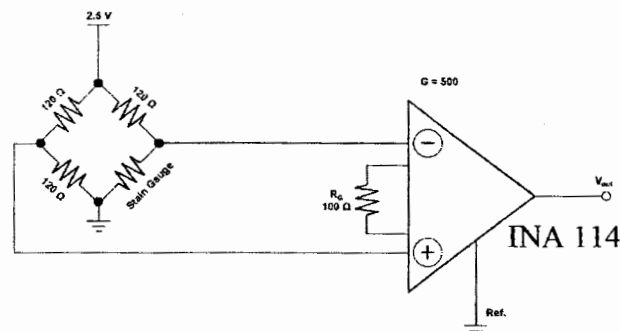


Figure 7 Amplifier circuit

The sample was vibrated at single frequency which ranges from 25 to 40 Hz. The control voltage for setting the vibration magnitude is held at 2.50 volt.

After a VFSS signal of a test mangosteen was recorded, the mangosteen was then peeled and the image data of the internal fruit was recorded with a digital camera (FujifilmFinePix F700 model). Figure 8 shows some sample images taken in this Thesis.

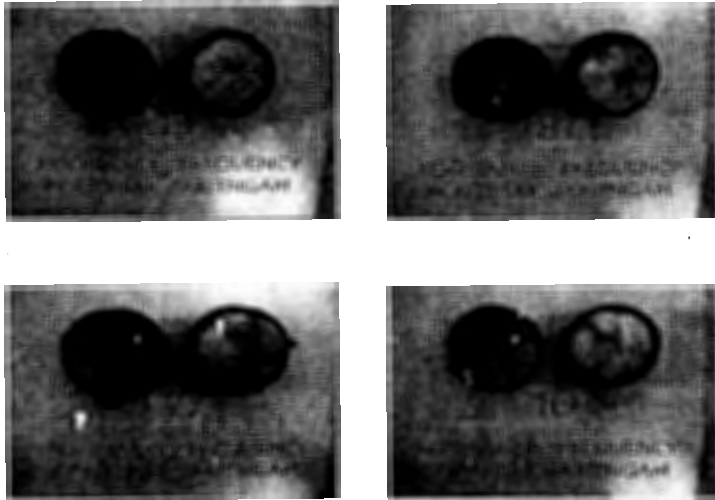


Figure 8 Images of test samples

Theoretically a VFSS signal depends on the modulus of elasticity, mass and shape of a mangosteen under test. Generally there are various vibration methods but the most common approaches are based on acoustic and mechanical techniques. A microphone or a piezoelectric sensor is applied to implement a technique based on an acoustic method. The frequency range of the acoustic technique lies in the audible frequency range, which is 0-20 kHz (Peleg, 1993). The acoustic response signal of the fruit is collected and transformed to frequency domain by the Fast Fourier Transform (FFT) technique. Resonance frequencies can be determined by considering the spectrum peaks.

In this Thesis, VFSS responses at 25, 30, 35 and 40 Hz will be investigated. In our analysis, the window length of VFSS samples is 256 ms such that a real-time signal processing can be achieved. This causes the delay for each VFSS sample to be less than 10 ms. The digitized VFSS signals will be recorded on a computer and techniques for detecting a good/defected mangosteen are applied.

2.3.2 Data analysis

The amplitude and frequency of vibration can be determined by several methods, for example ultrasonic, accelerometer, and laser doppler. The VFSS sensor is attached with the fruit to measure the response of vibration. A measurement is applied in a measurement of mangosteen vibration.

In this Thesis, the experimental procedure and the test set-up are as follows. The mangosteen under test is placed on the vibration base which can vibrate at a frequency range of 0-50 Hz. The signals from the VFSS sensor is transmitted to the instrument amplifier (IC = INA 114) and converted to digital data by an analogue-to-digital converter. These signals can be monitored on a program coding with

LABVIEW™ and post-processed by a program developed with the MATLAB program to detect a good/defected mangosteen.

The resonance frequency (f_R) is related to the characteristic of mechanical vibration which can be described as the energy radiated from the surface and propagates as a transversal wave in the medium. When f_V is less than 1 kHz, the velocity of transversal wave is related to the characteristic of medium (Kongrattanaprasert, 2001). This can be expressed as shown,

$$V_i = \frac{2\mu_1 \left(1 + \omega_v^2 \frac{\mu_2^2}{\mu_1^2} \right)}{\rho \left(1 + \sqrt{1 + \omega_v^2 \frac{\mu_2^2}{\mu_1^2}} \right)} \quad (2),$$

where V_i is the velocity of vibration. ρ is the density of the medium. ω_v is the angular frequency of vibration. μ_1 and μ_2 are the coefficients of shear elasticity and shear viscosity, respectively. Velocity of vibration is related to the frequency and wave propagation of vibration. Hence the property of shear elasticity can be found by measuring V_i and wave propagation at low frequency. If μ_1 is dominant comparing with μ_2 ($\mu_1 \gg \omega_v$ and μ_2 is satisfied), V_i can be simplified as

$$V_i \approx \sqrt{\frac{\mu_1}{\rho}} \quad (3)$$

The signal response of vibrated fruit (A) can be obtained from V_i and f_R as shown,

$$A = \frac{\alpha V_i}{f_R} \quad (4),$$

where A is the voltage of output vibration. α is voltage of output vibration from the prototype. f_R is the resonance frequency vibration, T is the output vibration time which is related to f_R as shown,

$$T = \frac{1}{f_R} \quad (5).$$

As previously stated, the amplitude and frequency of vibration can be determined by various methods such as ultrasonic, accelerometer and LDV methods. To obtain an accurate vibration, a specific position for installing a sensor at the pericarp should be carefully designed. f_V was chosen between 25 to 40 Hz and the vibration magnitude controlled voltage is 2.50 V. In system theory aspect, mangosteens with different internal properties should provide different responses regarding to their transfer functions. Therefore, the output response provides different amplitudes and frequencies depending on their physical properties such as internal air cavity, weight, diameter as well as texture property. The VFSS measurements evidently confirm this as shown in Figure 9(a-d)-12(a-d). A normal mangosteen has some specific signal patterns, which is different from a defected mangosteen which is affected from TFD and YGL.

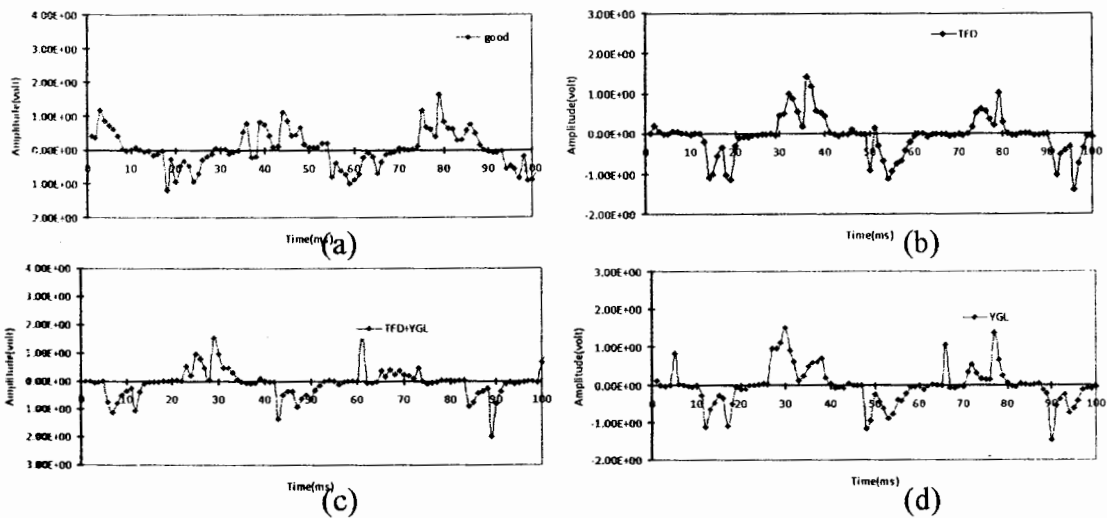


Figure 9 VFSS responses at f_v of a 25 Hz (a) good (b) TFD (c) TFD+YGL (d) YGL

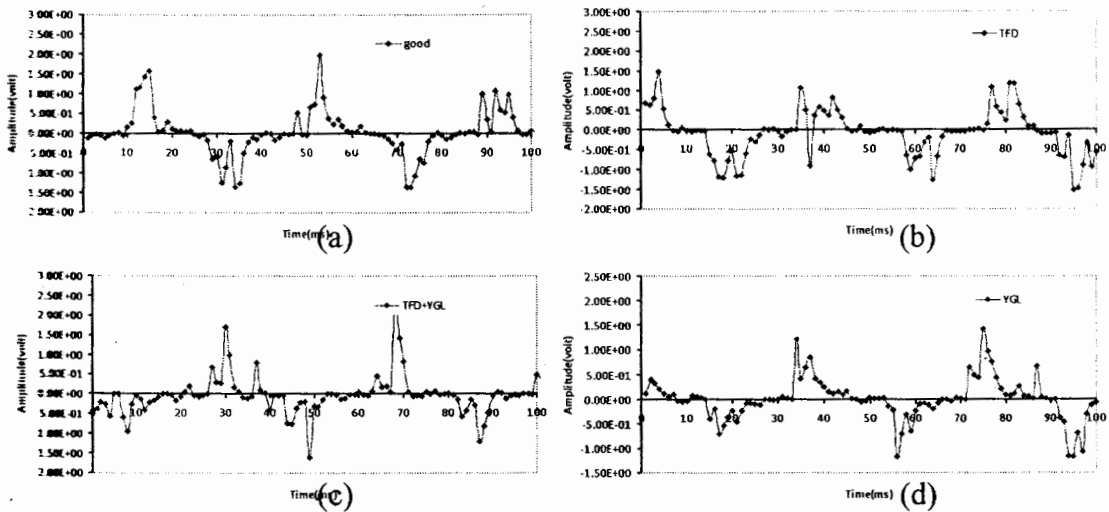


Figure 10 VFSS responses at f_v of a 30 Hz (a) good (b) TFD (c) TFD+YGL (d) YGL

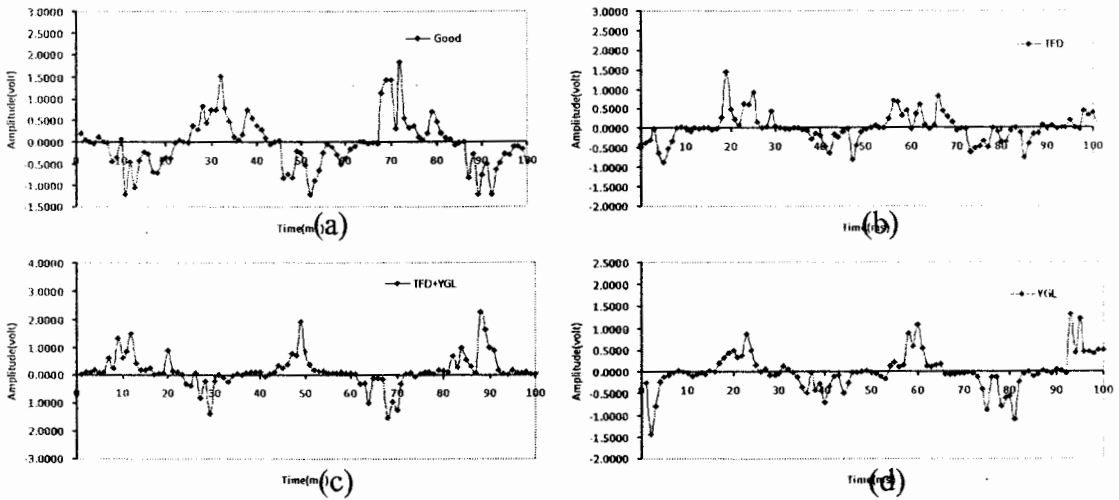


Figure 11 VFSS responses at f_v of a 35 Hz (a) good (b) TFD (c) TFD+YGL (d) YGL

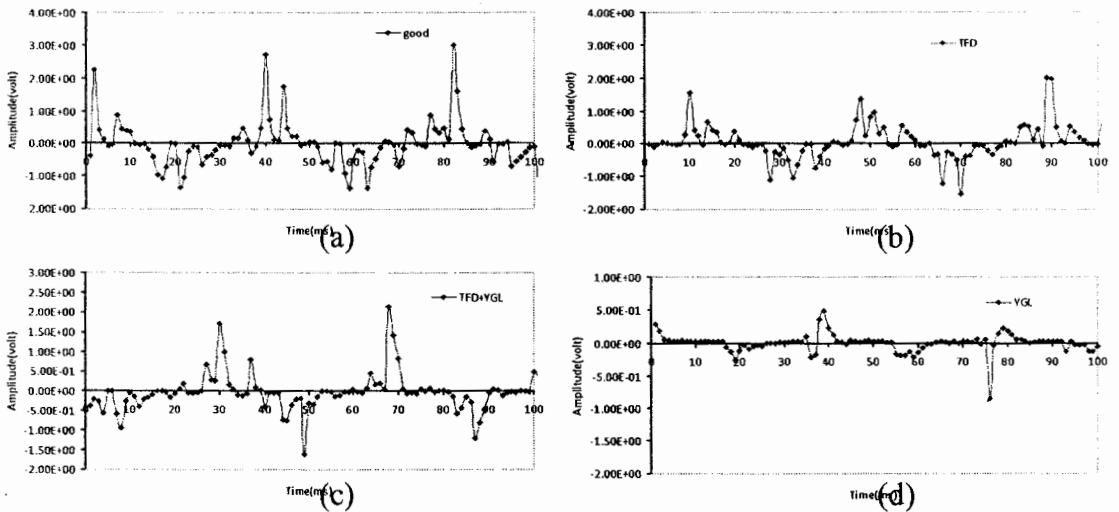


Figure 12 VFSS responses at f_v of a 40 Hz (a) good (b) TFD (c) TFD+YGL (d) YGL

2.3.3 Feature extraction

In this section, signal features in time domain are used to classify mangosteens. Because of simple implementation and computation, time-domain analysis is commonly used for feature analysis. There are nine time-domain features and can be implemented for real-time applications. These features are as follows,

2.2.3.1 Mean Absolute Value (MAV)

MAV is normally used as an onset index to detect an unusual signal activity. MAV is the average of the absolute value of VFSS signal amplitude, N is window Length (Points), $|X_n|$ is data within the window. It is defined as

$$MAV = \frac{1}{N} \sum_{i=1}^N |X_n| \quad (6)$$

2.2.3.2 Root Mean Square (RMS)

RMS is related to constant force and non-fatiguing contraction. Generally, it is similar to standard deviation which can be expressed as

$$RMS = \sqrt{\frac{1}{N} \sum_{i=1}^N x_n^2} \quad (7)$$

2.2.3.3 Waveform length (WL)

WL is the cumulative length of a waveform over a certain time segment (N). WL can be formulated as

$$WL = \sum_{n=1}^{N-1} |x_{n+1} - x_n| \quad (8)$$

2.2.3.4 Zero Crossing (ZC)

ZC is the number of times that the amplitude values of VFSS signal crosses zero in x-axis. An optimum threshold value is chosen to avoid from background noise. ZC provides an approximate estimation of frequency-domain properties. The calculation of ZC is obtained as shown,

$$ZC = \sum_{n=1}^{N-1} [\text{sgn}(x_n \times x_{n+1}) \cap |x_n - x_{n+1}| \geq \text{threshold}]$$

$$\text{sgn}(x) = \begin{cases} 1, & \text{if } x \geq \text{threshold} \\ 0, & \text{otherwise.} \end{cases} \quad (9)$$

2.2.3.5 Slope Sign Change (SSC)

SSC is related to ZC. It is another method to represent the frequency-domain properties of VFSS signal calculated in time domain. The number of changes

between positive and negative slope from three consecutive samples are performed. A threshold value is defined for avoiding background noise in VFSS signal. The SSC is given by

$$SSC = \sum_{n=1}^{N-1} [f[(x_n - x_{n-1}) \times (x_n - x_{n+1})]];$$

$$f(x) = \begin{cases} 1, & \text{if } x \geq \text{threshold} \\ 0, & \text{otherwise} \end{cases} \quad (10)$$

2.2.3.6 Willison amplitude (WAMP)

WAMP is the number of time resulting from the difference between VFSS signal amplitude of two adjoining segments that exceeds a predefined threshold, which is used to reduce background noises as similar to the calculation of ZC and SSC. It is given by

$$WAMP = \sum_{n=1}^{N-1} f(|x_n - x_{n-1}|),$$

$$f(x) = \begin{cases} 1, & \text{if } x \geq \text{threshold} \\ 0, & \text{otherwise} \end{cases} \quad (11)$$

The suitable value of threshold parameter of features in ZC, SSC, and WAMP is normally chosen between 10 and 100 mV, depending on the instrument gain (Angkoon, 2010). The optimal threshold for our VFSS analysis will be detailed later.

2.2.3.7 Autoregressive (AR) coefficients

AR model describes VFSS sample as a linear combination of previous VFSS samples (x_{n-i}) plus a white noise error term (w_n). In addition, p is the order of AR model, α_i are the autoregression coefficients, w_n is white noise. AR coefficients are used to model the VFSS spectrum. The definition of AR model is given by

$$x_n = -\sum_{i=1}^p \alpha_i x_{n-i} + w_n \quad (12)$$

2.2.3.8 Mean Absolute Value Slope (MAVSLP)

MAVSLP is a modified version of MAV. The difference between the MAV of adjacent segments is defined as

$$MAVSLP_i = MAV_{i+1} - MAV_i; \quad i = 1, \dots, I-1. \quad (13),$$

where I is the number of segments covering VFSS signal. When the number of segments increases, it improves the representation of the original signal over the traditional MAV.

2.2.3.9 Histogram (HIST)

HIST is an estimate probability distribution of the VFSS signal. It is given by

$$N = \sum_{i=0}^{M-1} H_i \quad (14),$$

where H_i is the histogram, N is the number of points in the signal, M is the number of points in the histogram.

2.3.4 Feature selection stage

Ankoon (2010) reviewed the quality in class separability aspect. The quality indicates the result of misclassification rate and the degree of experiment variation. From the explanation above, feature selection methods can be obtained based on either classifier or statistic measurement index. The selection of features based on statistical index was investigated where the statistic criterion method which can evaluate the distance between two scatter groups (separation index) was suggested. The statistic criterion method addresses the variation of feature in the same group (compactness index). Euclidean distance (ED) and standard deviation (SD) are the simplest tools selected by Ankoon(2010). Especially ED is most commonly used due to its simplicity and applicability. It is calculated as the root of square differences between co-ordinates of a pair of objects and is also as a separation index. The $ED(p,q)$ is defined as

$$ED(p, q) = |\bar{p} - \bar{q}| \quad (15),$$

where \bar{p} and \bar{q} is the feature means of VFSS signal from texture property in mangosteen.

SD is the most robust and widely used for variability measurement. SD is used as a compactness index which is given by,

$$SD = \sqrt{\frac{\sum_{w=1}^{N_w} (r_w - \mu)^2}{N_w}} \quad (16),$$

where r_w is the feature of the w^{th} window, N_w is the number of total number and μ is the feature mean of all windows. The ratio between ED and SD is RES_{pq} index, which is used as a statistic measured index in this paper. The RES_{pq} index can be expressed as

$$RES_{pq} = \frac{ED(p, q)}{SD} \quad (17).$$

In addition, the features calculated from VFSS response are normalized before calculating the ED and SD values. Good performance of classification is obtained when the ED value is high and the SD is low.

2.3.5 Artificial Neural Network (ANN)

An artificial neural network (ANN) or neural network (NN) is important mathematical models. The topologies of ANN and NN consist of several interconnected artificial neuron groups. ANN can be considered as an adaptive system that changes its structure regarding to the input or output data. Modern NNs are non-linear statistical model and can describe complex relationships between input and output data. The ANN and NN are widely used in several applications. These are:

- Function approximation or regression analysis: including time-series prediction, fitness approximation and modeling.
- Classification: including pattern and sequence recognition, novelty detection and sequential decision making.
- Data processing: including filtering, clustering, blind source separation and compression.
- Robotics: including directing manipulators, computer numerical control.

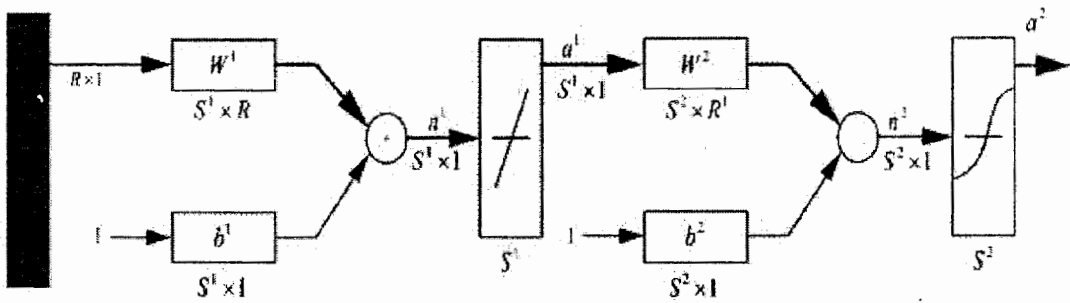


Figure 13 Structure of NN (Pituk, 2012)

NN topology was originated based on biological neural structure. Most NN structures begin with neuron node, as shown in Figure 13. The neuron section consists of multiple input and single output nodes. Each input node is modified by a weight which multiplies the input of ANN. The neuron will combine these weighted inputs and with reference to a threshold value and apply to activation function to determine the output of ANN. The ANN model follows the behavior of real neurons (Benkrose, 1996). Generally, the input layer is considered as a distributor of the signals from the external world. Hidden layers are considered to be categorizers or feature detectors of such signals. The output layer is considered as a collector of the features detected and responsible to producer the response which is given by,

$$\alpha^2 = f(W^2 \cdot a_1 + b^2) \quad (18)$$

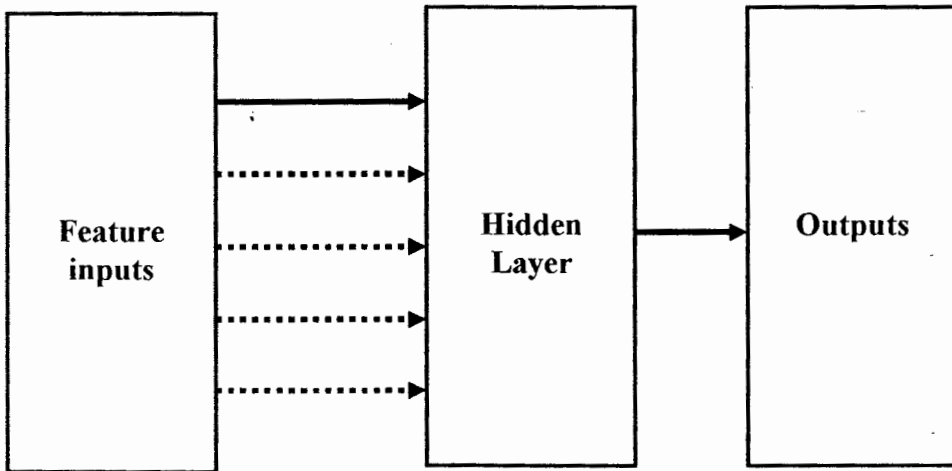


Figure 14 Proposed ANN

The ANN used in this Thesis has three layers based. The topology is feed-forward back propagation (FFBP). The structure is shown in Figure 14. Three layers of ANN consist of input, hidden and output layers. The weighting of each node depends on the application.

Chapter 3

Results and Discussion

3.1 TFD and YGL Detection

3.1.1 Frequency-domain features (paper I and IV)

In this section, VFSS spectrum is proposed as a feature. Four vibration frequencies (f_v) at 25, 30, 35 and 40 Hz are of interest. The vibration amplitude is controlled by applying 2.5 V to the motors. The time-domain VFSS signals are converted to spectrum using the FFT technique. A sampling frequency was selected at 1 kHz. After applying different f_v , resonance is occurred around 25.5-26 Hz as shown in Figure 15(a)-(d). Since the spectrum pattern of a good mangosteen is similar to the defected ones, other sophisticated techniques are recommended.

The transfer function of a mangosteen depends on the texture properties, peel thickness, fruit's weight and diameter. Therefore the amplitudes and phases of VFSS spectrum will be different as shown in Figure 15(a)-(d). From the experiment results, we have found that the weight and diameter of a mangosteen affect to the amplitude of spectrum. To reduce the effects of weight and diameter of fruits on the VFSS spectrum, we recommend to normalize VFSS spectrum with the weight and diameter of a mangosteen. Figure 16(a)-(b) show the normalized spectrum at 25.5-26 Hz with the weight and diameter. Figure 16(c) shows the normalized amplitude spectrum with the peel thickness. The normalized spectrum with peel thickness is smaller as compared with others. It is shown that classification using normalized spectrum will be possible if the f_v either at 35 or 40 Hz is chosen.

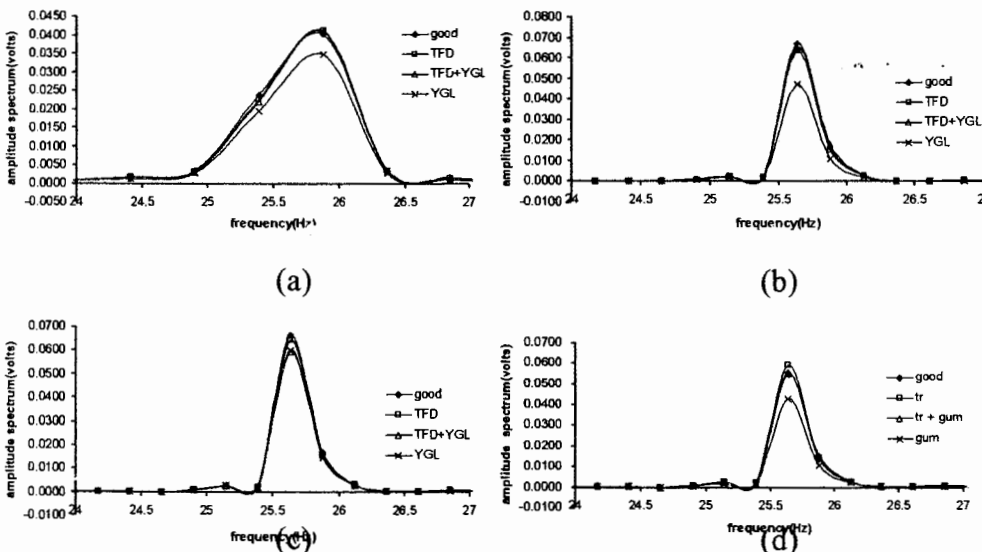
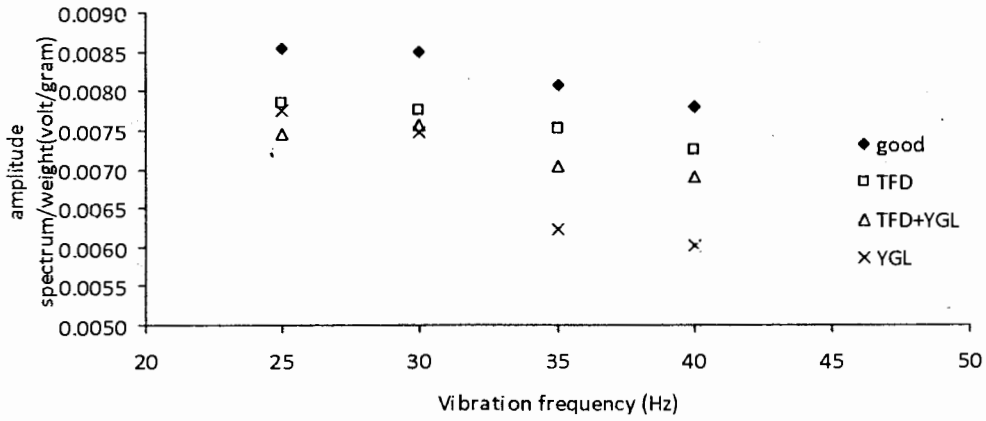
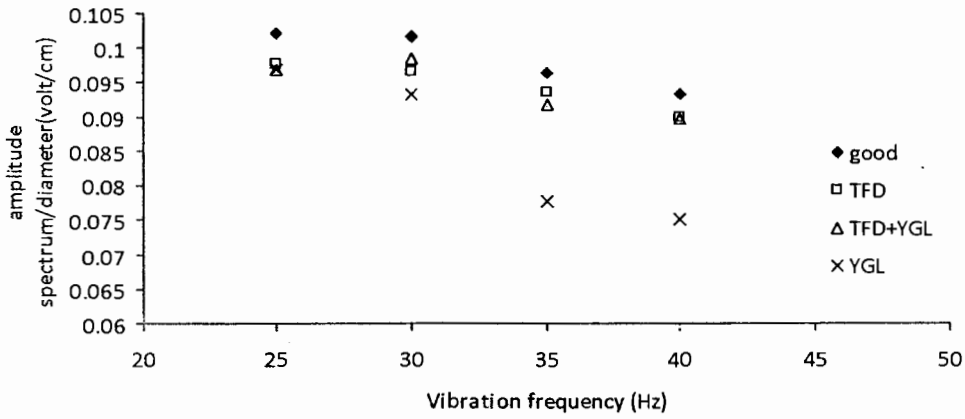


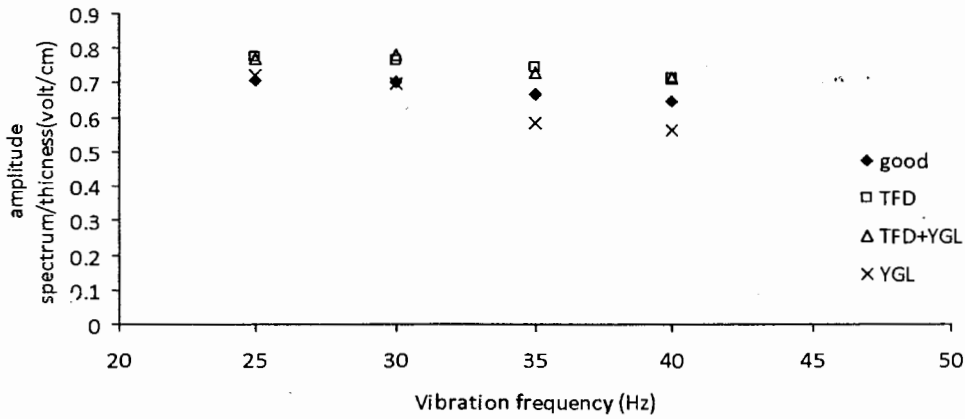
Figure.15 VFSS spectrum at f_v of (a) 25 Hz (b) 30 Hz (c) 35 Hz and (d) 40 Hz



(a)



(b)



(c)

Figure 16 Normalized spectrum with (a) weight (b) diameter and (c) peel thickness.

For clarity sake, the numeric values of spectrums shown in Figure 15 and 16 are listed in Table 3-6. Table 3 lists the amplitude of f_R at 25.5-26 Hz for four different values of f_v . It is shown that the spectrum amplitude at low f_v is larger than those at higher f_v . The amplitude spectrum of a good mangosteen is higher than the defected ones. Among three defected conditions, the VFSS spectrum obtained from a YGL mangosteen is lowest.

Table 3 VFSS spectrum (mV)

f_v (Hz)	Good	TFD	TFD&YGL	YGL
25	519.88	502.69	511.70	494.36
30	517.26	496.90	519.60	476.19
35	491.52	481.14	483.76	396.59
40	475.49	463.50	473.57	382.59

Table 4, shows the spectrums normalized by weight. From the experimental results at the same f_v , the normalized spectrums by weight of good fruit are higher than the defected fruits. The normalized spectrum is large at low f_v and is smaller when f_v increases. The results in Table 4 shows that high f_v is a promising feature to detect the defected fruits.

Table 4 Normalized VFSS spectrum with weight (mV/g)

f_v (Hz)	Good	TFD	TFD&YGL	YGL
25	8.53	7.85	7.45	7.76
30	8.49	7.76	7.56	7.48
35	8.07	7.52	7.04	6.23
40	7.80	7.24	6.89	6.01

Table 5, shows the voltage spectrum normalized with diameter of different mangosteen conditions. This normalized spectrum with diameter for good fruit is higher than the defected fruits. Larger normalized spectrum is obtained if low f_v is chosen. The normalized spectrum with diameter is smallest for a YGL mangosteen.

Table 5 Normalized VFSS spectrum with diameter (mV/cm)

f_v (Hz)	Good	TFD	TFD&YGL	YGL
25	102.10	97.69	97.01	96.93
30	101.58	96.56	98.50	93.37
35	96.53	93.50	91.71	77.76
40	93.38	90.00	89.78	75.02

Table 6 Normalized VFSS spectrum with peel thickness (mV/cm)

f_v (Hz)	Good	TFD	TFD&YGL	YGL
25	705.88	775.67	769.48	725.67
30	702.32	766.73	781.36	698.99
35	667.37	742.41	727.46	582.15
40	645.61	715.20	712.14	561.60

Table 6 shows the normalized amplitude spectrum with peel thickness for different mangosteen conditions. For each f_v value, the normalized spectrums for good mangosteens are smaller than the TFD and TFD&YGL fruits. The normalized spectrums for good fruits are larger than the YGL fruits condition except at f_v of 25 Hz.

3.1.2 Autoregression feature

In this section, the autoregression (AR) technique is applied to analyze the VFSS response signal obtained by vibrating base at 25, 30, 35 and 40 Hz. A hundred mangosteens were tested in this section. Several AR models were applied to these VFSS response signals. It is found that the 10th-order AR model is suitable to characterize the VFSS signal responses for each f_v . By applying the 10th-order AR model, the AR coefficients (a_i), which are obtained by modeling all VFSS signals resulted by vibrating base at 25 Hz, are shown in Figure 17. By inspection, the coefficient a_4 is suitable as a feature due to its well-separated distribution.

From the result, the values of a_4 can be classified to three groups. The first group is defined for coefficients which are smaller than -0.10. The second and the third groups are defined when the coefficient a_4 is greater than 0.10 and between -0.10 to 0.10, respectively. In the third group, only good samples fall in this category hence the third group will be discarded in our analysis. Only two groups of a_4 ($0.20 < a_4 < 0.10$ and $-0.20 < a_4 < -0.10$) are considered. Hence the test mangosteens are classified into two groups according to these two groups of a_4 .

When applying different values of f_v , a_4 feature is still applicable to classify. Other AR coefficients as a feature were investigated. Unfortunately none of them is suitable for this application, a_1 is less than -0.1.

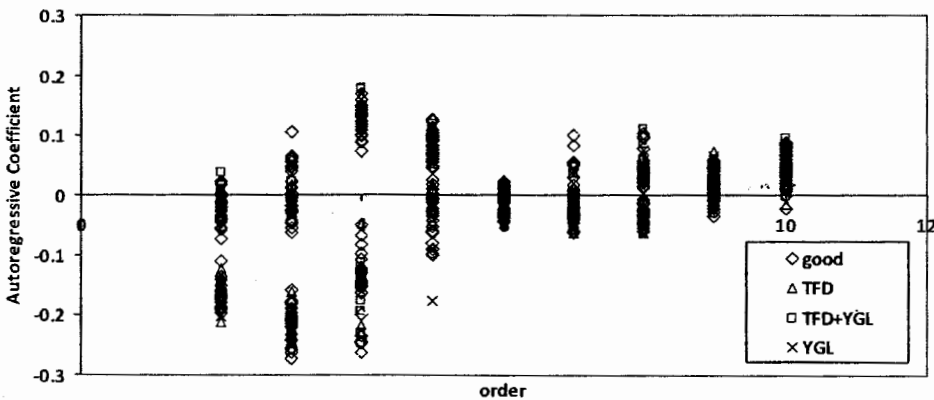


Figure 17 AR coefficients computed from VFSS response signals for 25 Hz f_v

3.1.3 Resonance frequency feature based on f_v at 40 Hz

Applying f_v at 25, 30, 35 and 40 Hz, two f_R at 77 and 187 Hz are appeared in the VFSS output spectrums as shown in Figure 18. Here we propose to classify mangosteens into two groups using f_R at 77 and 187 Hz. There are two resonances at 77 and 187 Hz appear for all VFSS spectrums. If the amplitude spectrum at 77 Hz is larger than the spectrum at 187 Hz, the VFSS is considered to resonate at 77 Hz and

vice versa for another. At f_v of 25 Hz, 88 mangosteens have f_R peaking at 77 Hz where other 12 samples have f_R peak at 187 Hz. At f_v of 30 Hz, 89 samples have dominant f_R at 77 Hz and only 11 samples have f_R at 187 Hz. At f_v of 35 Hz, 85 samples have dominant f_R at 77 Hz while 15 samples have f_R at 187 Hz. Finally when f_v at 40 Hz was applied, there are 51 and 49 fruits for the first (77 Hz) and second groups (187 Hz).

Table 7 shows the summary results using f_R to detect good/defected samples for different f_v . At a certain f_v , the number of mangosteens for each testing condition for each group is shown. When applying 40 Hz f_v , the distribution characteristic in each resonance group for each condition is more suitable for detecting a good/defected mangosteen. Hence f_v at 40 Hz is recommended to classify mangosteens.

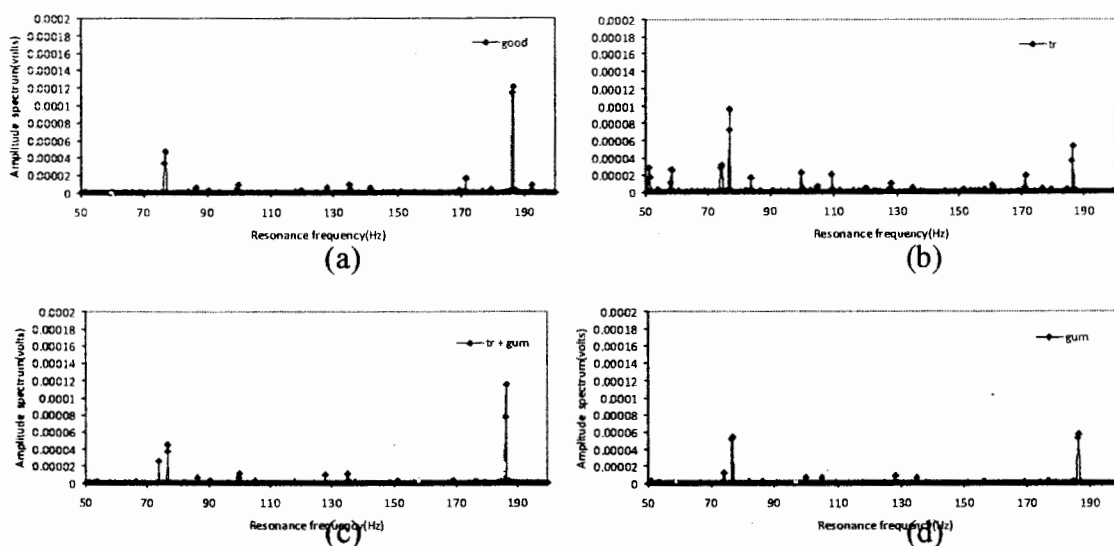


Figure 18 f_R at 77 and 187 Hz (f_v is 40Hz)

Table 7 Number of samples which have f_R at 77 and 187 Hz with negative AR and positive AR for different f_v

Condition	f_v (Hz)	25				30				35				40			
		77		187		77		187		77		187		77		187	
	f_R (Hz)	$-a_4$	$+a_4$	$-a_4$	$+a_4$	$-a_4$	$+a_4$	$-a_4$	$+a_4$	$-a_4$	$+a_4$	$-a_4$	$+a_4$	$-a_4$	$+a_4$	$-a_4$	$+a_4$
Good		15	15	5	0	2	29	4	0	10	21	4	0	10	7	10	8
TFD		8	16	1	1	7	17	0	2	7	15	0	4	2	9	7	8
TFD+YGL		9	9	1	1	3	15	1	1	6	11	1	3	5	5	5	5
YGL		3	1	0	0	0	4	0	0	0	4	0	0	2	0	0	2
Total		35	41	7	2	12	65	5	3	23	41	5	7	19	21	22	23

**** fifteen mangosteens is detected by AR model on f_v at 25Hz

Figure 19 shows the research methodology proposed in this Thesis. One hundred mangosteens were vibrated at 40 Hz. The sensors attached to the tested mangosteen sense the VFSS response. This time-domain VFSS response will be digitized and recorded. Hence there are 100 time-domain VFSS responses for 100 mangosteens which were vibrated at 40 Hz. Several frequency- and time-domain features were investigated. For frequency-domain feature, the VFSS output spectrums are computed using the FFT technique. Frequency resonances at 77 and 187 Hz are

utilized to classify samples. The spectrum estimation using AR technique is used to model the VFSS signal. The coefficient a_4 of tenth-order AR model is proposed for sample classification. The pre-classification process based on these two frequency domain features (AR and FFT) is introduced. Four groups of mangosteens; [group1 : a_4 is negative and second f_R at 77Hz], [group2 : a_4 is negative and second f_R at 187Hz], [group3 : a_4 is positive and second f_R at 77Hz], and [group4 : a_4 is positive and second f_R at 187Hz]; are obtained. Based on these four groups, eight time-domain features are computed from VFSS samples of each group. After pre-classification, feature extraction subsequent with good/defect detection were applied. Three different categories are proposed as shown in Table 8. The first technique is achieved by adopting an optimum pair of features from 36 possible pairs of features for each group by observation. From the scatter plot of the selected pair of features, the detection threshold is determined by observation. It is well known that observation by human can be bias. Therefore an artificial intelligence (AI) technique is introduced in the second technique. This technique employs the RES index for selecting an optimum pair of features while the threshold is still determined by human observation. The third technique applies the RES index for choosing an optimum pair of features and the neural network (NN) for detecting a good/defected mangosteen.

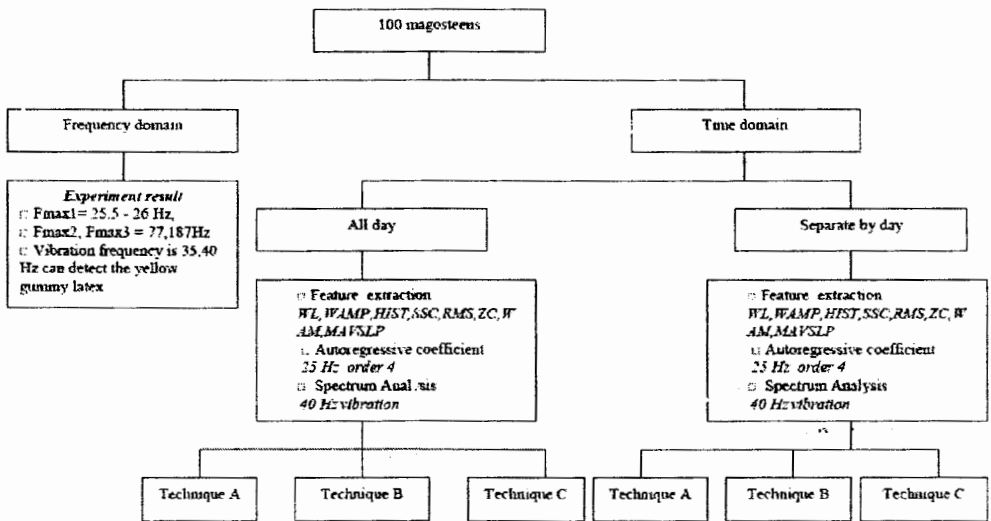


Figure 19 Methodology used in the research

Table 8 Techniques for feature selection and good/defected detection

<i>Technique</i>	<i>Feature selection</i>	<i>Good/defected detection</i>
A	Scatter plot	Scatter plot
B	RES index	Scatter plot
C	RES index	NN

3.2 Case Study

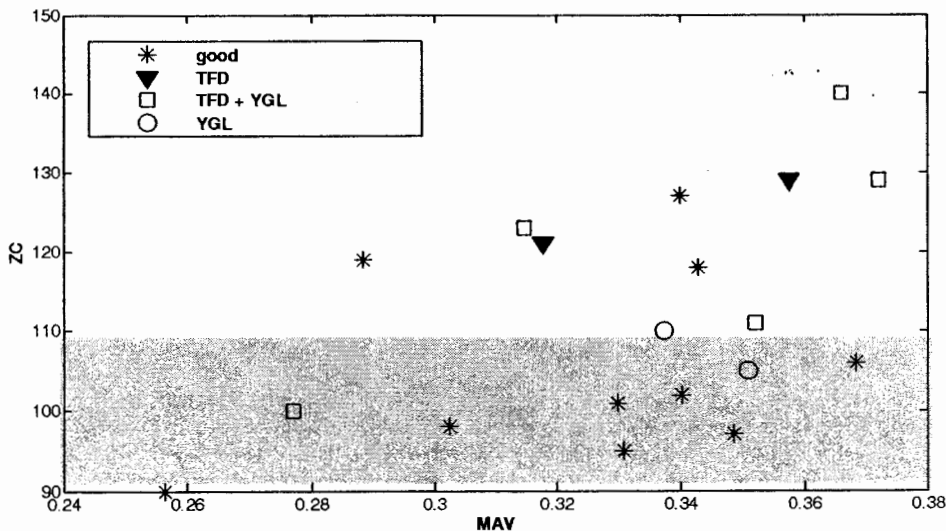
3.2.1 Case study 1: Pre-classification using AR and f_R

In this section, all VFSS output signals of 100 mangosteens are analyzed. These VFSS samples will be first classified using a_4 and f_R as described in Section 3.1.3. Four groups of VFSS samples; ([group1 : a_4 is negative and second f_R at 77Hz], [group2 : a_4 is negative and second f_R at 187Hz], [group3 : a_4 is positive and second f_R at 77Hz], and [group4 : a_4 is positive and second f_R at 187Hz]); will be obtained. For each VFSS group, time-domain features are computed and three techniques listed in Table 8 will be applied. The accuracy performances for each case are as follows:

3.2.1.1 Group1

(a) Technique A

The distribution characteristics of all 36 scatter plots are investigated and MAV-ZC feature pair is found to be optimum. Figure 20 shows MAV-ZC plot. The threshold for MAV and ZC at 0.24 - 0.38 and 107 is obtained by observation.

Figure 20 MAV-ZC plot ($[-a_4, 77 \text{ Hz}]$)

(b) Technique B

The average RES indexes of all features were calculated and the results are plotted in Figure 21. It is shown that MAVSLP and ZC provide two highest RES index values among other features.

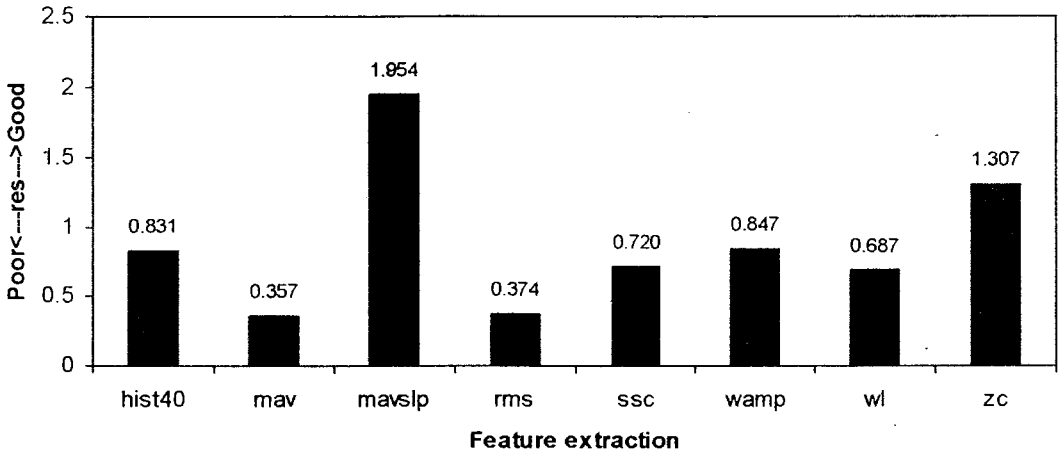


Figure 21 RES indexes of features ($[-a_4, 77 \text{ Hz}]$).

Figure 22 shows MAVSLP-ZC plot. A well separation of each mangosteen condition is obtained. By observation, the threshold values for MAVSLP and ZC are 0 - 0.027 and 102, respectively.

(c) Technique C

Based on the MAVSLP-ZC pair of features selected from RES index, NN technique is applied to detect a good/defected sample. The accuracy performances of detecting good and defected samples are only 66.67 and 44.44%, respectively. The overall accuracy performance of technique C is 50.00% only, which is lower accuracy than Technique A and B in $[-a_4, 77\text{Hz}]$ group.

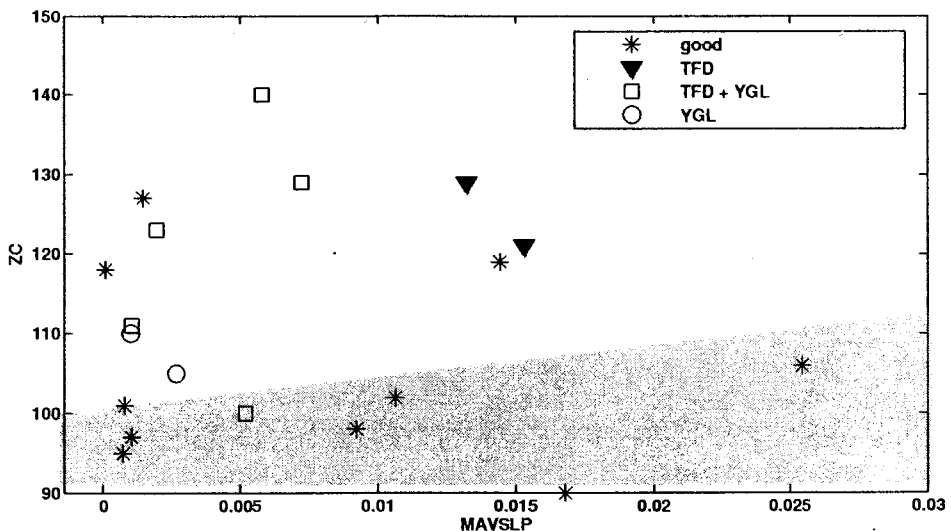


Figure 22 MAVSLP-ZC plot ($[-a_4, 77 \text{ Hz}]$).

Table 9 Summary of classification performances ($[-a_4, 77 \text{ Hz}]$).

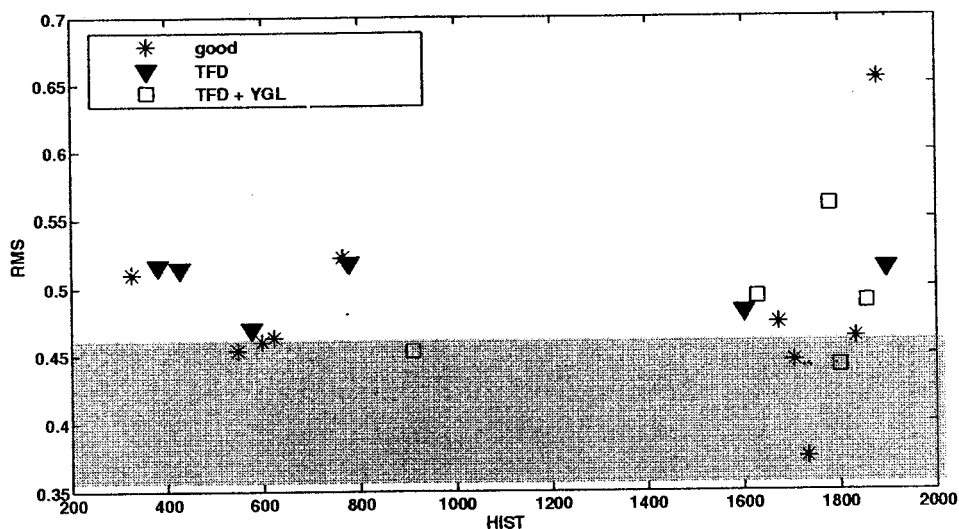
Technique	Performance (%)				Overall accuracy (%)
	Good	Accuracy	Defected	Accuracy	
<i>A</i>	70.00	77.78	77.78	70.00	73.68
<i>B</i>	70.00	87.50	88.89	72.72	78.95
<i>C</i>	28.57	66.67	80.00	44.44	50.00

Table 9 summarizes the accuracy performances obtained from three techniques applied to $[-a_4, 77 \text{ Hz}]$ group. It is shown that technique *B* shows accuracy of 78.95%, which is the best classification performance in this group. The worst performance is obtained from technique *C*.

3.2.1.2 Group2 .

(a) Technique *A*

The distribution characteristics of all 36 scatter plots are investigated and HIST-RMS feature pair is chosen. Figure 23 shows HIST-RMS plot. The threshold for HIST and RMS at 200 - 1900 and 0.47, respectively, is obtained by observation.

Figure 23 HIST-RMS plot ($[-a_4, 187 \text{ Hz}]$)

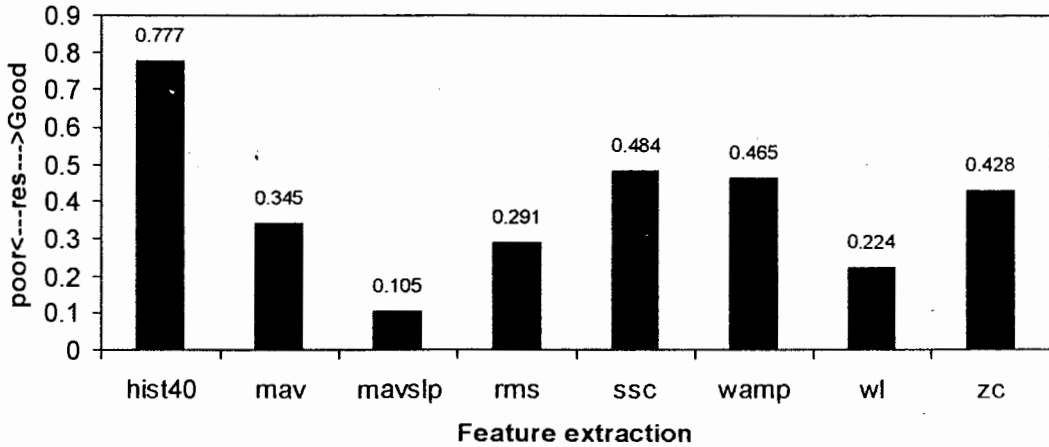


Figure 24 RES indexes of features ($[-a_4, 187 \text{ Hz}]$).

(b) Technique *B*

The RES indexes of all 36 features were calculated. Figure 24 shows the RES index values for all features. HIST and SSC provide two highest index values among other features.

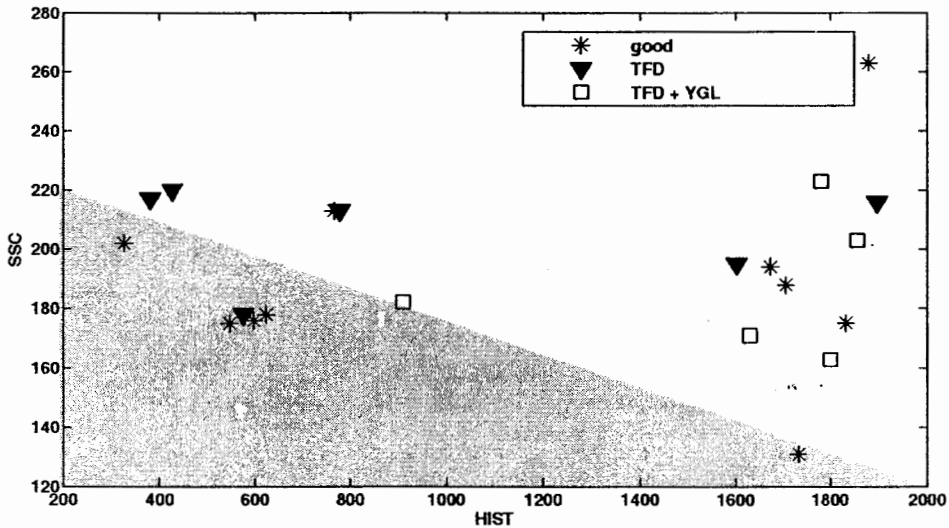


Figure 25 HIST-SSC plot ($[-a_4, 187 \text{ Hz}]$)

HIST-SSC plot is shown in Figure 25. By observation, the threshold values for these two features are 1900 and 210, respectively.

(c) Technique *C*

Based on the HIST-SSC pair of features selected from RES index, NN technique is applied to detect good/defected samples. The accuracy performances of detecting good and defected samples are 0.00 and 55.56%, respectively. The overall accuracy performance of technique *C* is 55.56% only, which is much lower accurate than technique *A* and *B*.

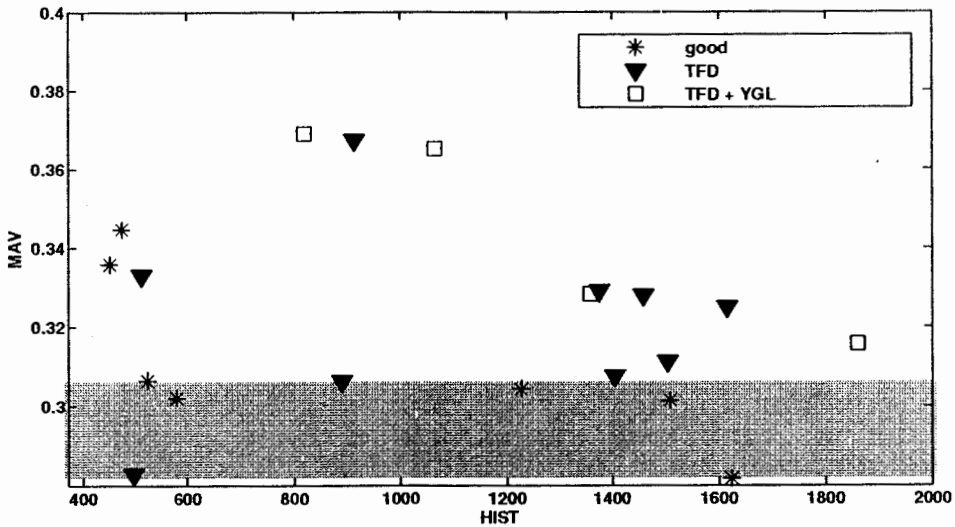
Table 10 Summary of classification performances ($[-a_4, 187 \text{ Hz}]$)

Technique	Performance (%)				
	Good	Accuracy	Defected	Accuracy	Overall accuracy (%)
<i>A</i>	70.00	70.00	72.73	72.73	71.43
<i>B</i>	50.00	83.33	90.91	66.67	71.43
<i>C</i>	0.00	0.00	100.00	55.56	55.56

Table 10 summarizes the accuracy performances obtained from three techniques applied to $[-a_4, 187 \text{ Hz}]$ group. It is shown that technique *A* and *B* show equal accuracy performance for 71.43%.

3.2.1.3 Group3

(a) Technique *A*

Figure 26 HIST-MAV plot ($[+a_4, 77 \text{ Hz}]$)

The distribution characteristics of all 36 scatter plots are investigated and HIST-MAV feature pair is chosen. Figure 26 shows HIST-MAV plot. The threshold for HIST and MAV at 400-2000 and 0.31, respectively, is obtained by observation.

(b) Technique B

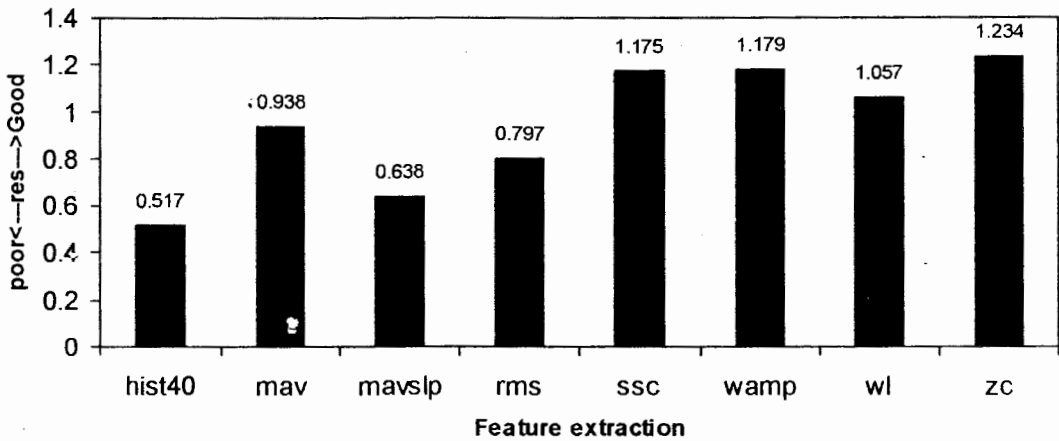
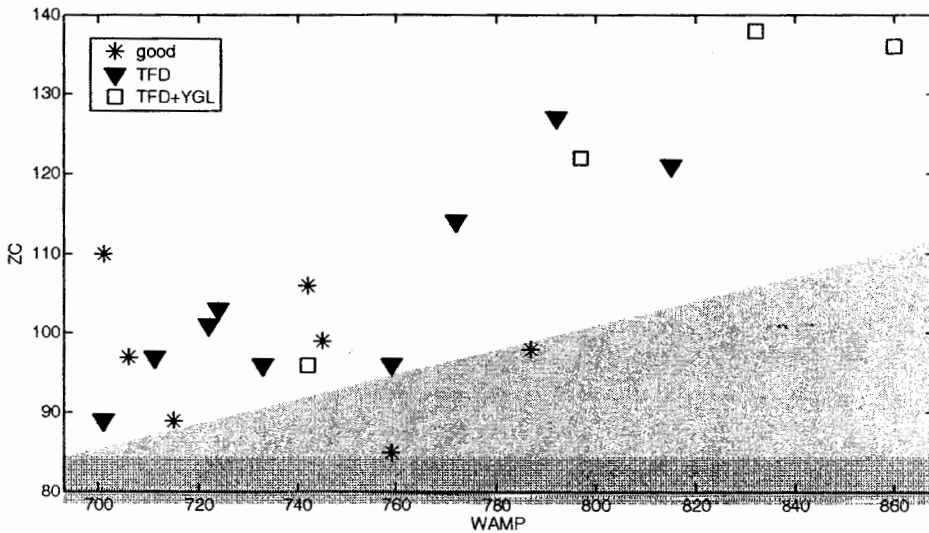
Figure 27 RES indexes of features ($[+a_4, 77 \text{ Hz}]$).

Figure 27 shows the RES index calculated for all features. It is shown that the RES index values of WAMP and ZC are highest among other features. WAMP-ZC plot is shown in Figure 28. The thresholds for these two features are 700 – 840 and 85, respectively.

Figure 28 WAMP-ZC plot ($[+a_4, 77 \text{ Hz}]$)

(c) Technique C

Based on the HIST-SSC feature pair selected from RES index, NN technique is applied to detect good/defected samples. The accuracy performances of detecting good and defected samples are 33.33 and 60.00%, respectively. The overall accuracy performance of technique C is 53.85% only, which is much lower accurate than technique A and B.

Table 11 Summary of classification performances ($[+a_4, 77 \text{ Hz}]$)

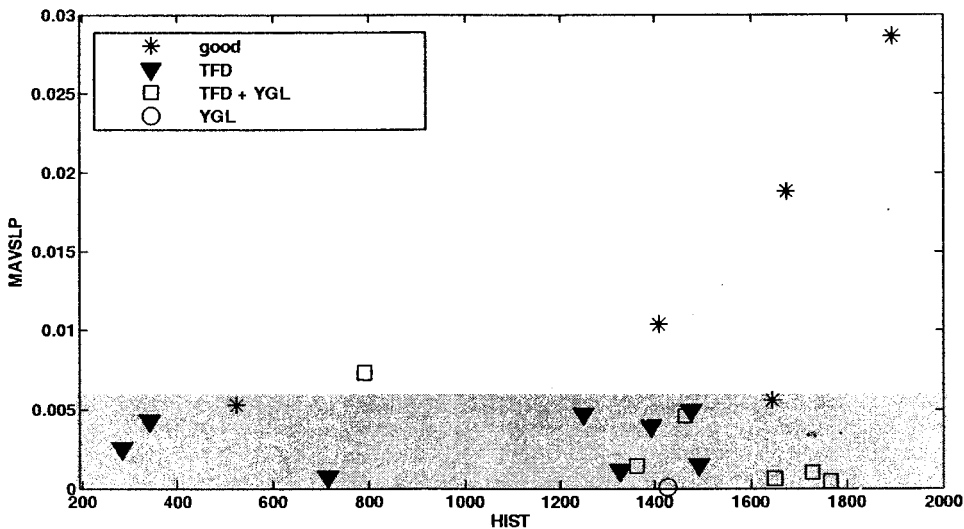
Technique	Performance (%)				
	Good	Accuracy	Defected	Accuracy	Overall accuracy
<i>A</i>	71.43	71.43	84.62	84.62	80.00
<i>B</i>	42.86	100.00	100.00	76.47	80.00
<i>C</i>	20.00	33.33	75.00	60.00	53.85

Table 11 summarizes that the accuracy performances obtained from three techniques applied to ($[+a_4, 77 \text{ Hz}]$) group. It is shown that technique *A* and *B* show equal accuracy performance for 80.00%.

3.2.1.4 Group4

(a) Technique *A*

The distribution characteristics of all 36 scatter plots are investigated and HIST-MAVSLP feature pair is chosen. Figure 29 shows HIST-MAVSLP plot. The threshold for HIST and MAVSLP at 0 to 2000 and 0.005, respectively, is obtained by observation.

Figure 29 HIST-MAVSLP plot ($[+a_4, 187 \text{ Hz}]$)

(b) Technique *B*

Figure 30 shows the RES index calculated for all features. It is shown that the RES index values of ZC and MAVSLP are highest among other features. Therefore these features are chosen to determine for detecting good/defected mangosteen in this case. Figure 31 plot MAVSLP and ZC. The thresholds for these two features are 0.3 and 180, respectively.

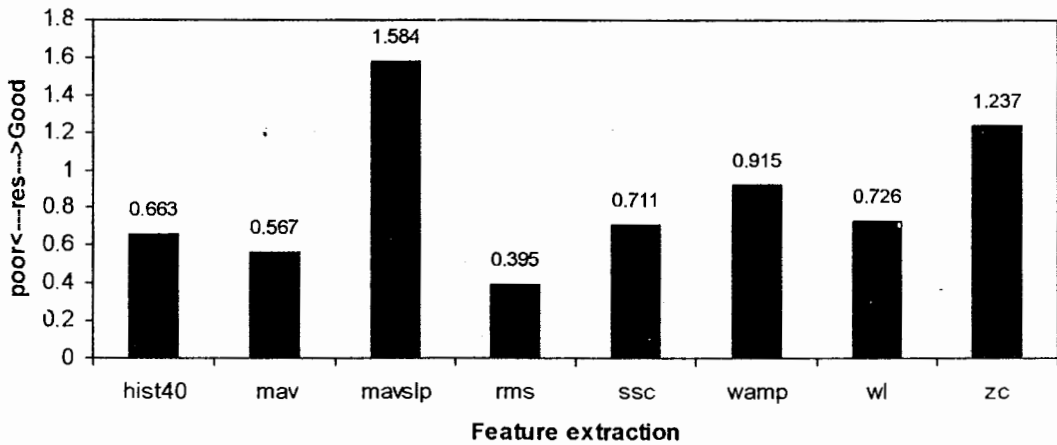


Figure 30 RES indexes of features ($[+a_4, 187 \text{ Hz}]$)

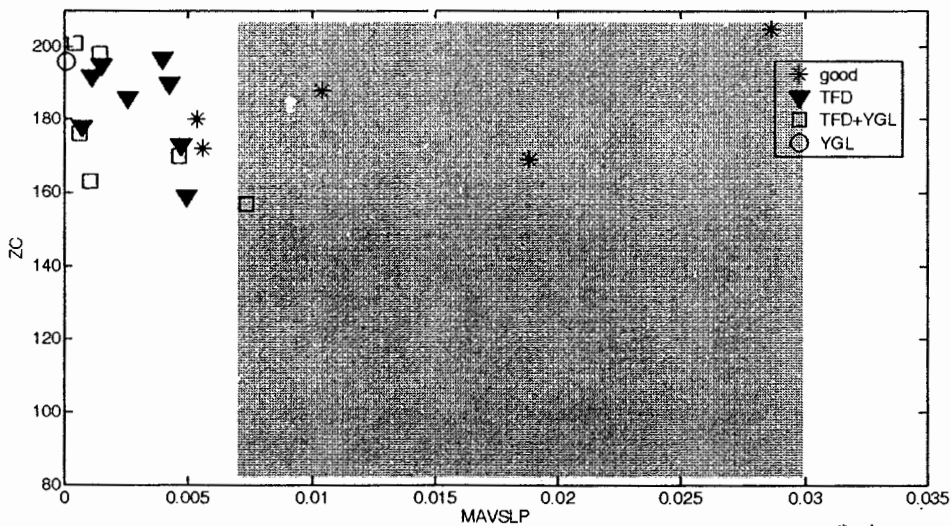


Figure 31 MAVSLP-ZC plot ($[+a_4, 187 \text{ Hz}]$)

(c) Technique C

Based on the MAVSLP-ZC feature pair selected from RES index, NN technique is applied to detect good/defected samples. The accuracy performances of detecting good and defected samples are 100.00 and 87.50%, respectively. The overall accuracy performance of technique C is 90.00% only, which is better than technique B.

Table 12 Summary of performances ($[+a_4, 187 \text{ Hz}]$)

Technique	Performance (%)				Overall accuracy (%)
	Good	Accuracy	Defected	Accuracy	
A	100.00	88.89	93.33	100.00	95.65
B	87.50	70.00	80.00	92.38	82.62
C	66.67	100.00	100.00	87.50	90.00

Table 12 summarizes that the accuracy performances obtained from three techniques applied to ($[+a_4, 187 \text{ Hz}]$) group. It is shown that technique *A* shows the best accuracy performance among other features.

3.2.2 Case study 2: All VFSS samples

In this experiment, 15 different techniques are applied to all VFSS output signals. Table 13 details these techniques regarding to the methods for spectrum estimation, feature selection and good/defected detection. The details for applying these 15 techniques to all VFSS samples are as follows:

Table 13 Summary of applied techniques

<i>Technique</i>	a_4	$f_R(\text{Hz})$	<i>Feature selection</i>	<i>Good/defected detection</i>
I	not used	not used	Scatter plot	Scatter plot
II	not used	not used	RES index	Scatter plot
III	not used	not used	RES index	NN
IV	not used	77	Scatter plot	Scatter plot
V	not used	187	Scatter plot	Scatter plot
VI	not used	77	RES index	Scatter plot
VII	not used	187	RES index	Scatter plot
VIII	not used	77	RES index	NN
IX	not used	187	RES index	NN
X	-	not used	Scatter plot	Scatter plot
XI	+	not used	Scatter plot	Scatter plot
XII	-	not used	RES index	Scatter plot
XIII	+	not used	RES index	Scatter plot
XIV	-	not used	RES index	NN
XV	+	not used	RES index	NN

(a) Technique I

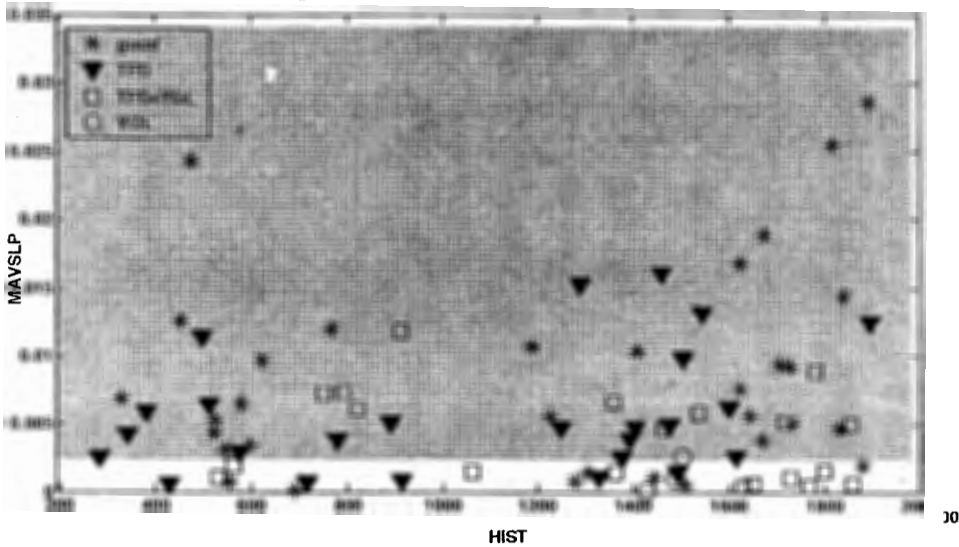


Figure 32 HIST-MAVSLP plot (All VFSS samples)

The distribution characteristics of all scatter plots are investigated and HIST-MAVSLP feature pair is chosen. Figure 32 shows HIST-MAVSLP plot. The threshold is chosen by setting HIST from 500 to 2000 and MASLP for 0.0025.

(b) Technique II

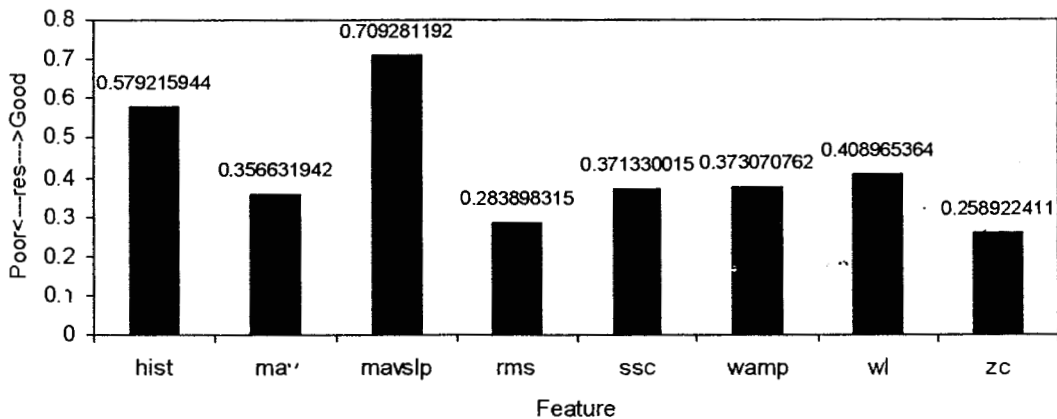


Figure 33 RES indexes of features (All VFSS samples)

Figure 33 shows the RES index of all features. It is shown that the RES index values of MAVSLP and HIST features are highest among other features. Therefore these two features are chosen for detecting good/defected mangosteen in this case. It is shown that two features obtained from technique II are the same features chosen by observation in the technique I. The MAVSLP-HIST plot is shown in Figure 32 and the threshold values for this plot based on observation are equal to the values obtained from technique I.

(c) Technique III

Applying NN method for detecting good/defected sample to the MAVSLP and HIST features, the overall accuracy performance is 68.42%.

(d) Technique IV

From this technique, the WAMP-WL plot as shown in Figure 34 is found to be the optimum features. The (WAMP,WL) threshold for detecting good/defected fruit is (760, 350-650).

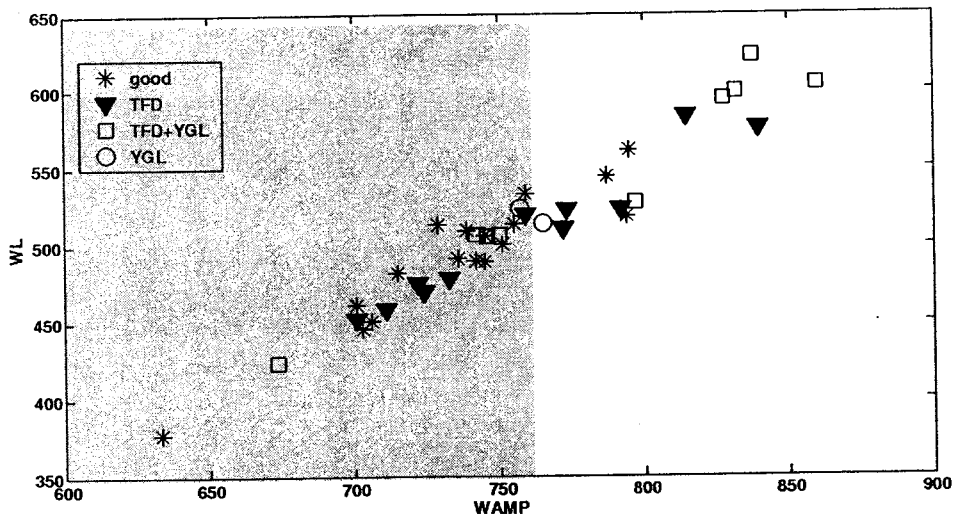


Figure 34 WAMP-WL plot (All VFSS samples)

(e) Technique V

From this technique, the HIST-MAVSLP plot as shown in Figure 35 is found to be optimum features. The threshold values for HIST and MAVSLP are 0 and 0.0025, respectively.

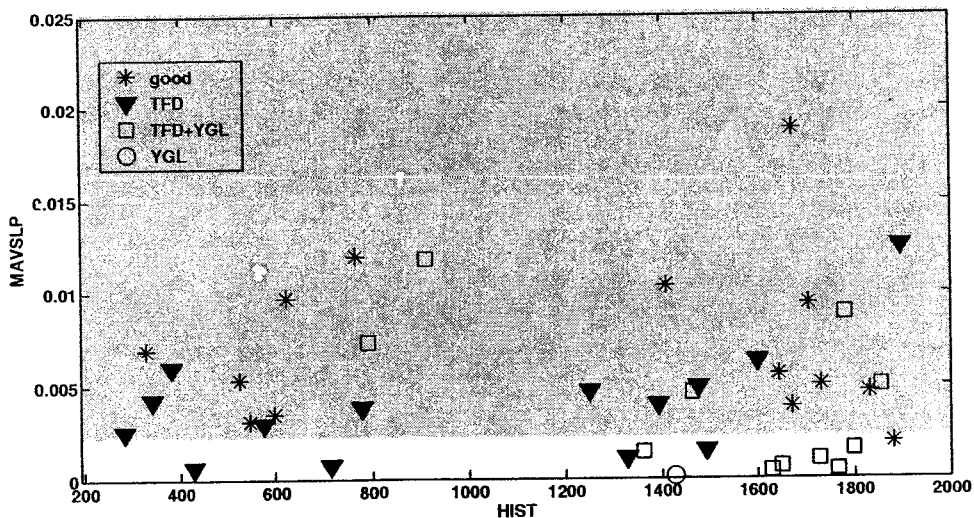


Figure 35 MAVSLP-HIST plot (All VFSS samples)

(f) Technique VI

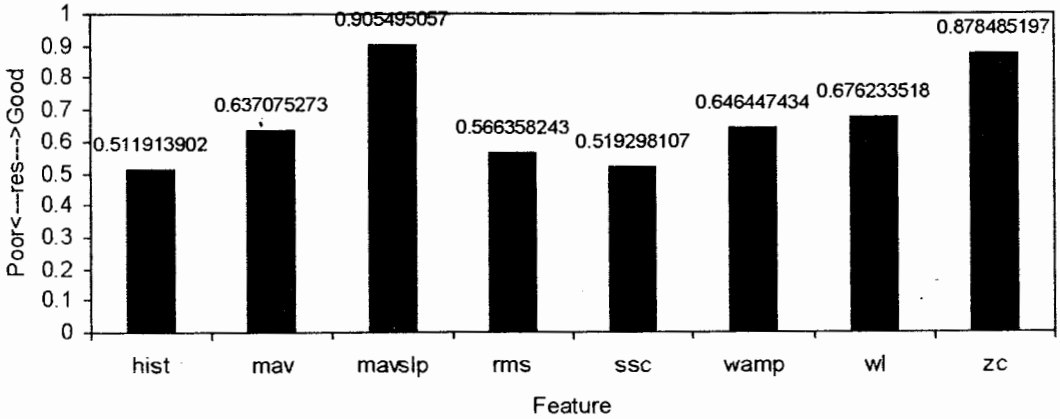


Figure 36 RES indexes of features (All VFSS samples)

RES indexes of 8 time-domain features were computed and are shown in Figure 36. It is shown that RES indexes of ZC and MAVSLP are highest among other features. Hence these two features are chosen for detecting a good/defected sample. Figure 37 shows MAVSLP-ZC plot. By observation, the thresholds values for MAVSLP and ZC are 0-0.03 and 138, respectively.

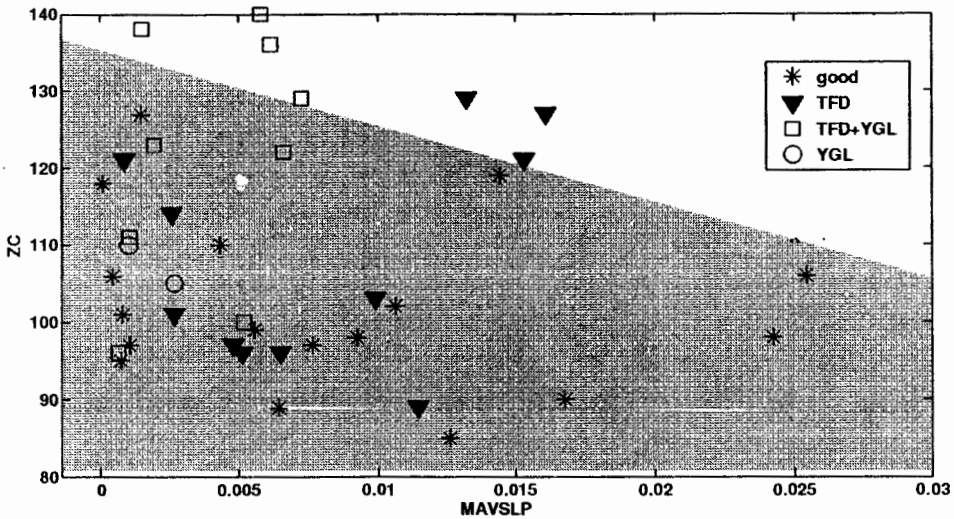


Figure 37 MAVSLP-ZC plot (All samples)

(g) Technique VII

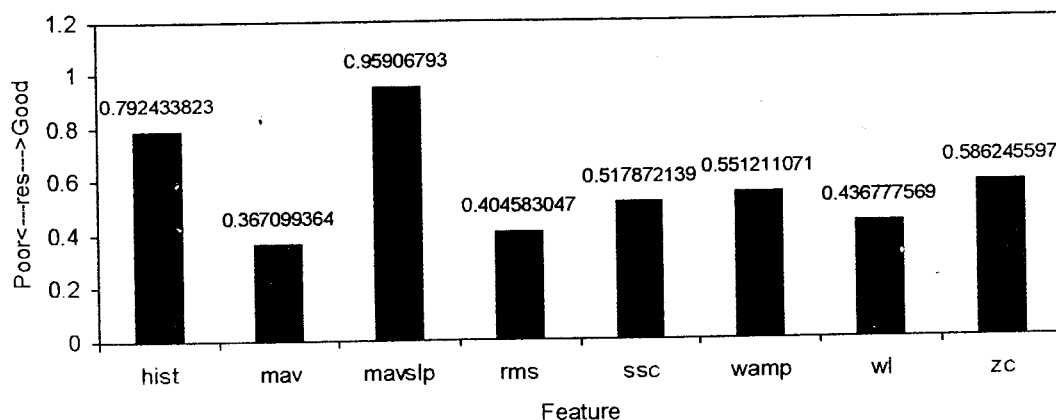


Figure 38 RES indexes of features (All samples)

In this case, RES indexes of 8 time-domain features are shown in Figure 38. It is shown that RES indexes of MAVSLP and HIST are highest among other features. Hence these two features are chosen for detecting a good/defected sample. The plot of MAVSLP-HIST is shown in Figure 35. Hence the threshold values for these features are the values previously obtained by technique V.

(h) Technique VIII

From the MAVSLP-ZC plot shown in Figure 33, a single-hidden NN is applied to detect a good/defected sample. It is found that the overall performance for this technique is 66.67%.

(i) Technique IX

From the MAVSLP-HIST plot shown in Figure 31, a single-hidden NN is applied to detect a good/defected sample. It is found that the overall performance for this technique is 62.5%.

(j) Technique X

The VFSS samples with $-a_4$ are analyzed and all possible feature pairs were plotted. Based on observation, the feature MAV and MAVSLP are found to be optimum. The MAV-MAVSLP plot is shown in Figure 39. The threshold values for (MAV, MAVSLP) are (0.24 to 0.42, 0.001 to 0.013).

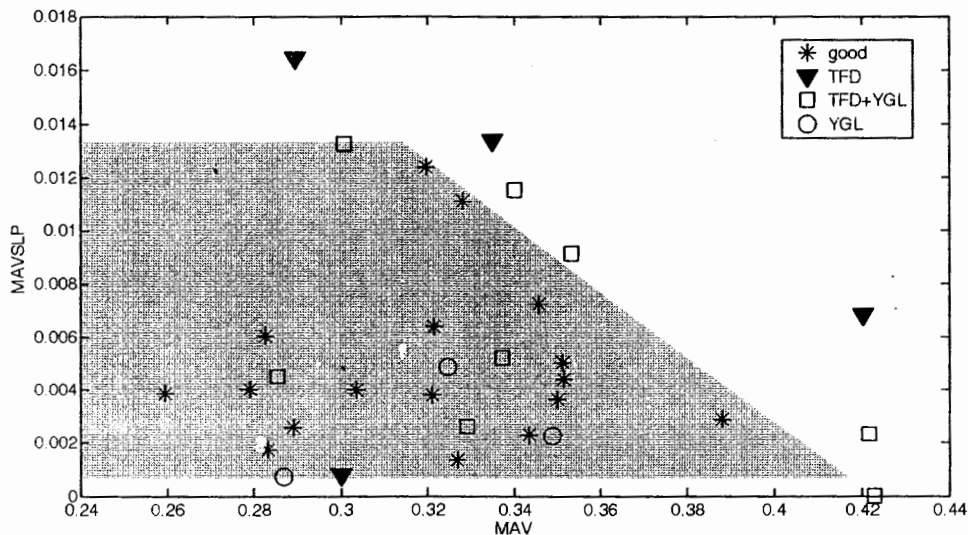


Figure 39 MAV-MAVSLP plot (All VFSS samples)

(k) Technique XI

The VFSS samples with have $+a_4$ are analyzed and all possible feature pairs were plotted. Based on observation, the feature SSC and ZC are found to be optimum. The MAV-MAVSLP plot is shown in Figure 40. The threshold values for (SSC, ZC) are (170,150).

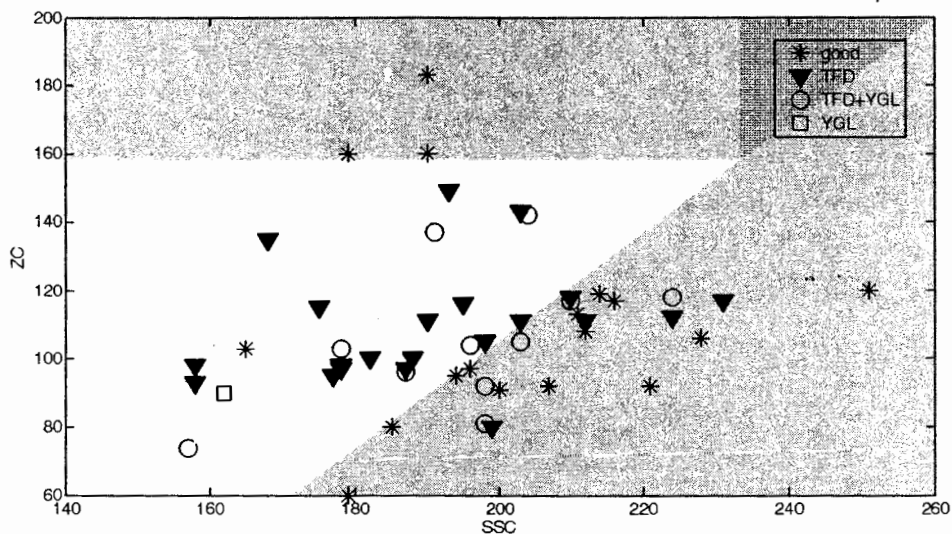


Figure 40 SSC-ZC plot (All VFSS samples)

(l) Technique XII

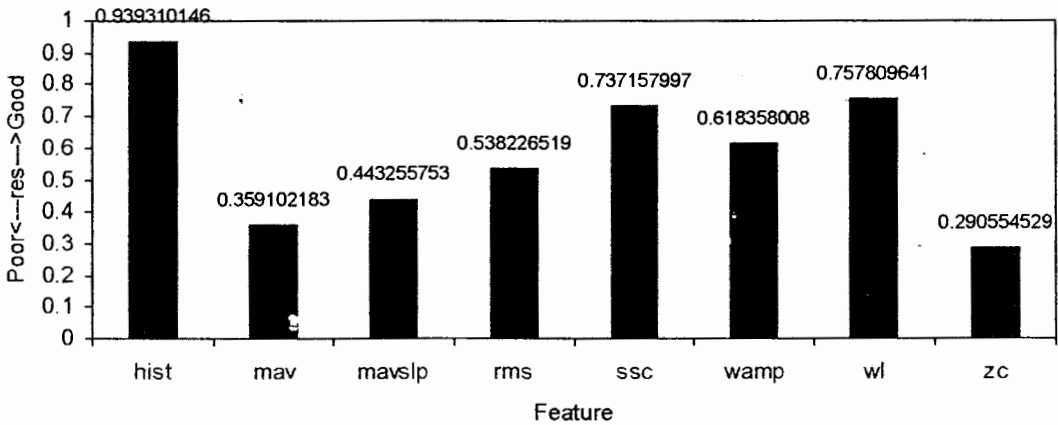


Figure 41 RES indexes of features (All samples)

The features of VFSS data samples that have $-a_4$ are computed. Their RES indexes are plotted in Figure 41. It is shown in Figure 41 that the RES index values of HIST and WL are highest among other features.

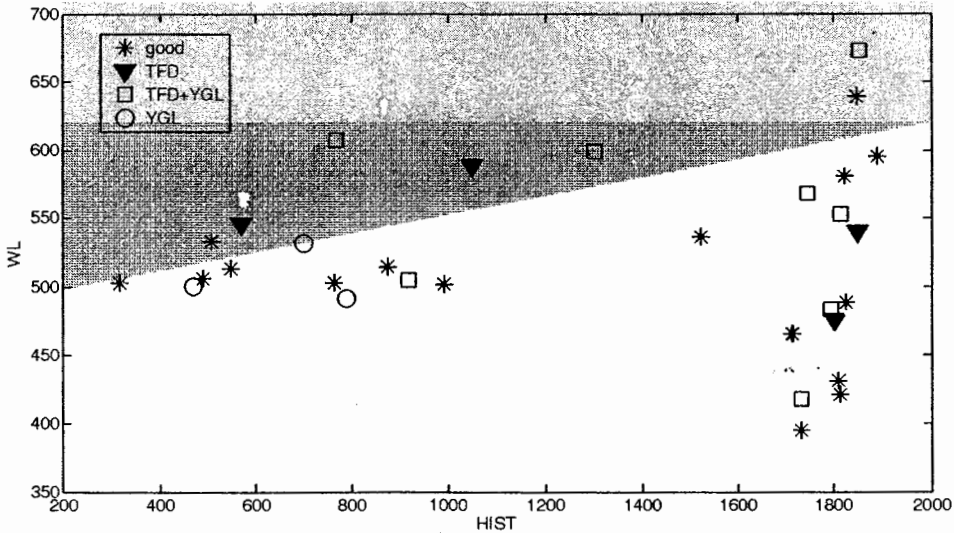


Figure 42 HIST-WL plot ($[-a_4]$, All samples)

Figure 42 shows HIST-WL plot. Based on observation, the thresholds values for HIST and WL are 0-2000 and 500, respectively.

(m) Technique XIII

The features of VFSS data samples that have $+a_4$ are computed. Their RES indexes are plotted in Figure 43. It is shown in Figure 43 that the RES index values of SSC and MAV are highest among other features.

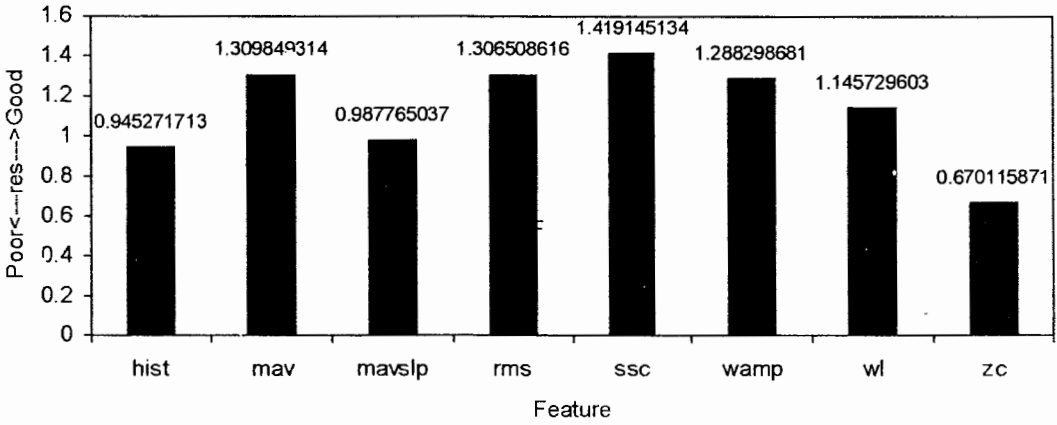


Figure 43 RES indexes of features (All VFSS samples)

Figure 44 shows MAV-SSC plot. Based on observation, the thresholds values for MAV and SSC are 0.26-0.40 to 0.31 and 170-220, respectively.

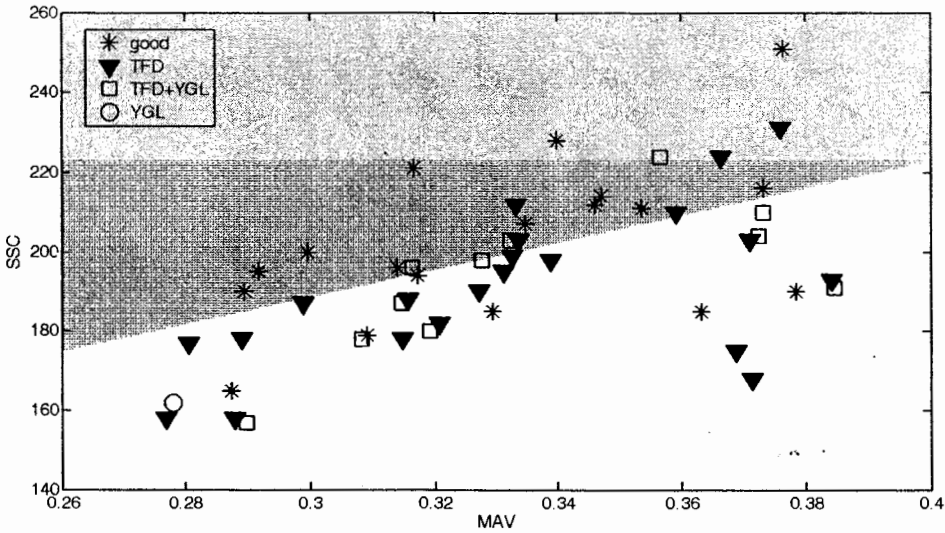


Figure 44 MAV-SSC plot (All VFSS samples)

(n) Technique XIV

From the features shown in Figure 41, a single-hidden layer NN is applied to determine the thresholds for detecting a good/defected sample. The overall accuracy performance obtained is 64%.

(o) Technique XV

From the features shown in Figure 43, a single-hidden layer NN is applied to determine the thresholds for good/defected sample detection. The overall accuracy performance obtained is 54.55%.

Table 14 Performances of techniques applied to all VFSS samples

Technique	Performance (%)				Overall accuracy (%)
	Good	Accuracy	Defected	Accuracy	
I	80.00	50.91	43.75	75.00	59.04
II	80.00	50.91	43.75	75.00	59.04
III	33.33	100.00	100.00	62.50	68.42
IV	82.35	56.00	50.00	78.57	64.10
V	94.44	56.67	50.00	92.86	68.18
VI	100.00	53.13	31.82	100.00	61.54
VII	94.44	56.67	50.00	92.86	68.18
VIII	100.00	56.25	41.67	100.00	66.67
IX	30.00	60.00	85.71	63.16	62.50
X	100.00	77.27	66.67	100.00	84.38
XI	94.44	68.00	75.76	96.15	82.35
XII	88.24	62.50	40.00	75.00	65.62
XIII	72.22	61.90	75.76	83.33	74.51
XIV	91.67	57.89	38.46	83.33	64.00
XV	50.00	30.00	56.25	75.00	54.55

Table 14 shows the accuracy performances of fifteen techniques applied to all VFSS signals measured from all mangosteen samples. The details of these techniques are summarized in Table 13. It is shown that technique X, which is based on using $-a_4$ for classification and observation for feature selection/detection, outperforms other techniques. It achieves 84.34% for overall accuracy performance. The second best performance is obtained from technique XI. The accuracy performance is 82.35%, which is comparable to Technique X. The process of technique XI is rather similar to Technique X. Only the classification process, which is relied on $+a_4$, differs from technique X. Table 15 shows the performances of combined techniques which apply to all VFSS samples. The results confirm to apply observation for feature selection and detection while using AR model for classification.

Table 15 Performances of combined techniques applied to all VFSS samples

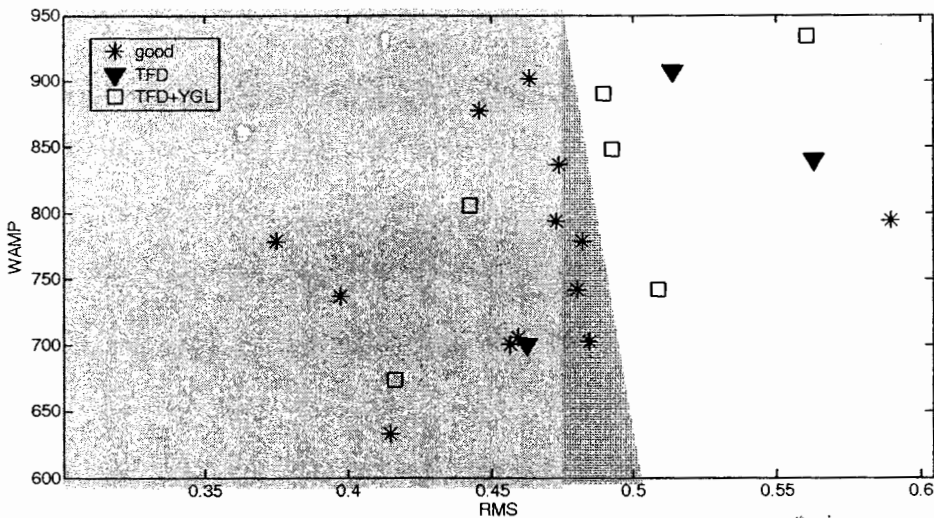
Technique	Performance (%)				Overall accuracy (%)
	Good	Accuracy	Defected	Accuracy	
I	80.00	50.91	43.75	75.00	59.05
II	80.00	50.91	43.75	75.00	59.04
III	33.33	100.00	100.00	62.50	68.42
IV&V	88.57	56.36	50.00	85.71	66.27
VI&VII	97.14	56.67	45.83	95.65	67.47
VIII&IX	63.16	63.16	70.83	70.83	67.44
X&XI	97.14	73.91	75.00	97.30	84.34
XII&XIII	80.00	62.22	64.58	81.58	71.08
XIV&XV	77.78	48.28	48.28	77.78	59.57

3.2.3 Case study 3: Classification by date

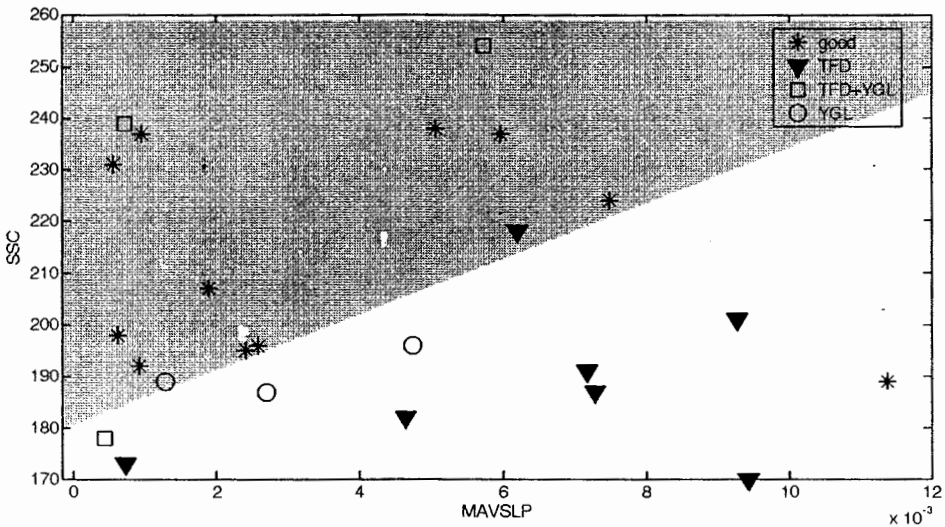
In this case study, a hundred mangosteens were prepared for experimenting three different days, called Day#1, Day#2 and Day#3. Fifteen techniques listed in Table 13 are applied. The detail results will be given as follows:

(a) Technique I

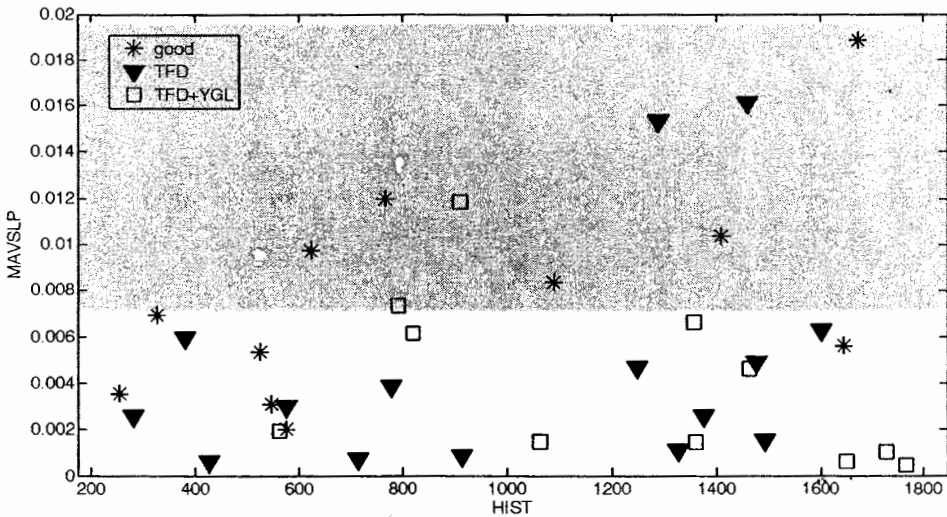
For each sample group, scatter plots of 36 feature pairs are observed. The optimum feature pair for each sample group was determined and the threshold values for detection will be selected by observation. Figure 45(a), (b) and (c) show the optimum feature pairs for samples of Day#1, Day#2 and Day#3, respectively. The optimum features for these three sample groups are RMS-WAMP, MAVSLP-SSC and HIST-MAVSLP, respectively. The threshold for Day#1 group is chosen by setting WAMP for 0-950 and RMS for 0.5. The threshold values for (MAVSLP, SSC) are (0-12, 180) for Day#2 group. Finally, the threshold for Day#3 group is set with MAVSLP and HIST for 0.007 and 200-1800.



(a)



(b)



(c)

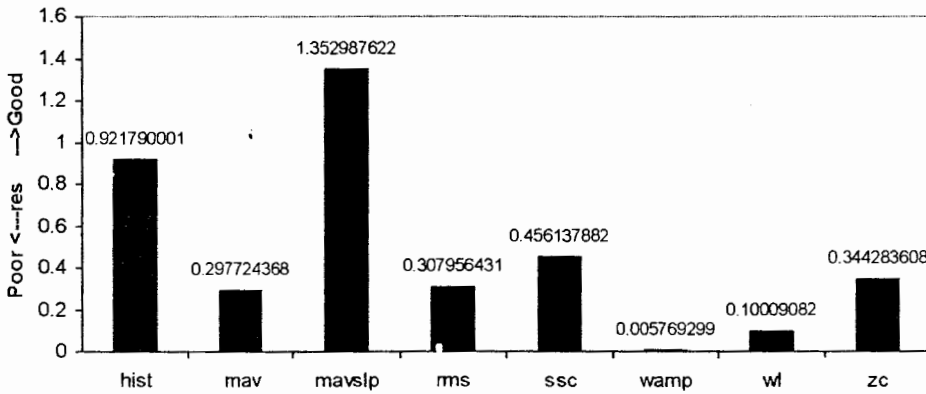
Figure 45 Optimum feature pairs based on (a) Day#1, (b) Day#2 and (c) Day#3

Table 16 Summary of performances obtained from Technique I

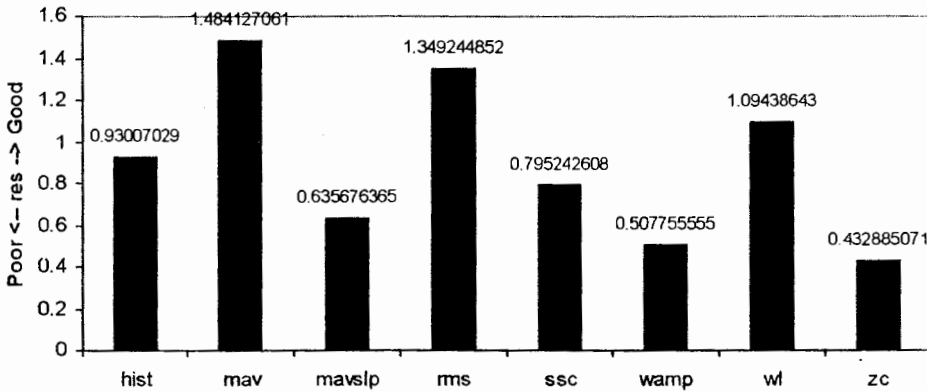
Sample	Performance (%)				Overall accuracy (%)
	Good	Accuracy	Defected	Accuracy	
Day#1	92.31	80.00	66.67	85.71	81.82
Day#2	90.91	71.43	69.23	90.00	79.17
Day#3	54.55	60.00	84.62	81.48	75.68

Table 16 summarizes the accuracy performances of technique I applied to three sample groups (Day#1, Day#2 and Day#3). The overall accuracy performances obtained from Day#1, Day#2 and Day#3 groups based on technique I are 81.82, 79.17 and 75.68%, respectively.

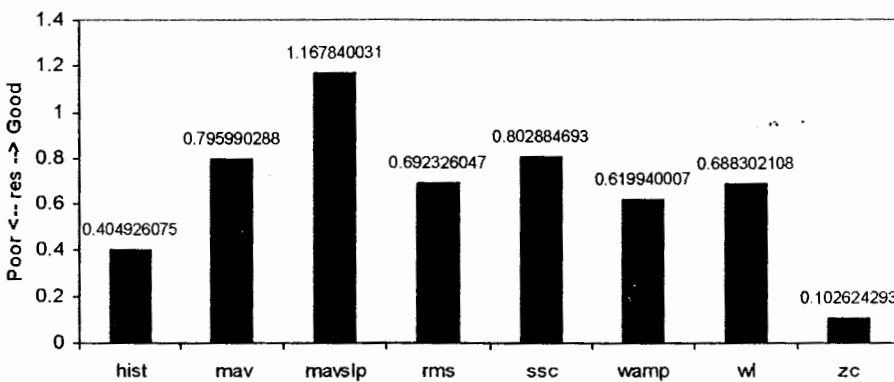
(b) Technique II



(a)



(b)

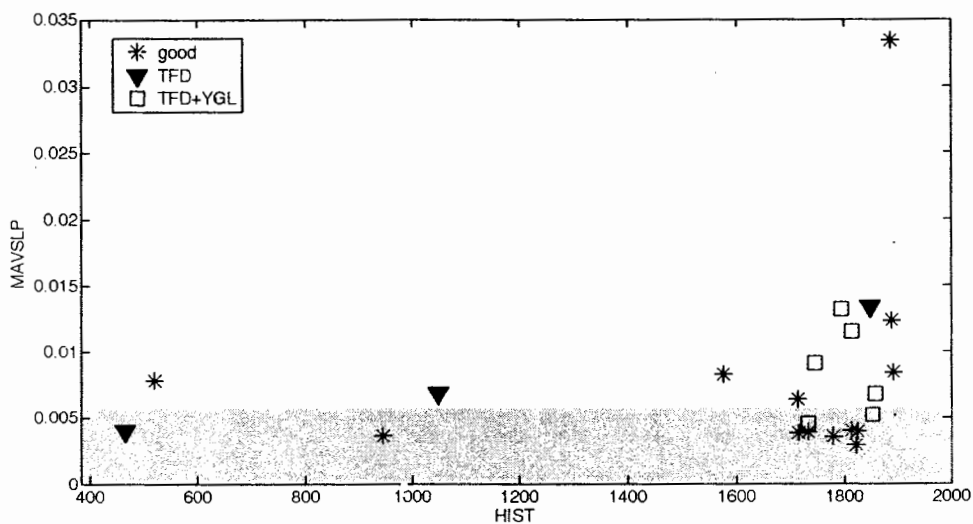


(c)

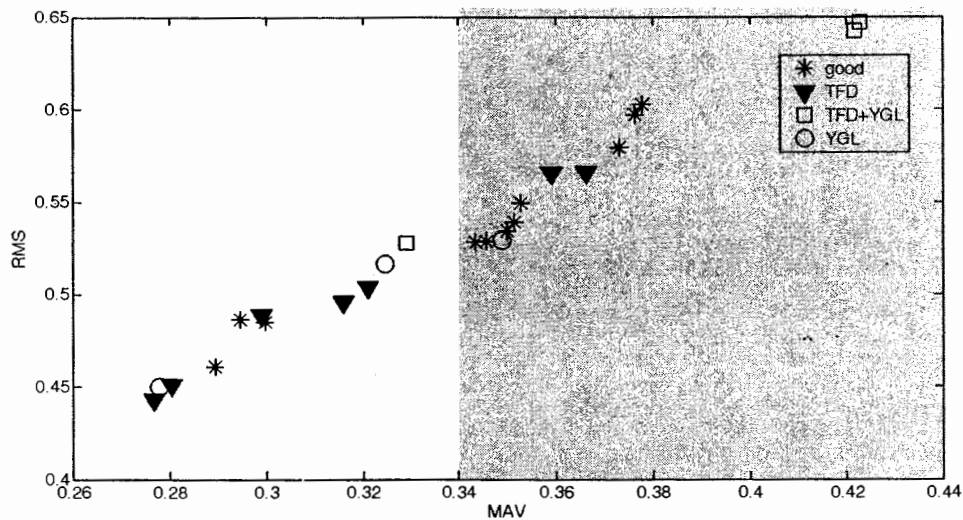
Figure 46 RES indexes of features based on (a) Day#1 (b) Day#2 and (c) Day#3

RES indexes of time-domain features computed from VFSS samples for Day#1, Day#2 and Day#3 are shown in Figure 46(a)-(c), respectively. Shown in Figure 46(a), MAVSLP and HIST provide RES indexes more than other six features. Hence MAVSLP and HIST are the optimum features for Day#1 sample. Figure 46(b) shows the RES index values of all features computed from Day#2 VFSS samples. It is shown that MAV and RMS are the optimum features for this case. For Day#3 sample,

MAVSLP and MAV provide highest *RES* index values among other features. Hence the optimum features for Day#3 sample are MAVSLP and MAV.



(a)



(b)

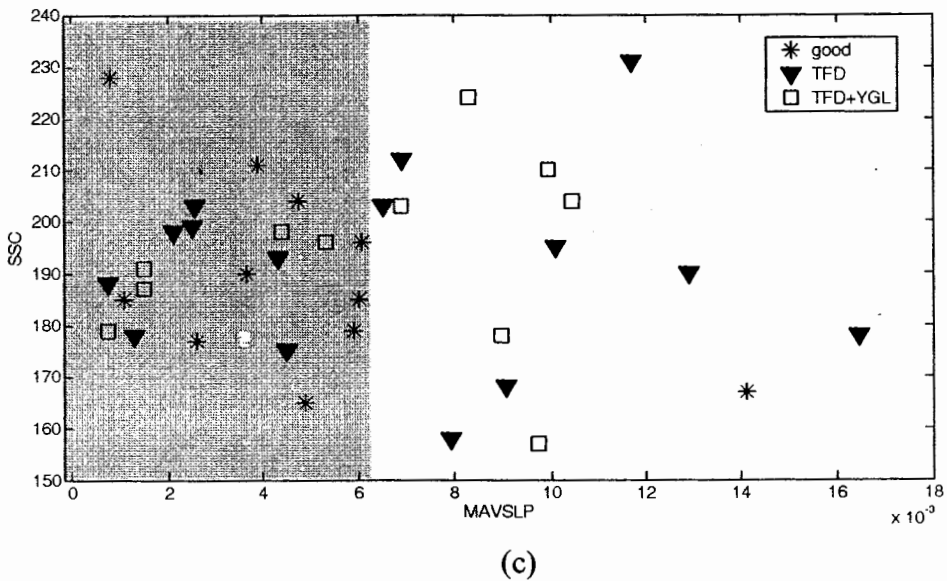


Figure 47 Optimum feature pairs based on (a) Day#1, (b) Day#2 and (c) Day#3

The plots of optimum feature pairs for Day#1, Day#2 and Day#3 samples are shown in Figure 47(a)-(c). In Figure 43(a), the threshold for MAVSLP is 0.006. For Figure 47(b) and 47(c), the threshold values for (MAV,RMS) and (MAVSLP,SSC) are (0.34,0.4-0.65) and (6.2,150-240) respectively.

Table 17 summarizes the accuracy performances of technique II applied to three sample groups (Day#1, Day#2 and Day#3). The overall accuracy performances obtained from Day#1, Day#2 and Day#3 groups based on technique II are 59.09, 66.67 and 64.86%, respectively.

Table 17 Summary of performances obtained from Technique II

Sample	Performance (%)				Overall accuracy (%)
	Good	Accuracy	Defected	Accuracy	
Day#1	53.85	70.00	66.67	50.00	59.09
Day#2	72.73	61.54	61.54	72.73	66.67
Day#3	90.91	45.45	53.85	93.33	64.86

(c) Technique III

Selected features obtained from technique II as shown in Figure 43(a)-(c) are applied to NN method. The overall accuracy performance obtained from Day#1 sample is 58.33%. For Day#2 sample, the overall accuracy performance is 42.86%. Finally, the total accuracy performance for Day#3 sample is 65.00% as shown in Table 18.

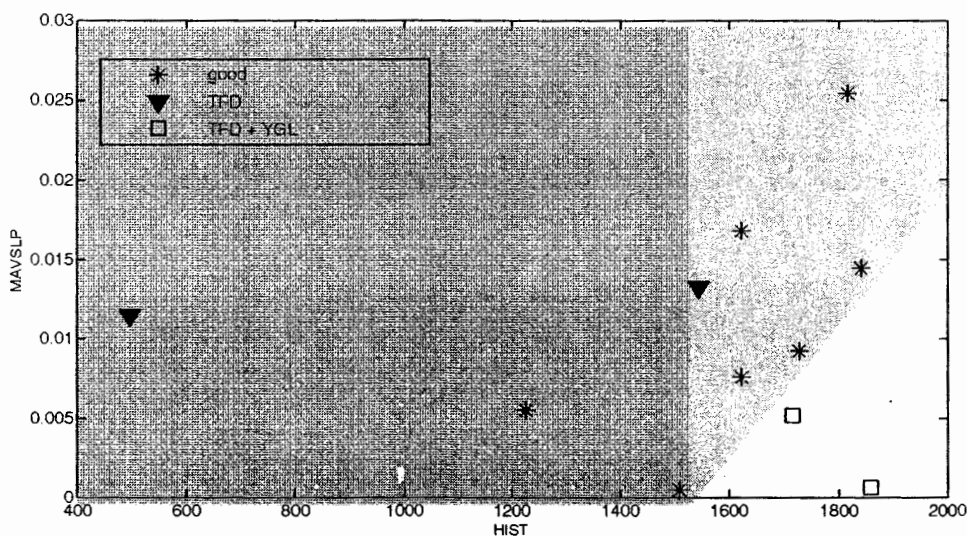
Table 18 Summary of performances obtained from Technique III

Sample	Performance (%)				Overall accuracy (%)
	Good	Accuracy	Defected	Accuracy	
Day#1	37.50	100.00	100.00	44.44	58.33
Day#2	14.29	33.33	71.43	45.45	41.86
Day#3	16.67	33.33	85.71	70.59	65.00

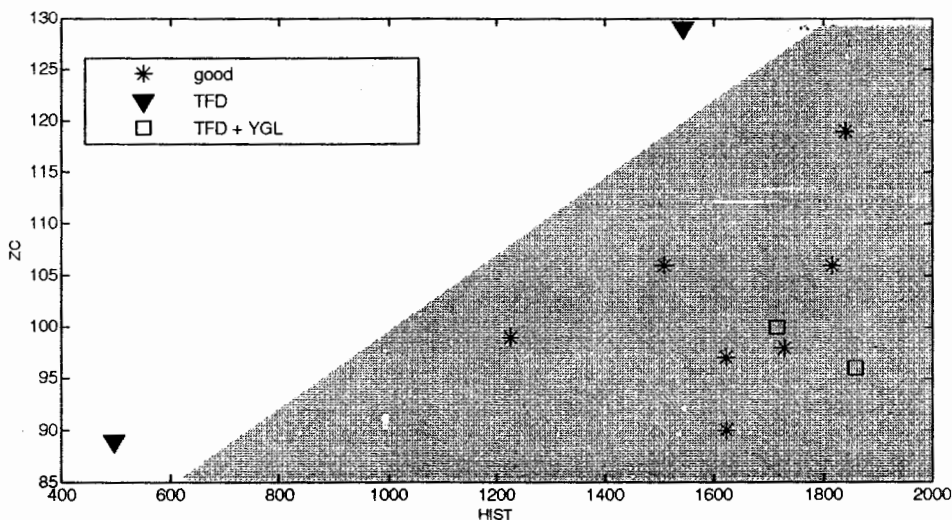
(d) Technique IV

In this section, the VFSS response samples which have f_R at 77 Hz are of interest. For Day#1 sample, HIST-MAVSLP and HIST-ZC are chosen for the optimum feature pairs. The HIST-MAVSLP plot is shown in Figure 48(a). The threshold values of HIST and MAVSLP are 1500 and 0-0.02, respectively. Figure 48(b) shows ZC-HIST plot and the threshold values for detecting a good/defected mangosteen are 85-130 and 600-1800, respectively.

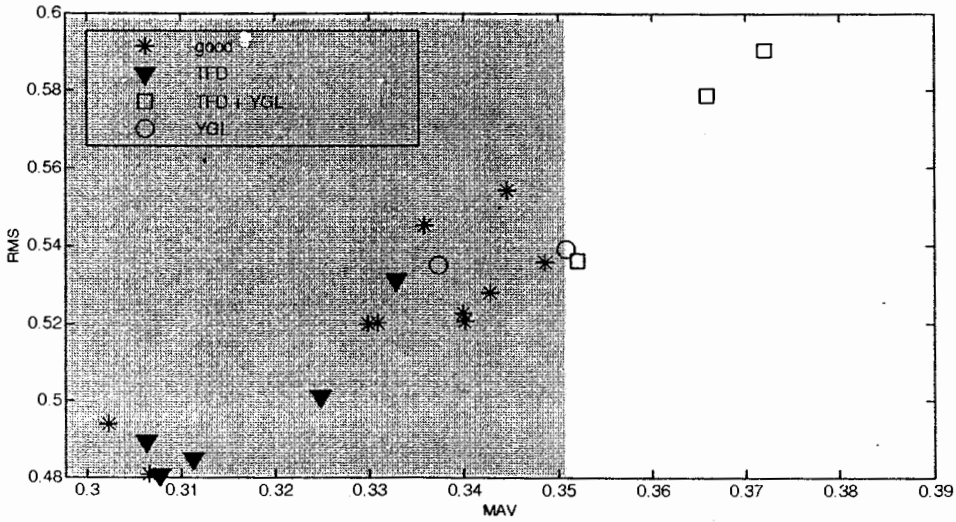
The mangosteen samples chosen for Day#2 sample are experimented as similar as the Day#1 sample. By observation, MAV-RMS and HIST-MAV are found to be the most optimum feature pairs for Day#2 sample. Figure 48(c)-(d) show MAV-RMS and HIST-MAV plots, respectively. The threshold values for RMS and MAV as shown in Figure 48(c) is 0.48-0.60 interval and 0.35, respectively. The threshold values for Figure 48(d) is chosen by setting MAV for 0.30-0.39 and HIST for 1300.



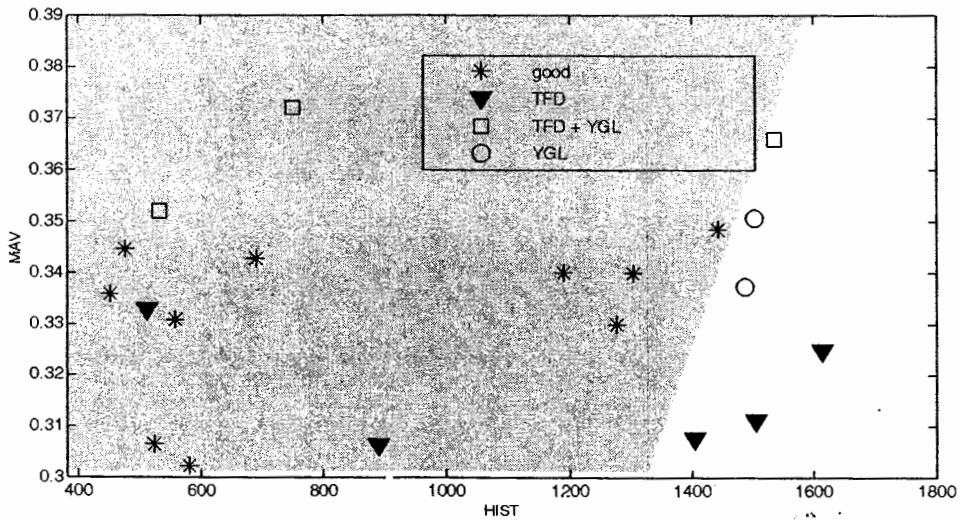
(a)



(b)



(c)



(d)

Figure 48 Optimum feature pairs based on (a)-(b) Day#1 and (c)-(d) Day#2 samples obtained from Technique III.

Table 19 Summary of performance obtained from Technique IV

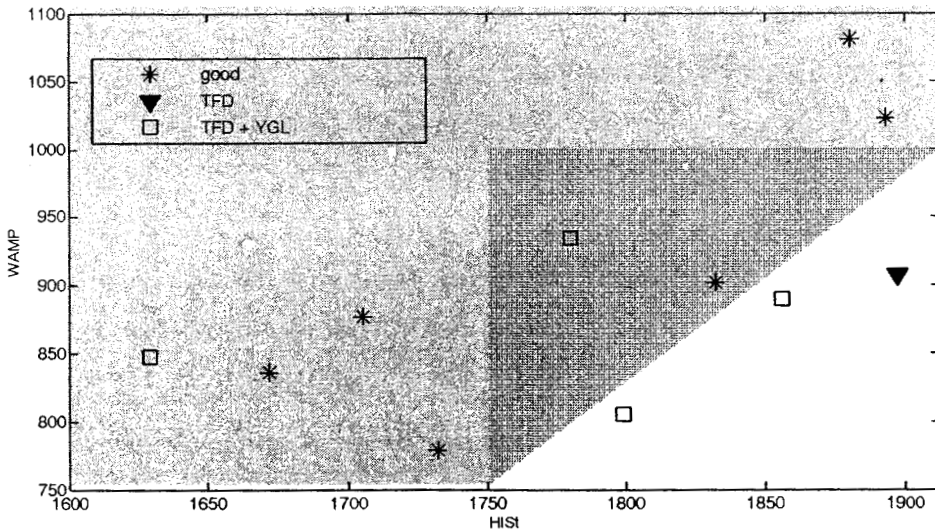
Sample	Performance (%)				Overall accuracy (%)
	Good	Accuracy	Defected	Accuracy	
Day#1	100.00	100.00	100.00	100.00	100.00
Day#2	90.00	81.82	80.00	88.89	85.00
Day#3	0.00	0.00	100.00	100.00	100.00

Table 19 summarizes the accuracy performances of technique IV applied to three sample groups (Day#1, Day#2 and Day#3). The overall accuracy performances obtained from Day#1, Day#2 and Day#3 samples based on technique III are 100.00, 85.00 and 100.00%, respectively.

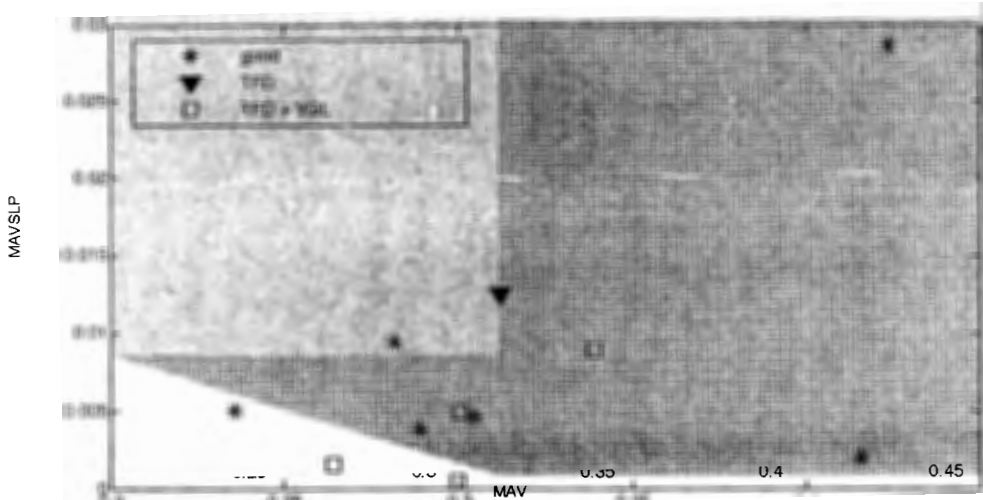
(e) Technique V

In this section, the VFSS response samples which have f_R at 187 Hz are of interest. For Day#1 group, HIST-WAMP and MAV-MAVSLP are chosen for the optimum feature pairs. The HIST-WAMP plot is shown in Figure 49(a). The threshold values of HIST and WAMP are 1750 and 750-1000, respectively. Figure 49(b) shows MAV-MAVSLP plot and the threshold values for detecting a good/defected mangosteen are 0.005 and 0.3, respectively.

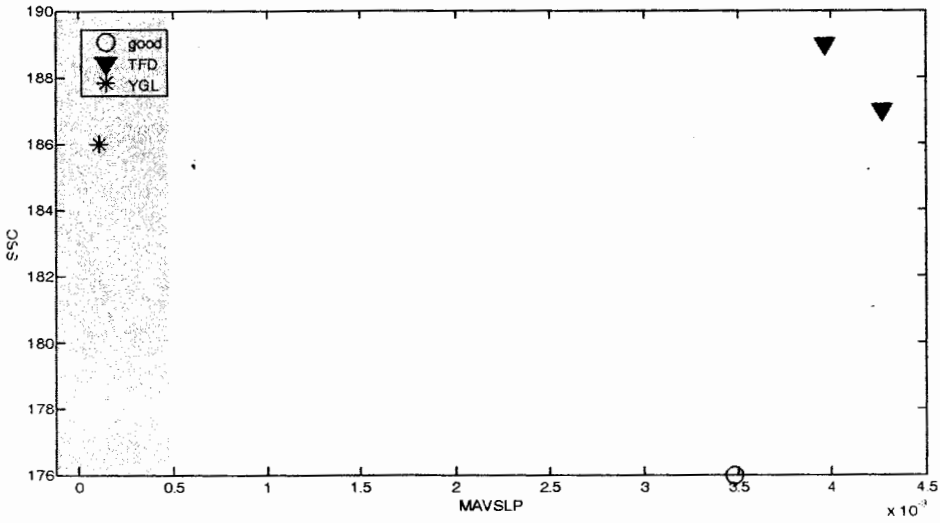
The mangosteen samples chosen for Day#2 sample are experimented as similar as the Day#1 sample. By observation, MAVSLP-SSC is found to be the most optimum feature pair for Day#2 group. Figure 49(c) shows MAVSLP-SSC plot. The threshold values for MAVSLP and SSC as shown in Figure 49(c) are 0.5 and 176-190, respectively. For Day#3 group, MAVSLP and WAMP are the best features among other time-domain features. Figure 49(d) shows the MAVSLP-MAV plot. The threshold values for MAVSLP and MAV are 0.007 and 0-0.34, respectively.



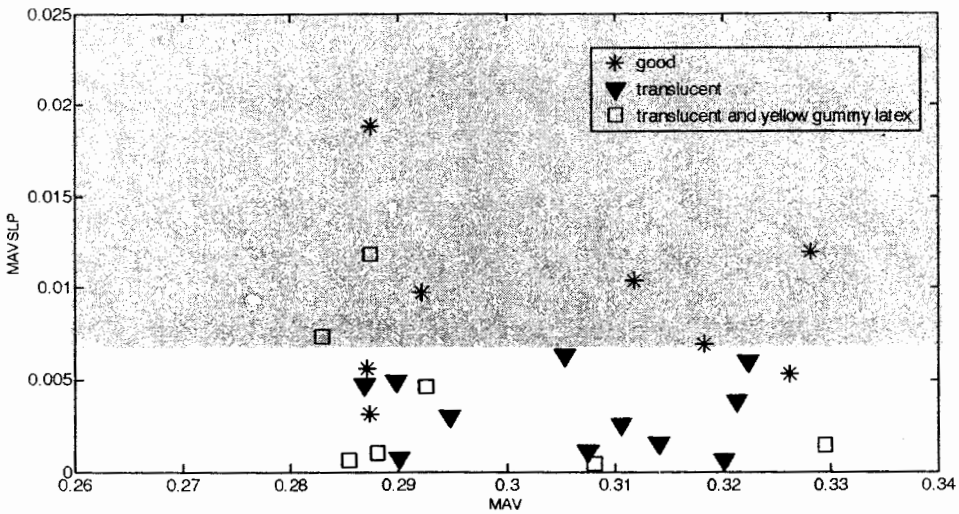
(a)



(b)



(c)

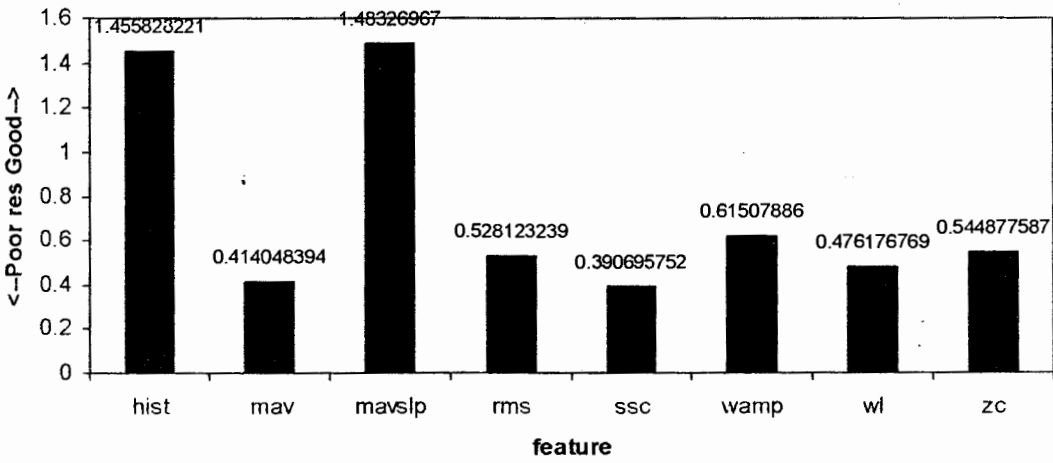


(d)

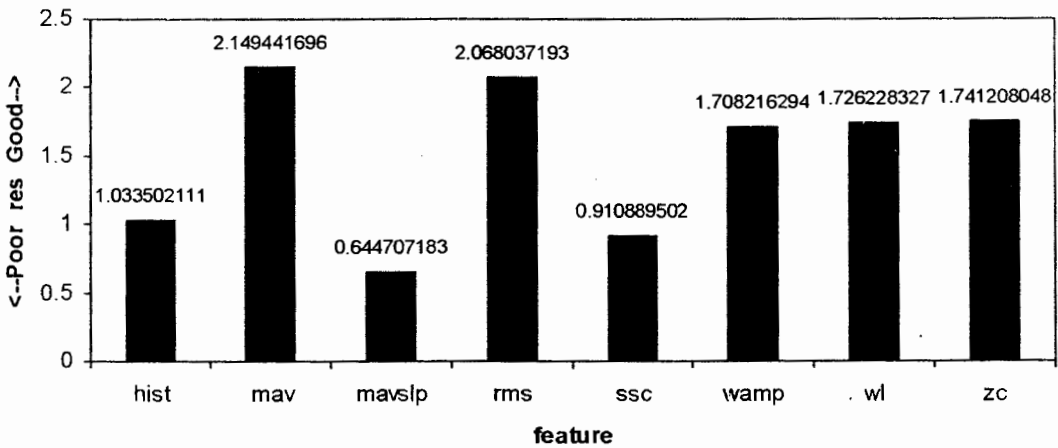
Figure 49 Optimum feature pairs based on (a)-(b) Day#1, and (c) Day#2 and (d) Day#3 samples obtained from technique V

(f) Technique VI

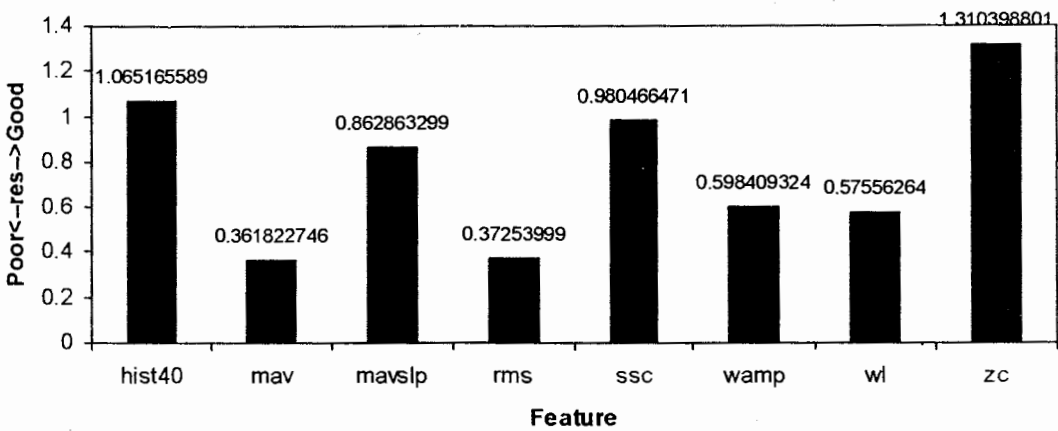
In this section, the VFSS response samples which have f_R at 77 Hz are of interest. RES indexes of eight time-domain features computed from the VFSS samples for Day#1, Day#2 and Day#3 are shown in Figure 50(a)-(c), respectively. For Day#1 group, the RES index values of MAVSLP and HIST features shown in Figure 50(a) are higher than other features. Figure 50(b) shows the RES index values obtained from the time-domain features performing on Day#2 group. It is shown in Figure 50(b) that the RES index values of MAV and RMS are highest among other features. Figure 50(c) shows the RES index values obtained for Day#3 group. It is shown that the RES index values of ZC and HIST features are higher than other features.



(a)



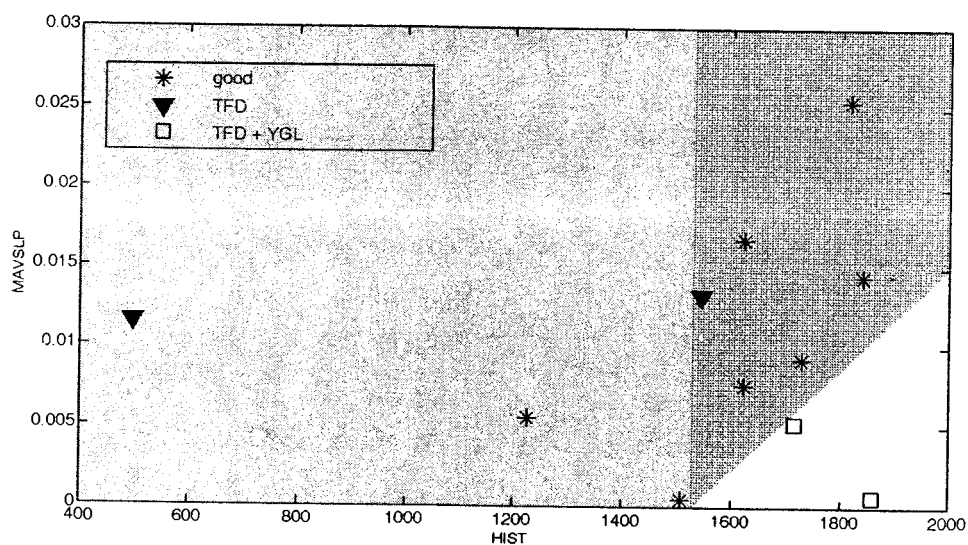
(b)



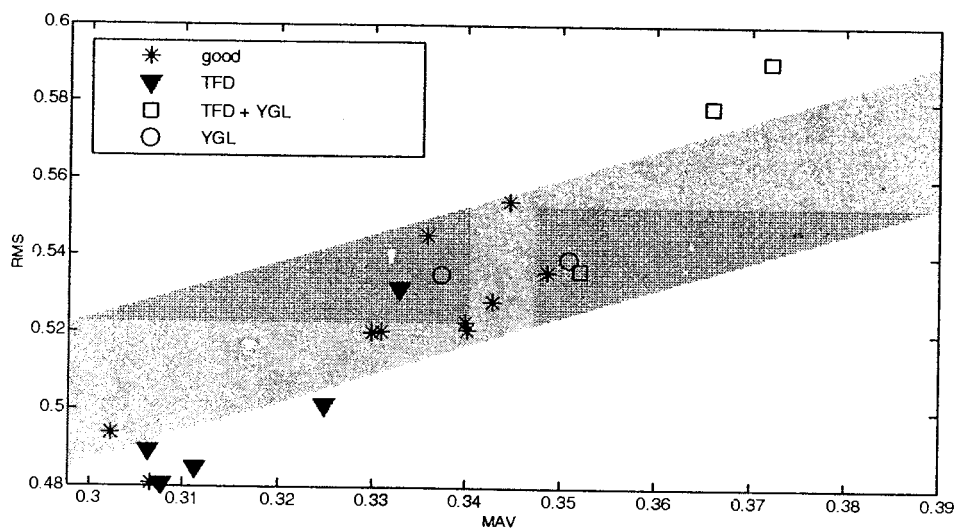
(c)

Figure 50 RES indexes of features based on (a) Day#1 (b) Day#2 and (c) Day#3 obtained from Technique VI

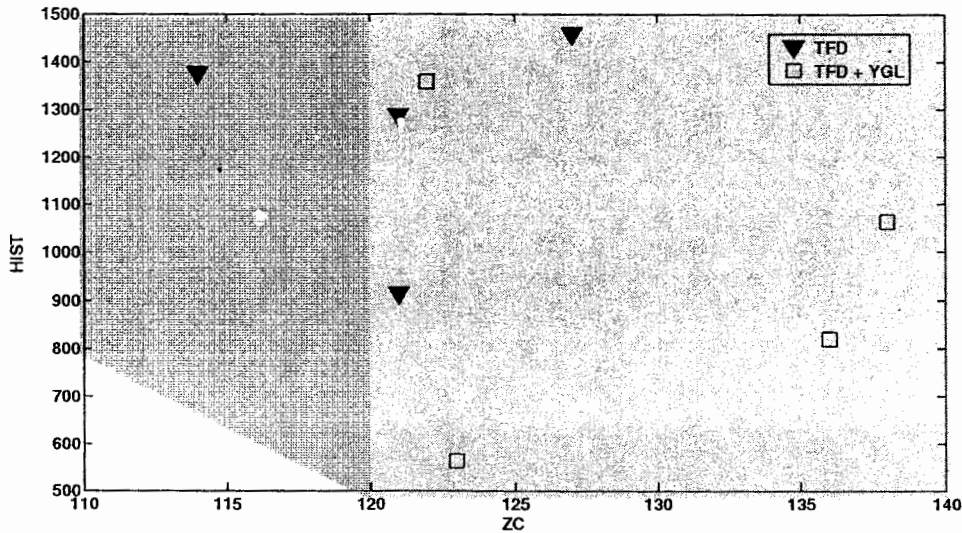
Figure 51(a) shows the plot of HIST-MAVSLP feature pair computed from VFSS samples on Day#1 group. The thresholds for MAVSLP and HIST are 0 - 0.015 and 1500, respectively. For Day#2 group which is shown in Figure 51(b), the MAV-RMS plot suggests to select the thresholds for MAV and RMS at 0.3-0.39 and 0.48-0.52, respectively. For Day#3 group, the thresholds for ZC and HIST are 120 and 800 as shown in Figure 51(c).



(a)



(b)



(c)

Figure 51 Optimum feature pairs based on (a) Day#1, (b) Day#2 and (c) Day#3 samples obtained from Technique VI

Table 20 shows the accuracy performances obtained by applying technique VI. The accuracy performances for Day#1, Day#2 and Day#3 groups are 81.82, 75.00 and 100.00%, respectively.

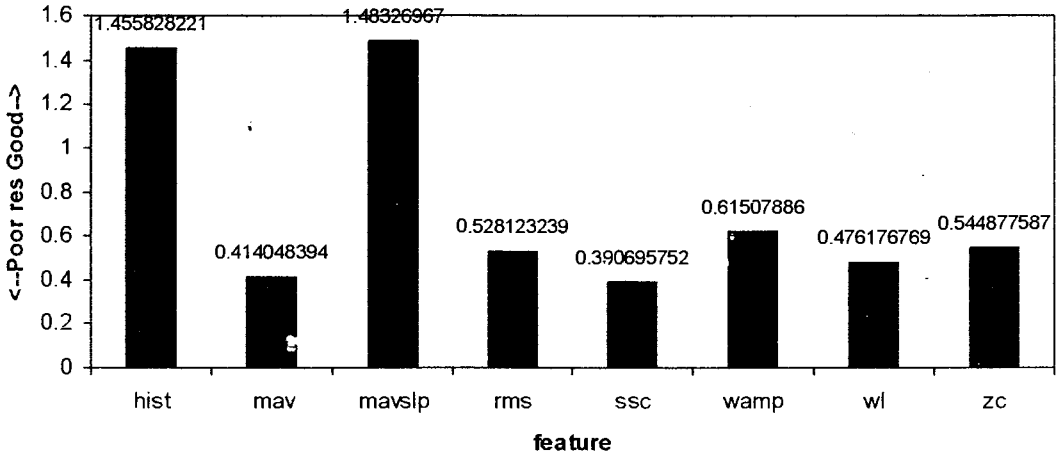
Table 20 Summary of performances Day#1-Day#3) using technique VI

Sample	Performance (%)				Overall accuracy (%)
	Good	Accuracy	Defected	Accuracy	
Day#1	100.00	77.78	100.00	100.00	81.82
Day#2	90.00	69.23	60.00	85.71	75.00
Day#3	0.00	0.00	100.00	100.00	100.00

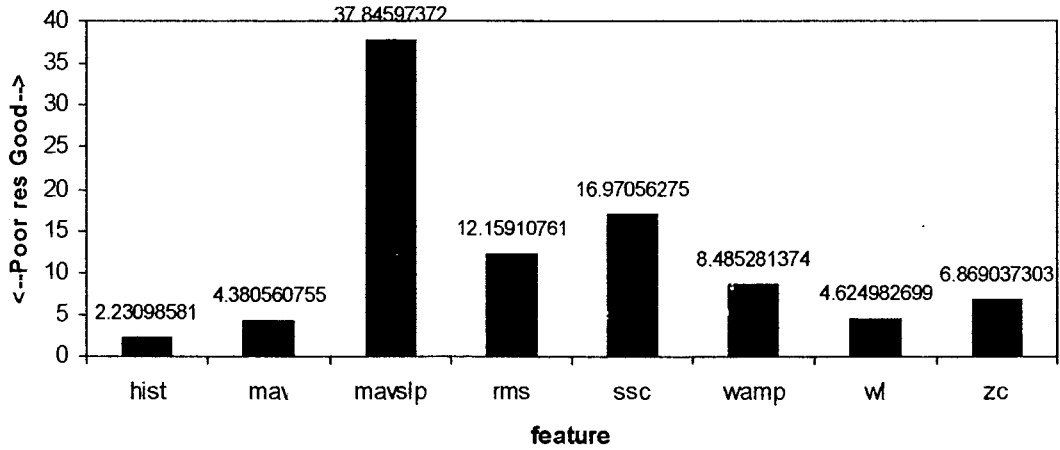
(g) Technique VII

In this section, the VFSS response samples which have f_R at 187 Hz are of interest. RES indexes of eight time-domain features computed from the VFSS samples for Day#1, Day#2 and Day#3 are shown in Figure 52(a)-(c), respectively. For Day#1 group, the RES index values of MAVSLP and HIST features shown in Figure 52(a) are higher than other features. Figure 52(b) shows the RES index values obtained from the time-domain features performing on Day#2 group. It is shown in Figure 52(b) that the RES index values of MAVSLP and SSC are highest among other features. Figure 52(c) shows the RES index values obtained for Day#3 group. It is shown that the RES index values of MAVSLP and WAMP features are higher than other features.

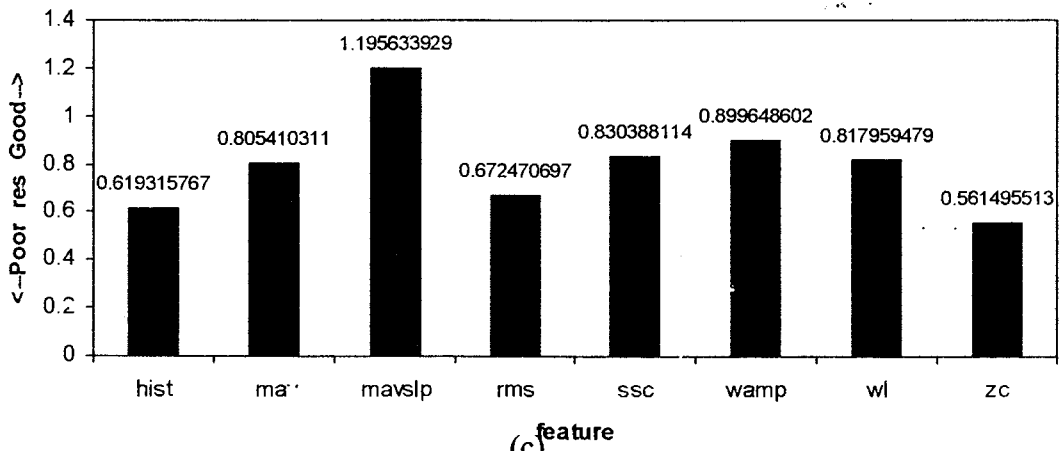
Figure 53(a) shows the plot of HIST-MAVSLP feature pair computed from VFSS samples on Day#1 group. The thresholds for MAVSLP and HIST are 0.0275 and 1700, respectively. For Day#2 group which is shown in Figure 53(b), the MAVSLP-SSC plot suggests to select the thresholds for MAVSLP and SSC at 0.50 and 176-190, respectively. For Day#3 group, the thresholds for MAVSLP and WAMP are 0-0.35 and 875 as shown in Figure 53(c).



(a)

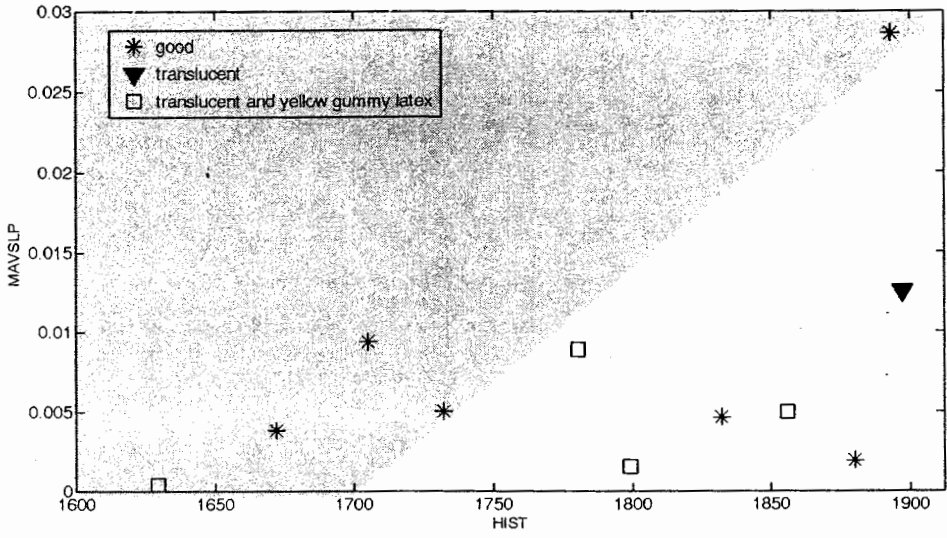


(b)

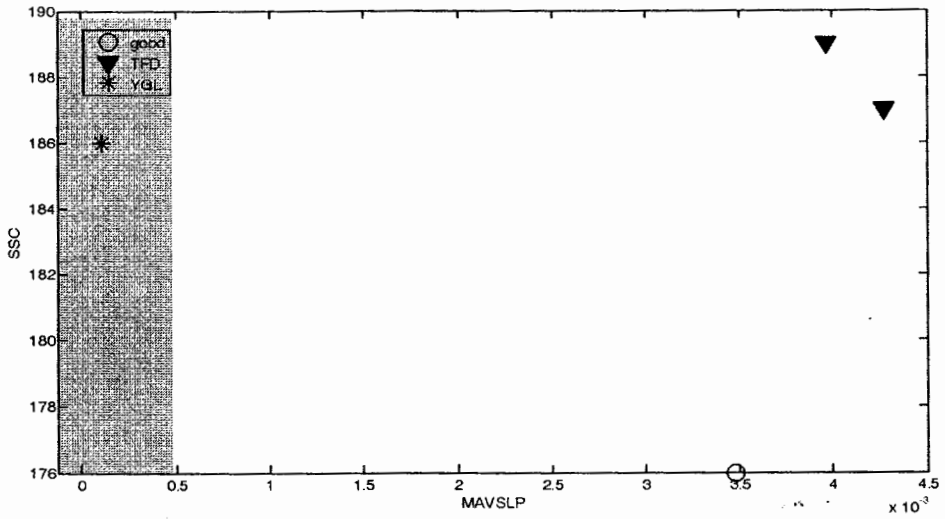


(c)

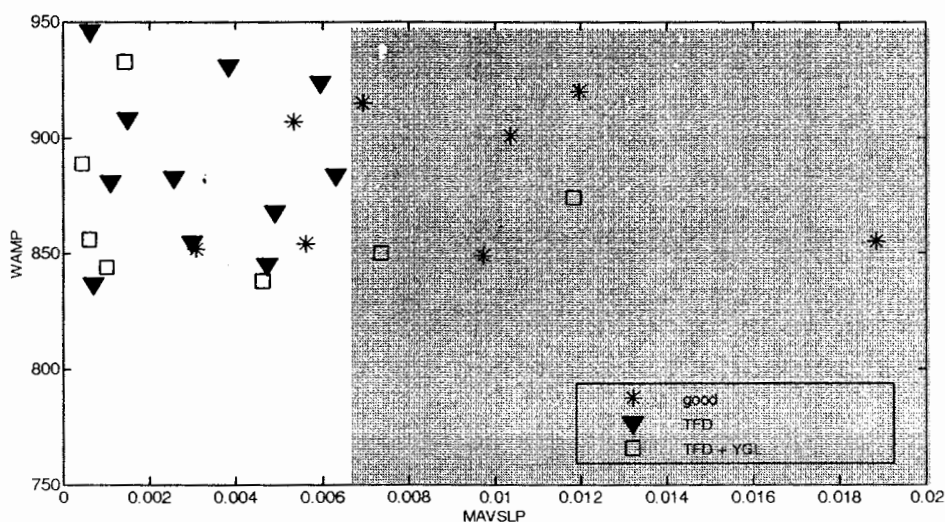
Figure 52 RES indexes of features based on (a) Day#1 (b) Day#2 and (c) Day#3 obtained from Technique VII



(a)



(b)



(c)

Figure 53 Optimum feature pairs based on (a) Day#1, (b) Day#2 and (c) Day#3 samples obtained from technique VII

Table 21 shows the accuracy performances obtained by applying technique VII. The accuracy performances for Day#1, Day#2 and Day#3 groups are 72.73, 100.00 and 82.76%, respectively.

Table 21 Summary of performances (Day#1-Day#3) using technique VII

Sample	Performance (%)				Overall accuracy (%)
	Good	Accuracy	Defected	Accuracy	
Day#1	66.67	80.00	80.00	66.67	72.73
Day#2	100.00	100.00	100.00	100.00	100.00
Day#3	72.73	80.00	57.14	84.21	82.76

(h) Technique VIII

From the features shown in Figure 48, a single-hidden layer NN is applied to determine the thresholds for good/defected sample detection. The overall accuracy performance obtained for Day#1, Day#2 and Day#3 groups as shown in Table 22 are 66.67, 55.56 and 100.00%, respectively.

Table 22 Summary of performances (Day#1-Day#3) using Technique VIII

Sample	Performance (%)				Overall accuracy (%)
	Good	Accuracy	Defected	Accuracy	
Day#1	50.00	50.00	100.00	50.00	66.67
Day#2	20.00	50.00	83.33	55.56	55.56
Day#3	100.00	100.00	100.00	100.00	100.00

(i) Technique IX

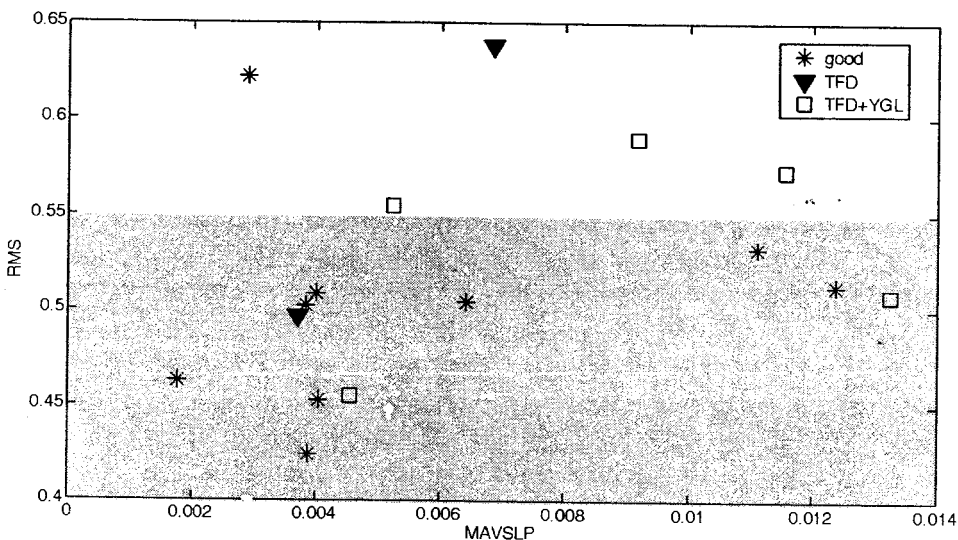
From the features shown in Figure 50, a single-hidden layer NN is applied to determine the thresholds for detecting a good/defected sample. The overall accuracy performance obtained for Day#1, Day#2 and Day#3 groups as shown in Table 23 are 100.00, 100.00 and 50.00%, respectively.

Table 23 Summary of performances ([187Hz], Day#1-Day#3) using Technique IX

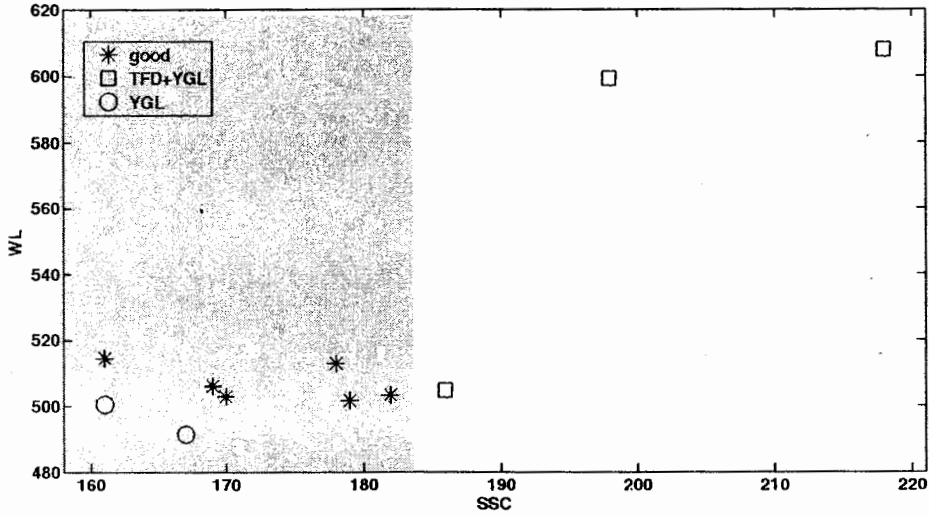
Sample	Performance (%)				Overall accuracy (%)
	Good	Accuracy	Defected	Accuracy	
Day#1	100.00	100.00	100.00	100.00	100.00
Day#2	100.00	100.00	100.00	100.00	100.00
Day#3	33.33	33.33	60.00	60.00	50.00

(j) Technique X

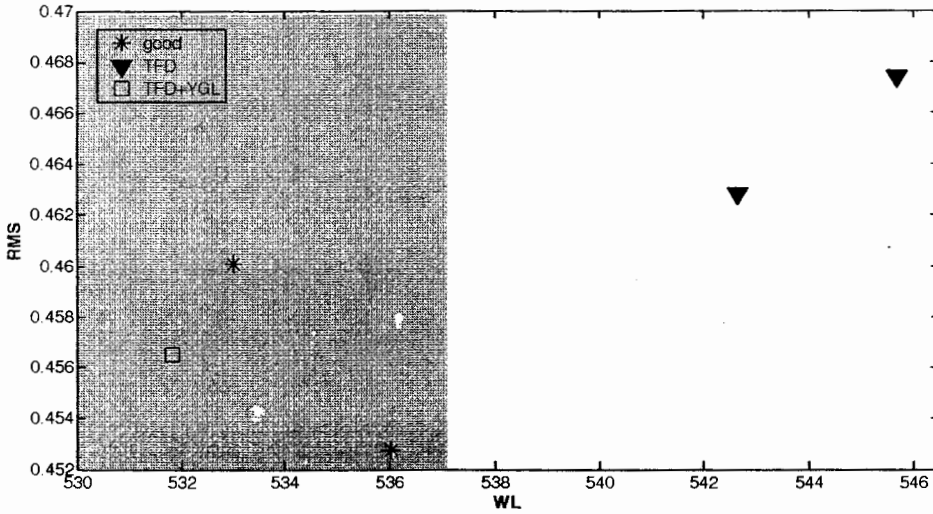
In this section, the VFSS response samples which have $-a_4$ are of interest. The technique is based on observation for choosing features and thresholds for detection. For Day#1 sample, MAVSLP-RMS pair is chosen for the optimum features. The RMS-MAVSLP plot is shown in Figure 54(a). The threshold values of RMS and MAVSLP are 0.55 and 0-0.014, respectively. Figure 54(b) shows SSC-WL plot. These two features are the optimum features for Day#2 group. The threshold values for detecting a good/defected mangosteen are 185 and 480-620, respectively. The mangosteen samples chosen for Day#3 sample are experimented as similar as the Day#1 and Day#2 groups. By observation, WL and RMS features are found to be the most optimum features. Figure 54(c) shows WL-RMS and plot. The threshold is set by choosing RMS and WL for 537 and 0.452-0.47, respectively.



(a)



(b)



(c)

Figure 54 Optimum feature pairs based on (a) Day#1, (b) Day#2 and (c) Day#3 groups obtained from technique X

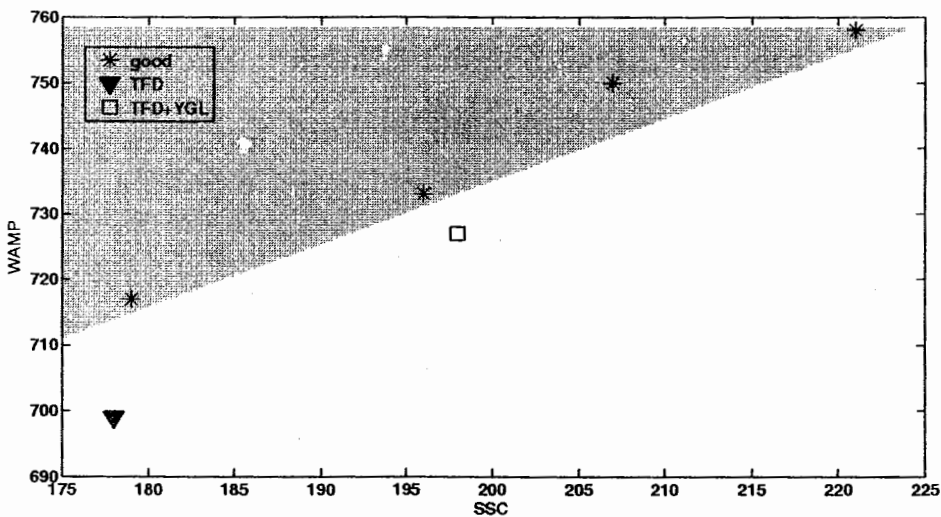
Table 24 shows the accuracy performances obtained by applying technique X. The accuracy performances for Day#1, Day#2 and Day#3 groups are 75.00, 81.82 and 80.00%, respectively.

Table 24 Summary of performances (Day#1-Day#3) using technique X

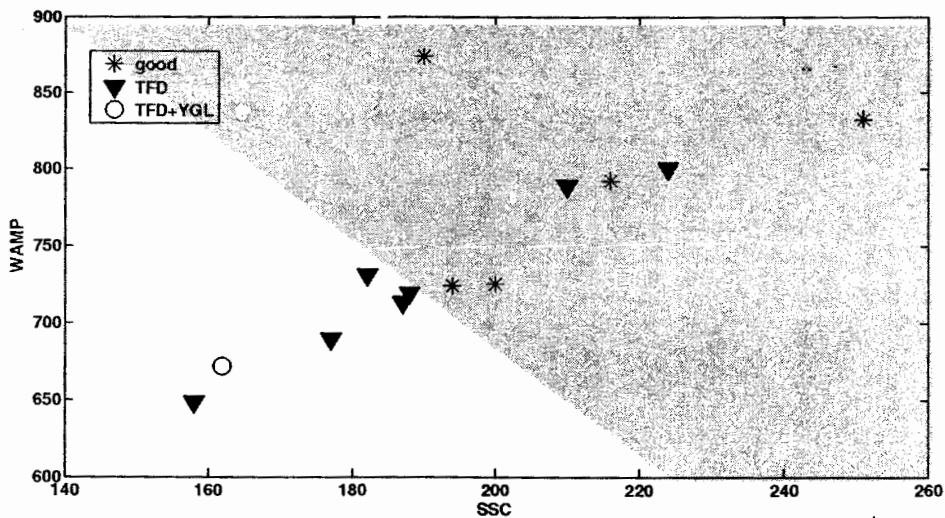
Sample	Performance (%)				Overall accuracy (%)
	Good	Accuracy	Defected	Accuracy	
Day#1	88.89	72.73	57.14	80.00	75.00
Day#2	100.00	75.00	60.00	100.00	81.82
Day#3	100.00	66.67	66.67	100.00	80.00

(k) Technique XI

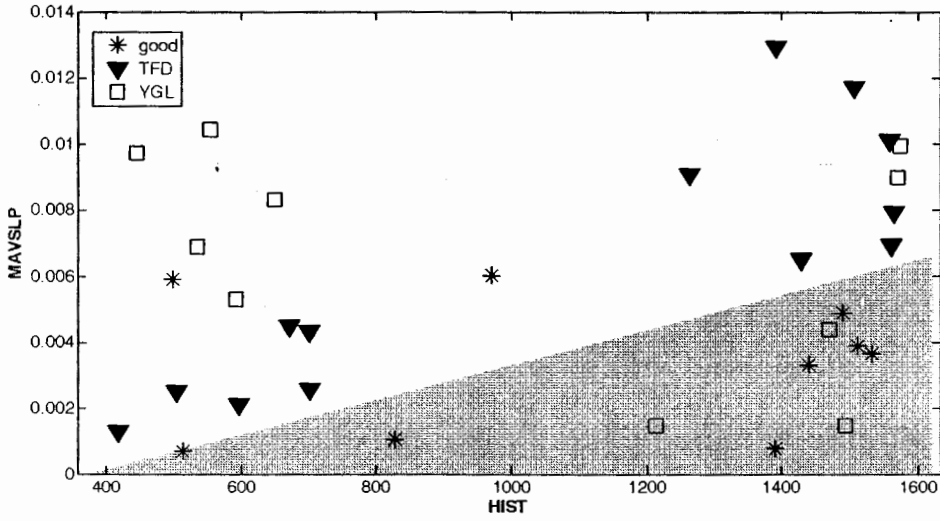
In this section, the VFSS response samples which have $+a_4$ are of interest. The technique is based on observation for choosing features and thresholds for detection. For Day#1 group, SSC-WAMP pair is chosen for the optimum features. The SSC-WAMP plot is shown in Figure 55(a). The threshold values of SSC and WAMP are 175-225 and 710, respectively. Figure 55(b) shows SSC-WAMP plot. These two features are the optimum features for Day#2 group. The threshold values for detecting a good/defected mangosteen, (SSC, WAMP), are (222, 900). The mangosteen samples chosen for Day#3 group are experimented as similar as the Day#1 and Day#2 groups. By observation, HIST and MAVSLP features are found to be the most optimum features. Figure 55(c) shows HIST-MAVSLP plot. The threshold is set by choosing HIST and MAVSLP for 0-1600 and 0.006, respectively.



(a)



(b)



(c)

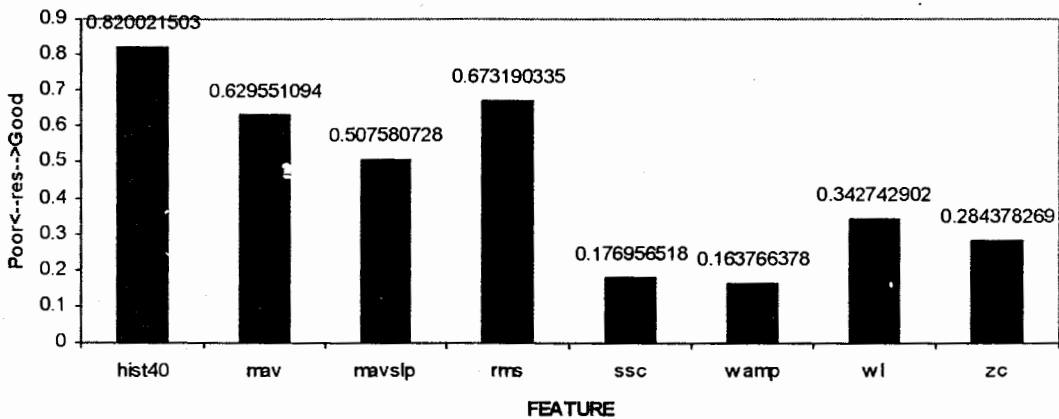
Figure 55 Optimum feature pairs based on (a) Day#1, (b) Day#2 and (c) Day#3 obtained from technique XI

Table 25 shows the accuracy performances obtained by applying technique XI. The accuracy performances for Day#1, Day#2 and Day#3 groups are 100.00, 84.62 and 81.82%, respectively.

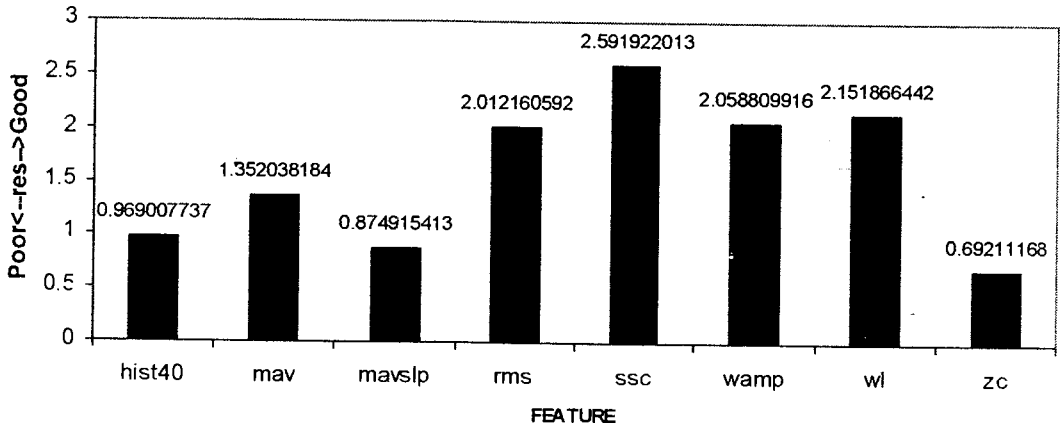
Table 25 Summary of performances (Day#1-Day#3) using technique XI

Sample	Performance (%)				Overall accuracy (%)
	Good	Accuracy	Defected	Accuracy	
Day#1	100.00	100.00	100.00	100.00	100.00
Day#2	100.00	71.43	75.00	100.00	84.62
Day#3	77.78	70.00	86.96	90.91	84.38

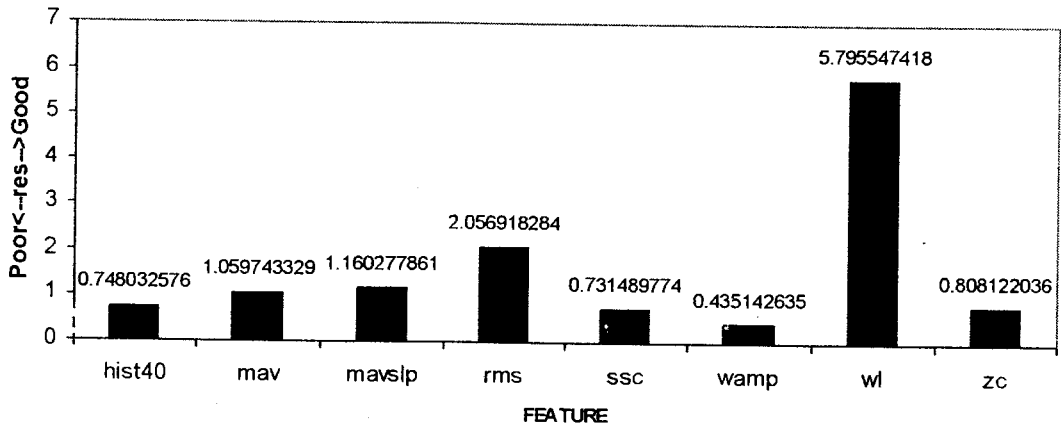
(l) Technique XII



(a)



(b)

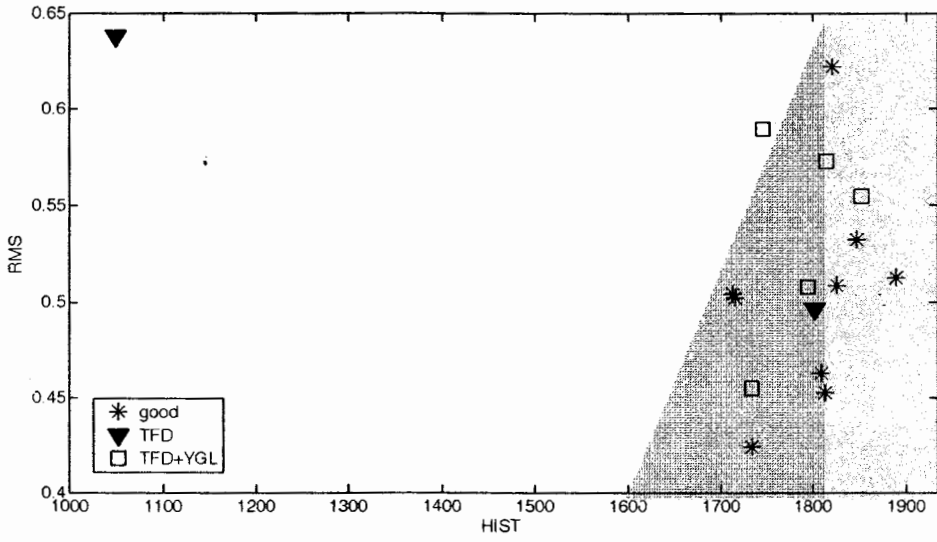


(c)

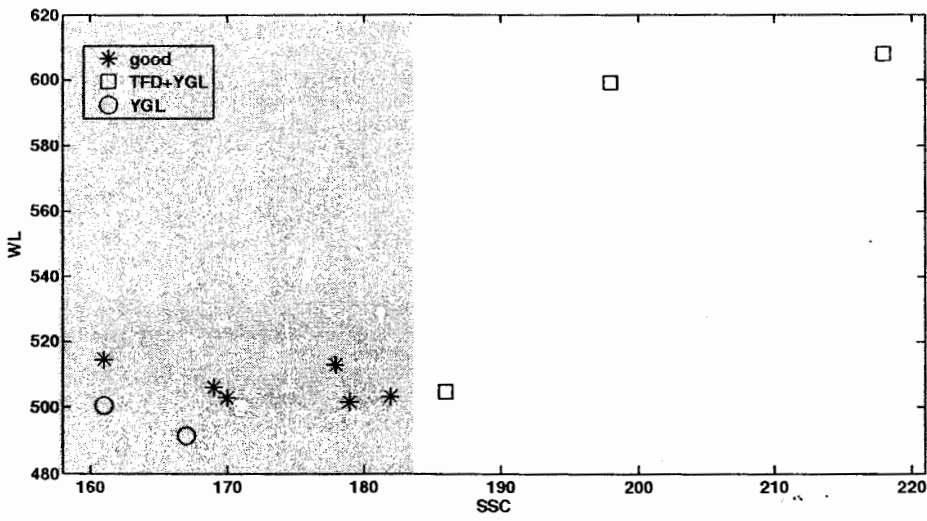
Figure 56 RES indexes of features based on (a) Day#1 (b) Day#2 and (c) Day#3 obtained from technique XII

In this section, the VFSS response samples which have $-a_4$ are of interest. RES indexes of eight time-domain features computed from the VFSS samples for Day#1, Day#2 and Day#3 are shown in Figure 56(a)-(c), respectively. For Day#1 group, the RES index values of HIST and RMS features shown in Figure 56(a) are higher than other features. Figure 56(b) shows the RES index values obtained from the time-domain features performing on Day#2 group. It is shown in Figure 56(b) that the RES index values of SSC and WL are highest among other features. Figure 56(c) shows the RES index values obtained for Day#3 group. It is shown that the RES index values of WL and RMS features are higher than other features.

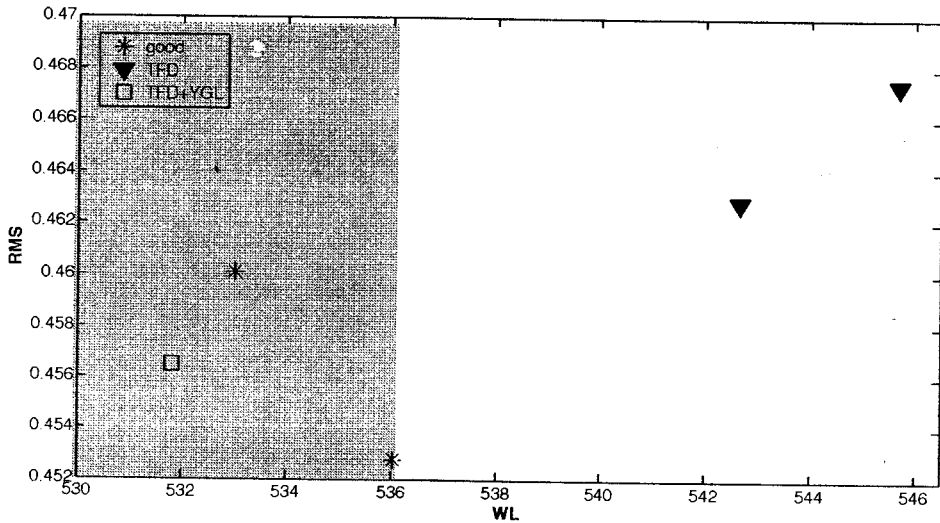
Figure 57(a) shows the plot of HIST-RMS feature pair computed from VFSS samples on Day#1 group. The thresholds for HIST and RMS are 1600 and 0.40-0.65, respectively. For Day#2 group which is shown in Figure 57(b), the SSC-WL plot suggests to select the thresholds for SSC and WL at 185 and 420-620, respectively. For Day#3 group, the thresholds for WL and RMS are 536 and 0.452-0.47 as shown in Figure 57 (c).



(a)



(b)



(c)

Figure 57 Optimum feature pairs based on (a) Day#1, (b) Day#2 and (c) Day#3 group obtained from technique XII

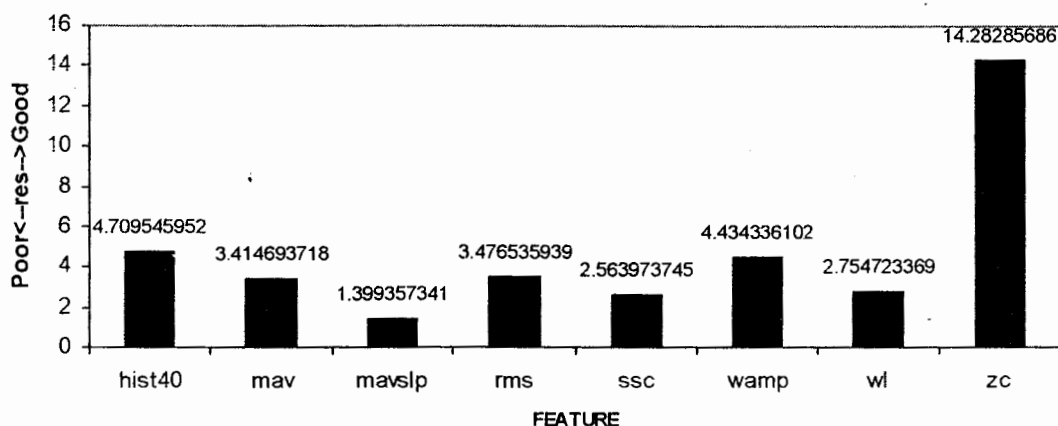
Table 26 Summary of performances (Day#1-Day#3) using technique XII

Sample	Performance (%)				Overall accuracy (%)
	Good	Accuracy	Defected	Accuracy	
Day#1	100.00	81.82	71.43	100.00	87.50
Day#2	100.00	75.00	60.00	100.00	81.82
Day#3	100.00	66.67	66.67	100.00	80.00

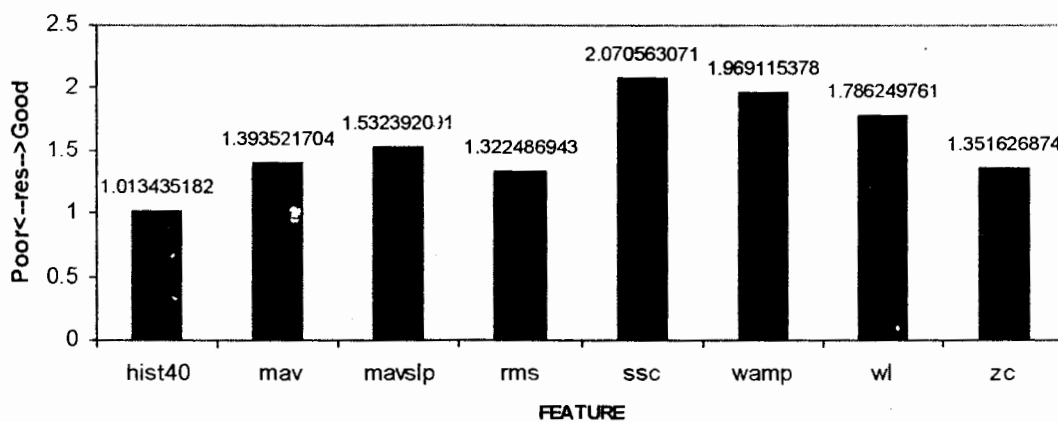
Table 26 shows the accuracy performances obtained by applying technique XII. The accuracy performances for Day#1, Day#2 and Day#3 groups are 87.50, 100.00 and 80.00%, respectively.

(m) Technique XIII

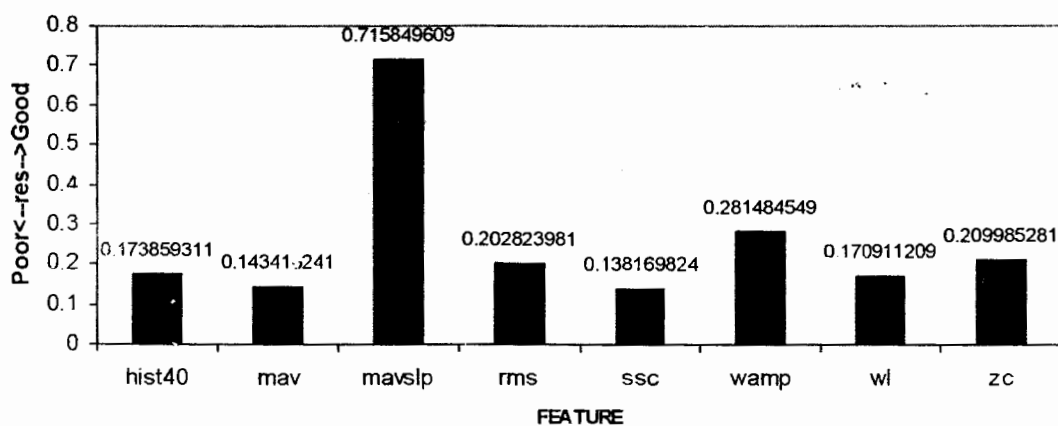
In this section, the VFSS response samples which have $+a_4$ are of interest. RES indexes of eight time-domain features computed from the VFSS samples for Day#1, Day#2 and Day#3 groups are shown in Figure 58(a)-(c), respectively. For Day#1 group, the RES index values of ZC and HIST features shown in Figure 58(a) are higher than other features. Figure 57(b) shows the RES index values obtained from the time-domain features performing on Day#2 group. It is shown in Figure 58(b) that the RES index values of SSC and WAMP are highest among other features. Figure 58(c) shows the RES index values obtained for Day#3 group. It is shown that the RES index values of MAVSLP and WAMP features are higher than other features.



(a)



(b)

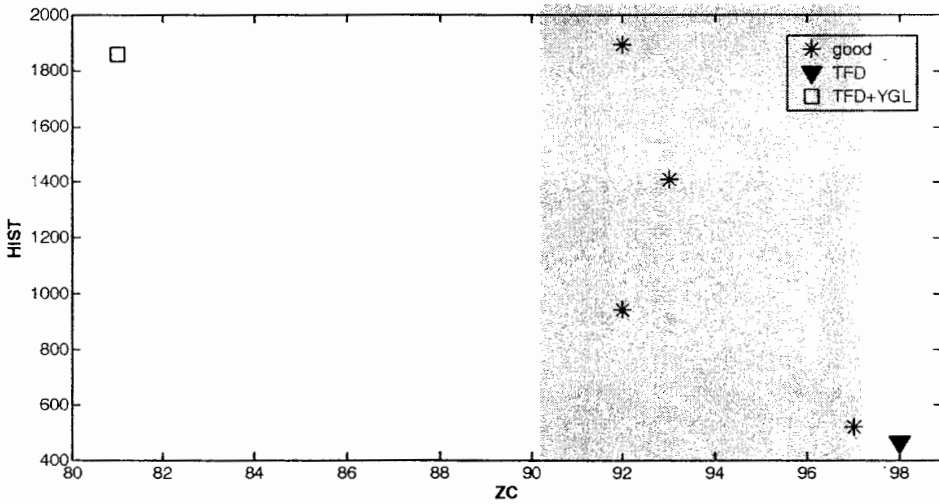


(c)

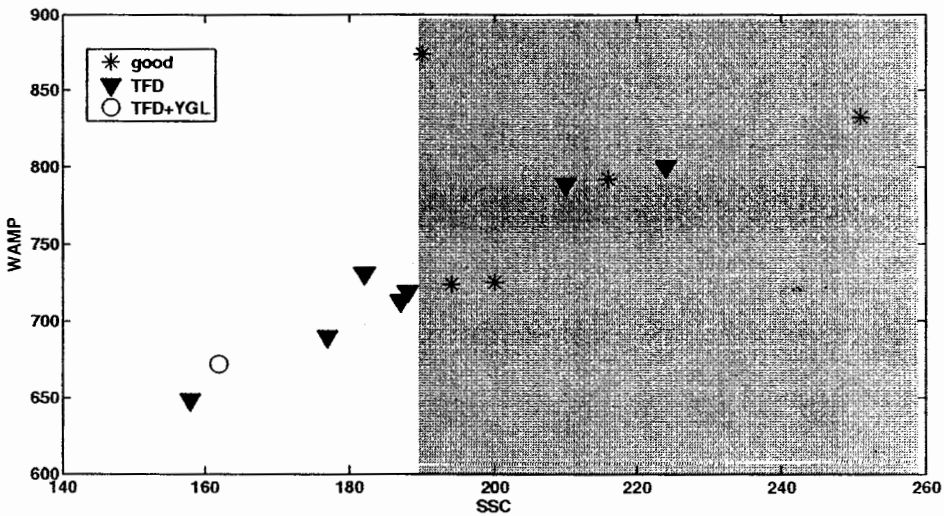
Figure 58 RES indexes of features based on (a) Day#1 (b) Day#2 and (c) Day#3 obtained from technique XIII

Figure 59(a) shows the plot of ZC-HIST feature pair computed from VFSS samples on Day#1 group. The thresholds for ZC and HIST are 90-97 and 400-2000,

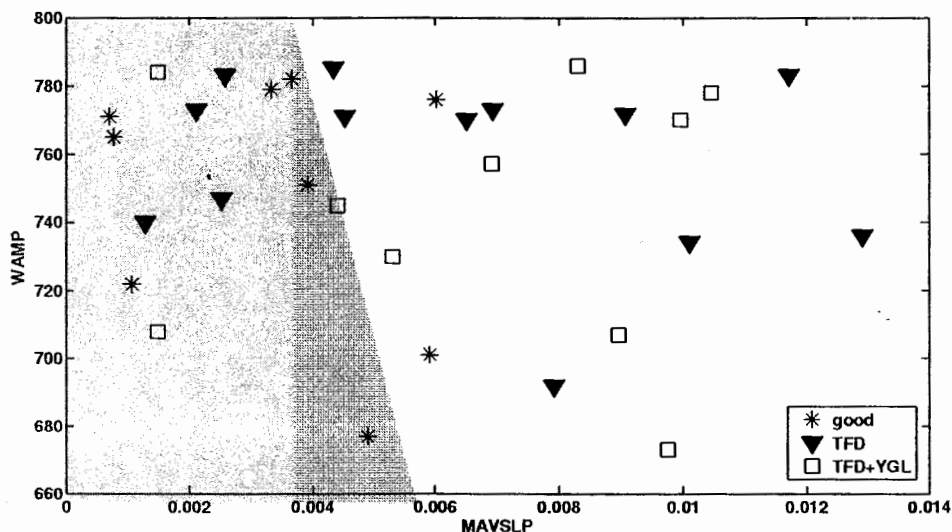
respectively. For Day#2 group which is shown in Figure 59(b), the SSC-WAMP plot suggests to select the thresholds for SSC and WAMP at 190 and 600-900, respectively. For Day#3 group, the thresholds for MAVSLP and WAMP are 0.005 and 660-800 as shown in Figure 59(c).



(a)



(b)



(c)

Figure 59 Optimum feature pairs based on (a) Day#1, (b) Day#2 and (c) Day#3 groups obtained from technique XIII

Table 27 shows the accuracy performances obtained by applying technique XIII. The accuracy performances for Day#1, Day#2 and Day#3 groups are 100.00, 80.00 and 33.33%, respectively.

Table 27 Summary of performances (Day#1-Day#3) using technique XIII

Sample	Performance (%)				Overall accuracy (%)
	Good	Accuracy	Defected	Accuracy	
Day#1	100.00	100.00	100.00	100.00	100.00
Day#2	100.00	71.43	60.00	100.00	80.00
Day#3	100.00	33.33	0.00	0.00	33.33

(n) Technique XIII

From the features shown in Figure 54, a single-hidden layer NN is applied to determine the thresholds for good/defected sample detection. The overall accuracy performance obtained for Day#1, Day#2 and Day#3 groups as shown in Table 28 are 80.00, 50.00 and 33.33%, respectively.

Table 28 Summary of performances (Day#1-Day#3) using technique XIV

Sample	Performance (%)				Overall accuracy (%)
	Good	Accuracy	Defected	Accuracy	
Day#1	100.00	71.43	60.00	100.00	80.00
Day#2	100.00	50.00	0.00	0.00	50.00
Day#3	100.00	33.33	0.00	0.00	33.33

(o) Technique XV

From the features shown in Figure 56, a single-hidden layer NN is applied to determine the thresholds for detecting a good/defected sample. The overall

accuracy performance obtained for Day#1, Day#2 and Day#3 groups as shown in Table 29 are 33.33, 62.50 and 64.71%, respectively.

Table 29 Summary of performances (Day#1-Day#3) using technique XV

Sample	Performance (%)				Overall accuracy (%)
	Good	Accuracy	Defected	Accuracy	
Day#1	100.00	33.33	0.00	0.00	33.33
Day#2	33.33	50.00	80.00	50.00	62.50
Day#3	60.00	42.86	75.00	80.00	64.71

3.3 Research Syntheses and Discussion

3.3.1 Background

The objectives are to study electrical based NTD techniques to detect internal defected mangosteens, which are TFD and YGL. A hundred mangosteens purchased directly from garden at Nakornsritummarat province were tested. The mangosteens were vibrated and their responses in the form of VFSS samples were recorded. The tested samples were vibrated at single frequency ranging from 25 to 40 Hz. The voltage amplitude of vibration is 2.5 volt.

3.3.2 Summary of Accuracy Performances

3.3.2.1 Pre-classification using AR and f_R

The accuracy performances based on applying pre-classification process using AR model and resonance spectrum are summarized in this section. There are four pre-classification techniques and three selection/detection techniques (A, B, C) as described in Table 8 applied to the classified VFSS groups. As shown in Table 30, there are 12 cases obtained from the combinations between pre-classification techniques developed from two frequency-domain features and three selection/detection techniques. Table 30 summarizes their accuracy performances. The best performance, which is 95.65%, is obtained by applying technique A to the VFSS samples which have $+a_4$ and f_R at 187 Hz. The second best performance is obtained by applying technique C to VFSS samples which have $+a_4$ and f_R at 187 Hz.

Table 30 Performances of techniques obtained by applying pre-classification methods

Case	a_4	f_R (Hz)	Technique	Performance (%)				Overall accuracy (%)
				Good	Accuracy	Defected	Accuracy	
1	-	77	A	70.00	77.78	77.78	70.00	73.68
2	-	77	B	70.00	87.50	88.89	72.73	78.95
3	-	77	C	28.57	66.67	80.00	44.44	50.00
4	-	187	A	70.00	70.00	72.73	72.73	71.43
5	-	187	B	50.00	83.33	90.91	66.67	71.43

6	-	187	C	0.00	0.00	100.00	55.56	55.56
7	+	77	A	71.43	71.43	84.62	84.62	80.00
8	+	77	B	42.85	100.00	100.00	76.47	80.00
9	+	77	C	20.00	33.33	75.00	60.00	53.85
10	+	187	A	100.00	88.89	93.33	100.00	95.65
11	+	187	B	87.50	70.00	80.00	92.31	82.61
12	+	187	C	66.67	100.00	100.00	87.50	90.00

Shown in Table 30, the technique that provides the best accuracy performance for each pre-classification group can be determined. There are six cases from four groups. These cases are 2, 4, 5, 7, 8 and 10 as shown in Table 30. Table 31 shows the accuracy performances of the techniques obtained by combining the best case for each pre-classification group. The cases obtained from these combinations are (2&4&7&10), (2&5&7&10), (2&4&8&10) and (2&5&8&10). It is shown in Table 31 that the case (2&4&7&10) provides the best accuracy performance among other cases.

Table 31 Performances of techniques obtained by applying a combination of pre-classification methods.

Case	Performance (%)				Overall accuracy (%)
	Good	Accuracy	Defected	Accuracy	
2&4&7&10	88.57	79.49	83.33	90.91	85.54
2&5&7&10	71.43	80.65	87.50	80.77	80.72
2&4&8&10	71.43	80.65	87.50	80.77	80.72
2&5&8&10	65.71	85.19	91.67	78.57	80.72

Table 32 Performances of applied techniques based on pre-classification method.

Technique	Performance (%)				Overall accuracy (%)
	Good	Accuracy	Defected	Accuracy	
A	77.14	77.14	83.33	83.33	80.72
B	62.86	81.48	89.58	76.79	78.31
C	26.32	62.50	88.00	61.11	61.36

Table 32 shows the overall performances of three feature selection/detection techniques. It is shown that technique A, which is based on observation, provides the best accuracy performance. The technique achieves 80.72%. Technique C, which is based on RES index and NN method, provides the worst accuracy performance among others.

3.3.2.2 All VFSS samples

Table 33 Performances of techniques applied to all VFSS samples

Technique	Performance (%)				Overall accuracy (%)
	Good	Accuracy	Defected	Accuracy	
I	80.00	50.91	43.75	75.00	59.04
II	80.00	50.91	43.75	75.00	59.04
III	33.33	100.00	100.00	62.50	68.42
IV	82.35	56.00	50.00	78.57	64.10
V	94.44	56.67	50.00	92.86	68.18
VI	100.00	53.13	31.82	100.00	61.54
VII	94.44	56.67	50.00	92.86	68.18
VIII	100.00	56.25	41.67	100.00	66.67
IX	30.00	60.00	85.71	63.16	62.50
X	100.00	77.27	66.67	100.00	84.38
XI	94.44	68.00	75.76	96.15	82.35
XII	88.24	62.50	40.00	75.00	65.62
XIII	72.22	61.90	75.76	83.33	74.51
XIV	91.67	57.89	38.46	83.33	64.00
XV	50.00	30.00	56.25	75.00	54.55

Table 33 shows the accuracy performances of fifteen techniques applied to all VFSS signals measured from all mangosteen samples. The details of these techniques are summarized in Table 13. It is shown that technique X, which is based on using $-a_4$ for classification and observation for feature selection/detection, outperforms other techniques. It achieves 84.34% for overall accuracy performance. The second best performance is obtained from technique XI. The accuracy performance is 82.35%, which is comparable to Technique X. The process of technique XI is rather similar to Technique X. Only the classification process, which is relied on $+a_4$, differs from technique X. Table 34 shows the performances of combined techniques which apply to all VFSS samples. The results confirm to apply observation for feature selection and detection while using AR model for classification.

Table 34 Performances of combined techniques applied to all VFSS samples

Technique	Performance (%)				Overall accuracy (%)
	Good	Accuracy	Defected	Accuracy	
I	80.00	50.91	43.75	75.00	59.05
II	80.00	50.91	43.75	75.00	59.04
III	33.33	100.00	100.00	62.50	68.42
IV&V	88.57	56.36	50.00	85.71	66.27
VI&VII	97.14	56.67	45.83	95.65	67.47
VIII&IX	63.16	63.16	70.83	70.83	67.44
X&XI	97.14	73.91	75.00	97.30	84.34
XII&XIII	80.00	62.22	64.58	81.58	71.08
XIV&XV	77.78	48.28	48.28	77.78	59.57

3.3.2.3 Classification based on experiment day

All mangosteen samples were divided into three groups based on experiment day. These three groups are named Day#1, Day#2 and Day#3. Fifteen techniques detailed in Table 13 were applied to each VFSS sample group. The accuracy performances of these techniques applied to each sample group are shown in Table 35-37. Some similar techniques were combined and applied to the VFSS samples for each group. The accuracy results are shown in Table 38-39. From Table 38, the accuracy performances obtained from Technique IV combined with V provides the best accuracy performance. It achieves 90.36%. The second best performance is obtained by applying technique X and XI. Considering the accuracy performances of combined technique applied to the individual group, Technique IV combined with V outperforms other combined ones.

Table 35 Performances of techniques applied to Day#1 VFSS samples

Technique	Performance (%)				Overall accuracy (%)
	Good	Accuracy	Defected	Accuracy	
I	92.31	80.00	66.67	85.71	81.82
II	53.85	70.00	66.67	50.00	59.09
III	37.50	100.00	100.00	44.44	58.33
IV	100.00	100.00	100.00	100.00	100.00
V	100.00	100.00	100.00	100.00	100.00
VI	100.00	77.78	100.00	100.00	81.82
VII	66.67	80.00	80.00	66.67	72.73
VIII	50.00	50.00	100.00	50.00	66.67
IX	100.00	100.00	100.00	100.00	100.00
X	88.89	72.73	57.14	80.00	75.00
XI	100.00	100.00	100.00	100.00	100.00
XII	100.00	81.82	71.43	100.00	87.50
XIII	100.00	100.00	100.00	100.00	100.00
XIV	100.00	71.43	60.00	100.00	80.00
XV	100.00	33.33	0.00	0.00	33.33

Table 36 Performances of techniques applied to Day#2 VFSS samples

Technique	Performance (%)				Overall accuracy (%)
	Good	Accuracy	Defected	Accuracy	
I	90.91	71.43	69.23	90.00	79.17
II	72.73	61.54	61.54	72.73	66.67
III	14.29	33.33	71.43	45.45	42.86
IV	90.00	81.82	80.00	88.89	85.00
V	100.00	100.00	100.00	100.00	100.00
VI	90.00	69.23	60.00	85.71	75.00
VII	100.00	100.00	100.00	100.00	100.00
VIII	20.00	50.00	83.33	55.56	54.55
IX	100.00	100.00	100.00	100.00	100.00
X	100.00	75.00	60.00	100.00	81.82
XI	100.00	71.43	75.00	100.00	84.62
XII	100.00	75.00	60.00	100.00	81.82
XIII	100.00	71.43	75.00	100.00	84.62
XIV	100.00	50.00	0.00	0.00	50.00
XV	33.33	50.00	80.00	50.00	62.50

Table 37 Performances of techniques applied to Day#3 VFSS samples

Technique	Performance (%)				Overall accuracy (%)
	Good	Accuracy	Defected	Accuracy	
I	54.55	60.00	84.62	81.48	75.68
II	90.91	45.45	53.85	93.33	64.86
III	16.67	33.33	85.71	70.59	65.00
IV	0.00	0.00	100.00	100.00	100.00
V	72.73	80.00	88.89	84.21	82.76
VI	0.00	0.00	100.00	100.00	100.00
VII	72.73	80.00	88.89	84.21	82.76
VIII	0.00	0.00	100.00	100.00	100.00
IX	33.33	33.33	60.00	60.00	50.00
X	100.00	66.67	66.67	100.00	80.00
XI	77.78	70.00	86.96	90.91	84.38
XII	100.00	66.67	66.67	100.00	80.00
XIII	77.78	53.85	73.91	89.47	75.00
XIV	100.00	33.33	0.00	0.00	33.33
XV	60.00	42.86	75.00	80.00	64.71

Table 38 Performances of combined techniques applied to Day#1-Day#3 VFSS samples

Technique	Performance (%)				Overall accuracy (%)
	Good	Accuracy	Defected	Accuracy	
I	80.00	76.92	76.47	79.59	78.22
II	72.00	72.00	72.55	72.55	72.28
III	23.81	55.56	84.00	56.76	56.52
IV&V	88.57	88.57	91.67	91.67	90.36
VI&VII	82.86	76.32	81.25	86.67	81.93
VIII&IX	42.11	61.54	84.38	71.05	68.63
X&XI	97.14	75.56	77.08	97.34	85.54
XII&XIII	100.00	72.92	72.92	100.00	84.34
XIV&XV	77.78	50.00	51.72	0.00	61.70

Table 39 Performances of combined techniques applied to three different sample groups

Technique	Sample group		
	Day#1	Day#2	Day#3
I	81.82	79.17	75.68
II	59.09	66.67	64.86
III	58.33	42.86	65.00
IV&V	100.00	87.50	86.49
VI&VII	77.27	79.17	86.49
VIII&IX	83.33	66.67	66.67
X&XI	81.82	83.33	83.78
XII&XIII	90.91	83.33	75.68
XIV&XV	69.23	57.14	60.00

3.3.2.4 Performance comparison

In this section, the accuracy performances of fifteen techniques and nine combined techniques previously presented in Section 3.3.2.2 (all VFSS samples) and 3.3.2.3 (Day#1, Day#2 and Day#3) are compared and summarized. The comparisons will lead to justify which technique is suitable to apply. Table 40 shows the comparison performances of 15 techniques applied to two conditions, without pre-classification and with pre-classification into three subgroups (by day). It is shown that technique IV by day with pre-classification provides the best accuracy performance while the technique X by all sample provides the best accuracy performance if no pre-classification is applied. However, the performance obtained from the first case is better, which is 10% more than the latter case. Table 41 shows the combined accuracy performance of the techniques. Results of nine experimental cases are shown. It is shown that the case applying technique IV and V by day with pre-classification is the most suitable choice among other cases.

Table 40 Comparison performances of techniques without and with pre-classification (by day)

Technique	Sample group	
	All samples	Day#1-#3
I	59.04	78.22
II	59.04	72.28
III	68.42	56.52
IV	64.10	94.87
V	68.18	88.64
VI	66.67	69.23
VII	68.18	93.18
VIII	66.67	63.16
IX	62.50	67.86
X	84.38	84.38
XI	82.35	78.12
XII	65.62	73.68
XIII	74.51	86.27
XIII	64.00	80.39
XV	54.55	60.71

Table 41 Comparison performances of the techniques applied to combined samples

Technique	Sample group	
	All samples	Day#1-#3
I	59.04	78.22
II	59.04	72.28
III	68.42	56.52
IV&V	66.27	90.36
VI&VII	67.47	81.93
VIII&IX	67.44	68.63
X&XI	84.34	85.54
XII&XIII	71.08	84.34
XIV&XV	59.57	61.70

Chapter 4

Conclusion and Future Works

4.1 Conclusion

The VFSS response data of a mangosteen has been proposed to apply for detecting good and internal-defected mangosteen. Two internal defects, TFD and YGL, are of interest. The VFSS response was obtained by sensing electrical signal of vibration response of a mangosteen under test. Four different vibration frequencies at various frequencies 25, 30, 35 and 40 Hz were investigated and several frequency-domain transfer functions were proposed. Several transfer functions were developed and the experimental results suggest to apply a 40 Hz vibration frequency to test mangosteen. It was found that pericarp hardness and fruit size should be taken into account. (paper IV).

Several frequency-domain and time-domain features were studied to apply for detecting good and defected condition. For frequency-domain technique, two spectrum estimation techniques, FFT and AR model were investigated. The FFT technique was applied to VFSS response samples to investigate the resonance characteristics. Two resonance frequencies, 77 and 187 Hz, are of interest and were applied to classify the internal quality of mangosteens. The second spectral estimation technique called AR model is proposed to model the VFSS outputs. Based on this work, a tenth-order AR model was chosen and the coefficient a_4 of the AR model as the feature provides the optimum result. Therefore the characteristic of a_4 with mangosteen condition was thoroughly investigated and the threshold for a_4 for detecting good and defected mangosteen was reported. (paper III).

Eight time-domain features (MAV, RMS, MAVSLP, WAMP, SSC, WL, ZC, HIST) computed from VFSS responses were thoroughly investigated. Two-dimensional feature was established by plotting a scatter plot of two time-domain features. There are 28 possible two-dimensional features which can be applied to detect mangosteen condition. The author proposed two techniques for the feature selection. They are scatter plot and RES index. The final procedure is to detect good/defected fruits. We proposed to apply either scatter plot or NN method to determine the threshold value from 2-D features.

A hundred mangosteens with different conditions, weights, sizes, pericarp thickness and color indexes were tested at vibration of 40 Hz. Three sample groups classified as Day#1, Day#2 and Day#3 groups were experimented with the test setup to investigate the vibration response. The VFSS responses were digitized and collected. Various techniques formed by combining frequency-domain and time-domain features were proposed to three VFSS sample groups. The accuracy performance of each technique for each case was evaluated. The accuracy performances obtained from these techniques suggest on the feasibility of the proposed techniques for detecting good/defected mangosteen (paper II).

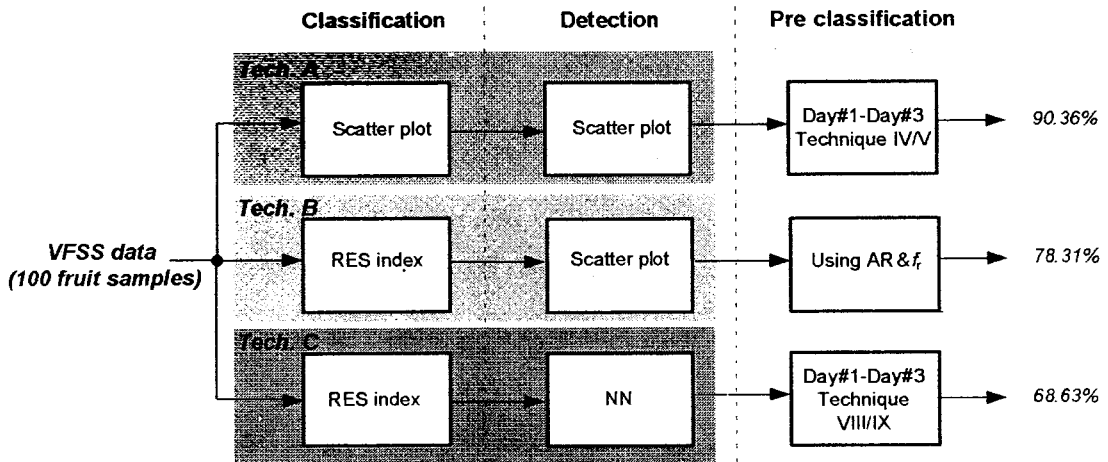


Figure 60 Summary of the accuracy performances

Applying different combinations techniques, from the pre-classification to the detection procedure, the accuracy performance results are summarized to three main categories as shown in Figure 60. The best accuracy performance obtained from the proposed methodology in this Thesis is 90.36%. This is obtained when pre-classifying the tested fruits into three subgroups, applying the resonance technique, and using scatter plot in both classification and detection procedures. The second best accuracy performance is 78.31%. It is obtained by applying AR and frequency resonance techniques for pre-classification combining with RES index and scatter plot during classification and detection processes. Finally, applying the RES and NN in the classification and detection processes, sampling VFSS data to three subgroups and employing the resonance technique, we achieve the accuracy performance for 68.63% only.

From the proposed technique that provides the best accuracy performance, Table 42 compares the accuracy performances obtained from this work with other three works that were previously proposed. Our proposed technique and another two techniques (SG and Microwave) detect good and defected fruits with the same degree of accuracy. Considering the overall accuracy performances, our proposed technique outperforms other techniques. Comparing with microwave and NIR, our technique is more suitable to be applied in practice because it is based on a low-frequency electronic design, which is low cost.

Table 42 Performances of the proposed and three previously proposed techniques.

Technique	Performance (%)				Overall accuracy (%)
	Good	Accuracy	Defected	Accuracy	
Resonance(our technique)	88.57	88.57	91.67	91.67	90.36
SG(Tanachai,1996)	88.00	82.09	80.80	87.07	84.40
Microwave(Tawatchai,2004)	82.00	77.36	76.00	80.85	79.00
NIR(Sontisuk,2007)	98.00	58.33	30.00	93.75	64.00

4.2 Future Works

With a wide variety of mangosteens, several difficulties during the experiment appeared. The proposed technique needs to measure VFSS at pericarp fruit. This requires a strain gage sensor attached at pericarp of the test sample. The accuracy performances obtained by pre-classification the samples into three days provide the best results. Especially, the sample number of experimental day#1 is high accuracy. It is found that some spots on fruit pericarp of a mangosteen can possibly distort the readout VFSS data, which in turn reduces accuracy performance. To obtain undistorted VFSS data, a suitable installing position of sensor should be investigated and a laser sensor may be applied.

In the experiment, all mangosteens were collected from the 7 year old plants. The fruit pericarp from the plants from this age becomes harden and this can affect to the response of the VFSS. Therefore, more investigation should be performed with other plant ages.

Finally, the new transfer function formulated with the ratio between the VFSS and the vibration signal of the plate. This may facilitate to classify mangosteens and detect the good and defect fruits.

References

1. Abbott J.A., Massie D.R., 1998. Nondestructive sonic measurement of kiwifruit firmness. *J Amer Soc Hort Sci* 123(2), 317-322.
2. Angkoon Phinyomark, Saowaluck Hirunviriyaya, Chusak Limsakul, Pornchai Phukpattaranont. 2010. Evaluation of EMG Feature Extraction for Hand Movement Recognition Based on Euclidean Distance and Standard Deviation. The 7th annual international conference on Electrical Engineering/Electronics, Computer, Telecommunications and Information technology, Chiang Mai, Thailand. pp. 856-860
3. Chen P., Ruiz-Altisent M., Barreiro P., 1996. Effect of impacting mass on firmness sensing of fruits. *T ASAE* 39(3), 1019-23.
4. De Belie N., Schotte S., Lammertyn J., Nicolai B., De Baerdemaeker J. 2000. Firmness changes of pear fruit before and after harvest with acoustic impulse response technique. *J. Agr Eng Res.* 77(2):183-91.
5. Delwiche M. J., McDonald T., Bowers S.V., 1987. Determination of peach firmness by analysis of impact forces. *T ASAE* 30(1), 249-54.
6. Desmet M., Lammertyn J., Scheerlinck N., Verlinden B.E., 2002. A pendulum for testing puncture injury susceptibility of tomatoes. *Proc Intl Conf Agricultural Engineering*. Budapest, June 30-July 4. Paper 02-PH-038.
7. Diezma B., Ruiz-Altisent M., Orihuel B. 2002. Acoustic impulse response for detecting hollow heart in seedless watermelon. *Acta Horticulture*. 599: 249-256.
8. F. J. García-Ramos, C. Valero, I. Homer, J. Ortiz-Cañavate and M. Ruiz-Altisent. 2005. Non-destructive fruit firmness sensors: a review. *Spanish Journal of Agriculture Research* 3(1):61-73.
9. García - Ramos, C. Valero, I. Homer, J. Ortiz-Cañavate J., Ruiz-Altisent M., Diez J., Flores L., Homer I., Chavez J.M., 2003. Development and implementation of an online impact sensor for firmness sensing of fruit. *J Food Eng* 58(1), 53-57.
10. Jaren C., García -Pardo E., 2002. Using non-destructive impact testing for sorting fruits. *J Food Eng* 53(1), 89-95.
11. Jaren C., Ruiz-Altisent M., Perez De Rueda R., 1992. Sensing physical stage of fruits by their response to non-destructive impacts. *Proc Intl Conf on Agricultural Engineering*. Uppsala. June 1-4. Paper 9211-113.

12. Junichi Sugiyama, Muhammad Imran Al-Haq and Mizuki Tsuta. 2005. Application of Portable Acoustic Firmness Tester for Fruits. The fifth International Conference on Information and Technology for Sustainable Fruit and Vegetable Production, Montpellier, France. P 439-443.
13. Kongrattanaprasert, S., Arunrungrusmi, S., Pungsiri, B., Chamnongthai, K., and Okuda, M. 2001. Nondestructive Maturity Determination of Durian by Force Vibration. The IEEE International Symposium on Circuits and System (ISCAS), Sydney, Australia. P 441-444.
14. L. Lleó, P. Barreiro, A. Fernández, M. Bringas ,B. Diezma and M. Ruiz-Altisent. 2005. Evaluation of the storability of Piel de Sapo melons with sensor fusion. The fifth International Conference on Information and Technology for Sustainable Fruit and Vegetable Production, Montpellier, France. P523-531.
15. Migdalia A., A. Bello, L. Rastrelli, M. Montelie, L. Delgado and C. Panfet. 2011. Antioxidant properties of pulp and peel of yellow mangosteen fruits. Emir. J. Food Agric. 2011. 23 (6): 517-524.
16. Mohsenin N., 1970. Physical properties of plant and animal materials. Gordon and Breach Science Publishers. USA. 734 pp.
17. Muramatsu N., Sakura N., Yamamoto R., Nevins D.J., Takahara T., Ogata T. 1997. Comparison of non-destructive acoustic method with an intrusive method for firmness measurement of kiwifruit. Postharvest Biology. and Technology. 12:221-228.
18. Nourain Jamal, Ying Yi-bin, Wang Jian-ping, Rao Xiu-qin and Yu Chao-gang. 2005. Firmness evaluation of melon using its vibration characteristic and finite element analysis. Journal of Zhejiang University. 6B(6):483-490.
19. Ortiz C., Barreiro P., Correa E., Ruiz-Altisent M., Riquelme F., 1999. Identificación de melocotones lanosos mediante técnicas no destructivas de impacto yespectroscopía en el infrarrojo cercano. Proc VIII Congreso Nacional de Ciencias Hortícolas, Murcia, Spain, April, pp. 210-223.
20. Osman, M. and Rahman Milan, A. (2006). Mangosteen—Garcinia mangostana. Southampton Centre for Underutilised Crops, University of South Hampton, Southampton, UK.
21. Pankasemsuk, T.,O.Garner, J., B. Malta,F., and L. Silva, J. 1996. Translucent fresh disorder of mangosteen(Garcinia mangostana L.). HortScience. 31(1):112-113.
22. Peleg K., 1993. Comparison of non-destructive measurement of apple firmness. J Agr Eng Res 55(3), 227-238.

23. Roedhy Poerwanto, Dorly, Indah Wulandari and Febriyaqnti (2009). International Seminar on Recent Developments in the Production, Postharvest Management and Trad of Minor Tropical Fruits. Best Western Seri Pacific Hotel, Kuala Lumpur, Malaysia.
24. Rittisak jaritngam, Chusak Limsakul, Sayan Sdoodee, Saravut Jaritngam and Mareena Mani. 2001. To Detect Gummy Fruit of Mangosteen (*Garcinia mangostana* Linn.) by the Autoregressive Model Analysis Method. *Journal of Agricultural Science*. 32:1-4.
25. Sdoodee, S and S. Limpun-Udom (2002). Effect of excess water on the incidence of translucent flesh disorder in mangosteen (*Garcinia mangostana* L.). *Acta Hort. (ISHS)* 575:813-820.
26. Shmulevich I., Galili N., Rosenfeld D., 1996. Detection of fruit firmness by frequency analysis. *T ASAE* 39(3), 1047-55.
27. Shoji Terasaki, Naoki Sakurai, Jacek Zebrowski c,g, Hideki Murayamad, Ryoichi Yamamotoe, Donald J. Nevins f. 2006. Laser Doppler vibrometer analysis of changes in elastic properties of ripening 'La France' pears after postharvest storage. *Postharvest Biology and Technology*. 42:198-207.
28. Somchai Arunrungrusmi, Dejwoot Khawaparisuth, Kosin Chamnongthai. 1999. Nondestructive 2D Cross-Sectional Visualization of A Mangosteen. The fifth International Symposium an Signal Processing and its Applications, Brisbane, Australia. P 443-445.
29. Sontisuk Teerachaichayut. 2007. Non-destructive prediction of translucent flesh disorder in intact mangosteen by short wavelength near infrared spectroscopy. *Postharvest Biology and Technology*. 43:202-206.
30. Sriyont Chaichumpan. 1986. The Study on Neua Gaew a Physiological disorder of mangosteen(*Garcinnia magostana* Linn). Undergraduate Student , Department of Horticulture, Faculty of Agriculture, Kasetsart University, Thailand.
31. Studman C.J, 1999. Fruit and vegetables: fruit and vegetable quality. CIGR ed. *CIGR Handbook of Agriculture Engineering*, Vol. IV. pp. 243-72.
32. Tawatchai Tongleam, Nutthacha Jittiwaranghl, Pinit Kumhoml, Kosin Chamnongthai. 2004. Non-Destructive Grading of Mangosteen by Using Microwave Moisture Sensing. International Symposium on Communications and Information Technologies, Sapporo, Japan. P 650-653.
33. Timoshenko S.P., Goodier J., 1951. *Theory of elasticity*, 2nd ed. McGraw-Hill. NY.

34. Voraphat Luckanatinvong. 1996. Effect of Water on Physiological Disorders of Mangosteen Fruit (*Garcinia Mangostana* Linn). Developmental Physiology, Master of Science (agriculture) Department of Horticulture, Kasetsart University, Thailand.
35. Yantarasi, T., C. Sivasomboon, J. Uthaibutra and J. Sornsrivichai. 1996. X-ray and NMR for nondestructive internal quality evaluation of durian and mangosteen fruits. *Acta Horticulture*. 464:97-101.

Appendix A

Conference/Journals

A.1 International conference

(1) Rittisak Jaritngam, Chusak Limsakul and Booncharoen Wongkittiserka, "The relation between the resonance frequency with the property for detect the translucent and yellow gummy latex of mangosteens (*Garcinia mangostana* Linn.)," *Proceedings of the International Conference on Arts, Social Sciences & Technology*, Penang, Malaysia, 2012.

A.2 International journals

(1) Rittisak Jaritngam, Chusak Limsakul and Booncharoen Wongkittiserka, "The translucent and yellow gummy latex of mangosteen by using the VFSS Measurement," *Journal of Biology, Agriculture and Healthcare*, vol. 2, no. 1, pp 83-91, 2012 (EBSCO).

(2) Rittisak Jaritngam, Chusak Limsakul and Booncharoen Wongkittiserka, "The translucent and yellow gummy latex of mangosteen by using autoregressive coefficient method," *Journal of Innovative Systems Design and Engineering*, vol. 3, no. 5, pp. 33-40, 2012 (EBSCO).

(3) Rittisak Jaritngam, Chusak Limsakul and Booncharoen Wongkittiserka, "The relation between the texture properties of mangosteen (*Garcinia mangostana* Linn.) with the resonance frequency for detect the translucent and yellow gummy latex," *Emirates Journal of Food and Agriculture*, vol. 25, no. 2, 2013. (SCOPUS).

Paper I

Rittisak Jaritngam, Chusak Limsakul and Booncharoen, " The Relation between the Resonance Frequency with the property For Detect the translucent and yellow gummy latex of mangosteens (*Garcinia mangostana* Linn.)," Proceedings of the International Conference on Arts, Social Sciences & Technology, Penang, Malaysia, pp.xxx-xxx, 2012.

The Relation between the Resonance Frequency with the property For Detect the translucent and yellow gummy latex of mangosteens (*Garcinia mangostana* Linn.)

Rittisak Jaritngam¹, Chusak Limsakul² and Booncharern Wongkittiserksa³

¹Faculty of Engineer, Prince of Songkla University(PSU), Thailand
rittisak.ja@chaiyo.com

²Faculty of Engineer, Prince of Songkla University(PSU), Thailand
chusak.l@psu.ac.th

³ Faculty of Engineer, Prince of Songkla University(PSU), Thailand
booncharoen.w@psu.ac.th

ABSTRACT

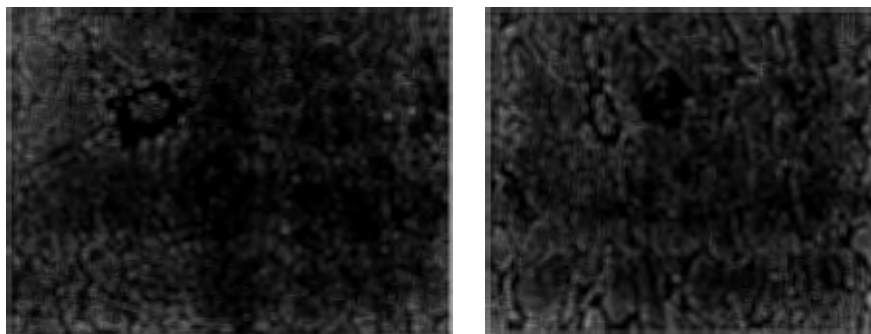
In Thailand, mangosteens are the queen of fruits because of their flavors. Generally, the good quality of mangosteen, which are accepted by consumers a reconsidered from the appearance, color, size and no translucent or yellow gummy latex. So that the electronic, measurement solve this problem. The Vibration Fruit base on Strain gage Sensor (VFSS) is the nondestructive measurement for detect the translucent and yellow gummy latex in mangosteen; the most important step is method. In this research, we present a spectrum plot by 100 samples, vibration is 25 Hz, 30 Hz, 35 Hz and 40 Hz. From the experimental results, mass is the best comparing with the other property. This measurement can detect the yellow gummy latex in mangosteen at 35 Hz and 40 Hz.

Keywords : Vibration Fruit base on Strain gage Sensor (VFSS), feature extraction, yellow gummy latex and translucent.

1. INTRODUCTION

The mangosteen is the queen of fruit and one of the high economical fruits that Thailand is exported for several years. The most problem and quality of mangosteen are determining internal factors such as translucent fresh disorder and yellow gummy latex which are also very important for consumer acceptance. There are many methods to determine their qualities non-destructive measurement. In quality determination of mangosteen, the physiological disorder of mangosteen using a destructive technique [11]. The effect of water to translucent flesh disorder using chemical technique [15],[16]. In non-destructive measurement of mangosteen in Thailand, A floating technique using differences in specific gravity is non-destructive detection of translucent fresh disorder in mangosteen [8]. Similarly, microwave technique used to classify the mangosteen with a translucent fresh disorder out from the good one finding of a threshold in term of magnitude of the reflect microwave signal through a mangosteen, the monopole probe is chosen [14]. Non-destructive 2D cross-sectional visualization of a mangosteen [12]. Near infrared spectroscopy used to accurate mangosteen [13]. A nondestructive hardness inspection of mangosteen using Near Infrared (NR) Transmittance [1]. X-ray and NMR used to nondestructive internal quality evaluation of durian and mangosteen fruits [17]. The resonance frequency used to measurement by knocking to detect translucent fresh disorder and yellow gummy latex [9].

From the physiological disorder of mangosteen are reliable with the water and hollow in the fruit are shown in Table 1. In recent year, the nondestructive vibration to determine the maturity levels of durian [5].



(a)

(b)

Fig 1 (a) normal of mangosteen (b) translucent fresh disorder of mangosteen

Table 1: The different of property in mangosteen;

No.	Property	Translucent solution	Yellow Gummy latex	Normal	Reference
1	Opening of Cell		-	Air	Sriyon,1986
2	S.G.	Higher than 1	-	Lower than 1	Vorapat,1996
3	Water Volume		Higher than normal 1.21%		Vorapat,1996
4	Air Volume		Lower than normal 15		Vorapat,1996
5	Density		Higher than normal 3		Vorapat,1996

The acoustic measurement and a intrusive method for determining tissue firmness were compared to assess the textural properties of kiwifruit [6], Firmness measurement of muskmelons by acoustic impulse transmission [4]. The vibration element analysis to determine firmness evaluation of melon [7]. A Laser Doppler Vibrometer(LDV) technique was monitor ripening behavior temperature [11]. The acoustic impulses were detected internal hollow in watermelon [2]. The acoustic response evaluation of the storability of Piel de Sapo melons[3].

In this paper, we propose a nondestructive inspection of mangosteen by using technique detect the translucent fresh disorder and yellow gummy latex.

2. MATERIALS AND METHODS

2.1 System Architecture of VFSS Measurement

The amplitude and frequency of vibration determine have many methods such as ultrasonic and accelerometer and Laser Doppler method can fix sensor with the fruit, there have response of vibration and accuracy. VFSS measurement has used in the vibration measurement of mangosteen.

The prototype system architecture for determination translucent fresh disorder and yellow gummy latex is shown in figure. The first, we put the mangosteen on the base of the prototype, base on vibration set (1) which can vibrate with frequency 0 – 50 Hz. Second, the strain gauge sensor (2) is adjusted by fix on the mangosteen. After that signals from this one sent to amplifier (3) by instrument amplifier circuit (IC = INA 114) to A/D converter (4). Respectively, we can observe these signal on computer (5) by labview programming and process them by matlab programming for classification of translucent fresh disorder and yellow gummy latex of mangosteen

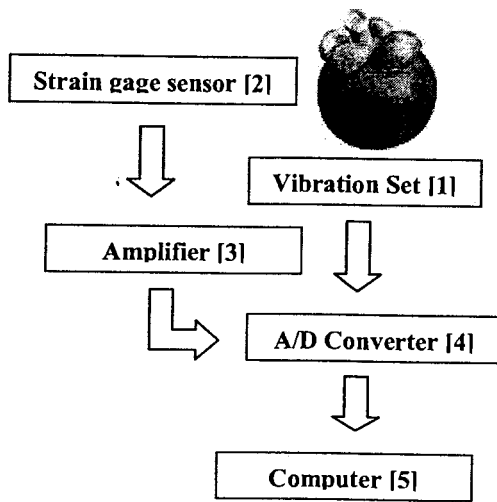


Figure 2. the system architecture for determination translucent and yellow gummy latex of mangosteen

2.2 Signal of VFSS Measurement

The resonance frequency in this case, the characteristic of mechanical vibration most parts of the energy radiated from the surface propagates as a transversal wave in the medium when the frequency of low frequency vibration is less than about 1 kHz [3], the velocity of transversal wave in medium related to characteristic of medium are given by

$$V_i = \left(\frac{2(\mu_1^2 + \omega_b^2 \mu_2^2)}{\rho(\mu_1 + \sqrt{\mu_1^2 + \omega_b^2 \mu_2^2})} \right)^{1/2} \quad (1)$$

Where V_i is velocity of vibration. ρ is the density of the medium. ω_b is the angular frequency of vibration and μ_1 and μ_2 are the coefficients of shear elasticity and shear viscosity. Respectively. Velocity of vibration related to frequency and wave propagation of vibration. So, property of shear elasticity can be found by velocity measurement of vibration and wave propagation at low frequency. In (1) if the shear elasticity is dominant compared with the shear viscosity so that $\mu_1, \gg \omega_b \mu_2$ is satisfied. the velocity is written as

$$V_i = (\mu_1 / \rho)^{1/2} \quad (2)$$

The signal of output vibration, when reference voltage of output vibration from the prototype for determine velocity of vibration which can be obtained from

$$V_i = \frac{A}{\alpha T} \quad (3)$$

$$A = \frac{\alpha V_i}{F} \quad (4)$$

where A is the voltage of output vibration. T is the time of output vibration. α is voltage of output vibration from the prototype. F is the resonance frequency vibration

The amplitude and frequency of vibration determining have many methods such as ultrasonic and accelerometer and Laser Doppler method can fix sensor on sample, there have response of vibration accuracy. In this paper, we used VFSS measurement has used in the vibration measuring of mangosteen. In this paper, we choose the frequency vibration between 25 to 40 Hz and input signal is 2.5 Volt, for the mangosteen with difference texture property when transfer input signal. Output signal has difference amplitude and frequency has related to internal air cavity, weight and diameter follow to texture property of mangosteen. In fig 2(a) the good mangosteen have pattern signal difference with unusual mangosteen, translucent and yellow gummy latex.

3 RESULT AND DISCUSSION

From the experiment, In Fig 5 has shown the differential real time signal of texture property of mangosteen. We can observe that output signal in the differential on texture property of mangosteen have different pattern. The result, frequency at 25 Hz is the best VFSS compared with the other vibration as we can observe from Fig 6. That frequency obtains the amplitude spectrum as 2.5 volt, there is higher than secondary vibration about 30 and 35 Hz are the secondary frequency vibration.

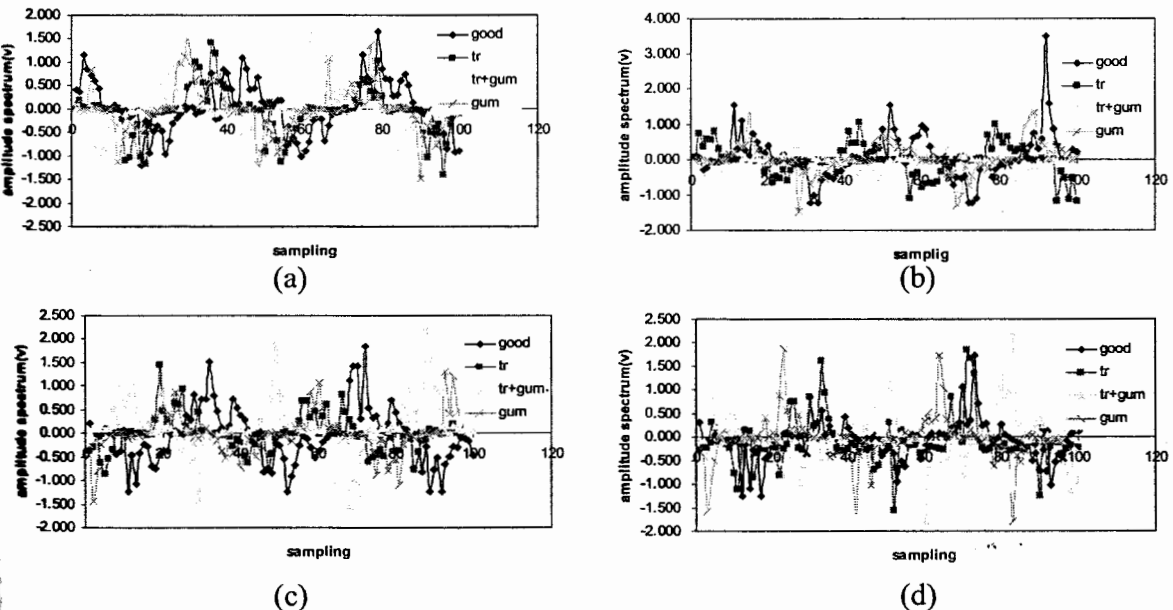


Fig 5 the differential real time signal of texture property of mangosteen
 (5a) time domain at 25 Hz vibration base, (5b) time domain at 30 Hz vibration base
 (5c) time domain at 35 Hz vibration base, (5d) time domain at 40 Hz vibration base

A Fast Fourier Transform (FFT) converts the time signal into a frequency spectrum. For each mangosteen the frequency spectrum for 0 up to 500 Hz after the nondestructive measurement with the VFSS technique, translucent fresh order and yellow gummy latex of the mangosteen. The typical spectrums for texture property are represented in Fig 7a, 7b, 7c and 7d respect. For the resonance frequency, there is usually a high peak, while the spectrum with good mangosteen shown usually one high peak at 26 Hz. From the result, weight and diameter have related with amplitude spectrum. Ratio of amplitude spectrum with weight at 25 Hz of base vibration is the best compared with the other as we can observe from Fig 8, there are obtains the ratio as 0.00853 volt. There are higher than secondary base vibration about 0.00005 volt, frequency at 30 and 35 Hz base vibration are the secondary. The ratio is

greater than 0.0080 and 40 Hz is very poor. From table 2, Shown the data of amplitude and ratio of amplitude with the texture property, this measurement can be detect the yellow gummy latex in mangosteen at the 35 and 40 Hz, the amplitude is lowest compared with the other frequency.

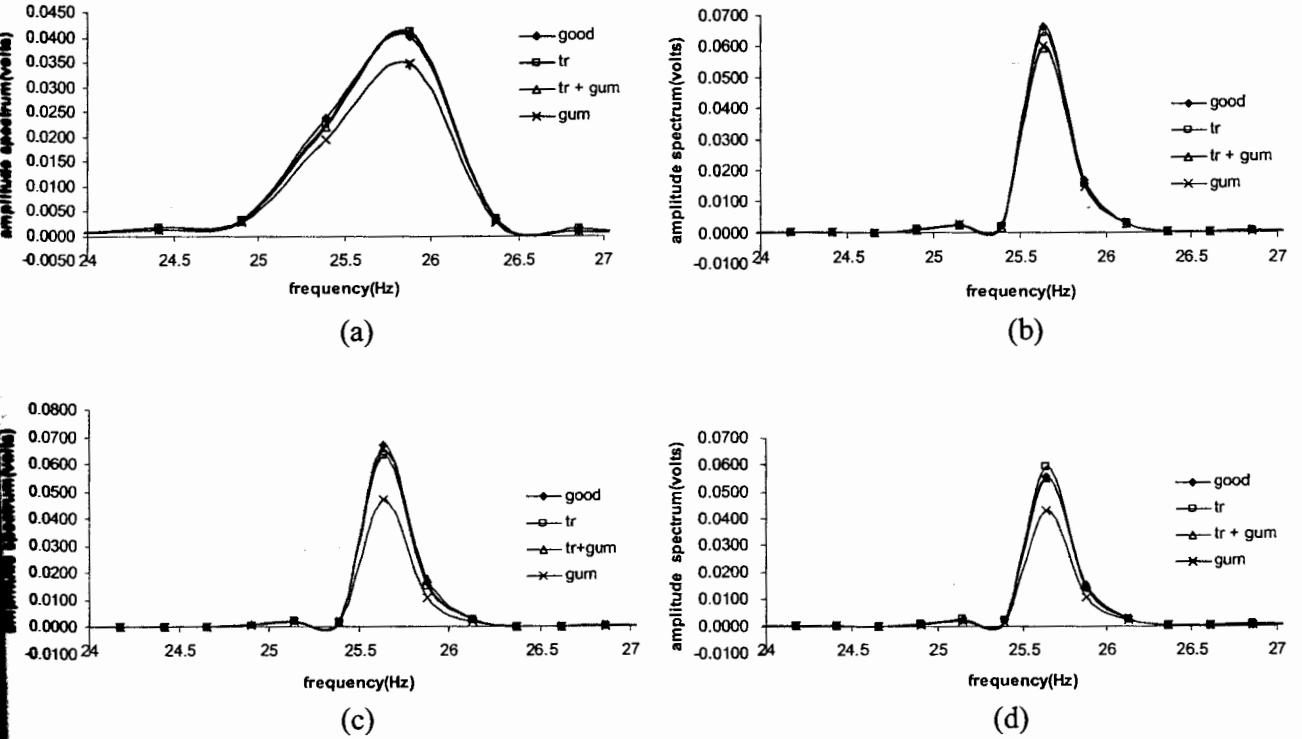


Fig 6 The typical spectrums for texture property
 (6a) frequency at 25 Hz vibration base, (6b) frequency at 30 Hz vibration base
 (6c) frequency at 35 Hz vibration base, (6d) frequency at 40 Hz vibration base

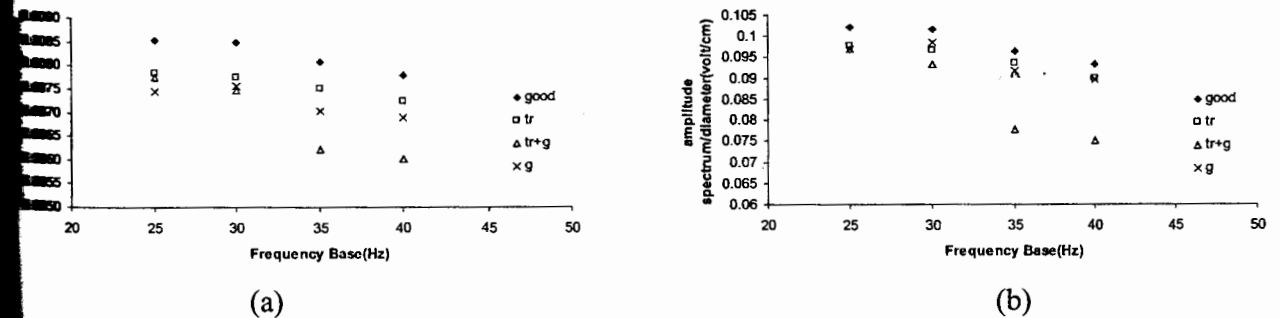


Fig 7 the frequency are the best by VFSS measurement compared with the other vibration. (7a) ratio of amplitude spectrum/weight and
 (7b) ratio of amplitude spectrum/diameter

Table 2: Mean amplitude spectrum of the texture property in mangosteen;

Frequency(Hz)	mean amplitude spectrum(Volt)			
	good	translucent	translucent + yellow gummy latex	yellow gummy latex
Amplitude				
25	0.519877	0.50269462	0.5117037	0.4943593
30	0.517261	0.496899	0.5196019	0.476186
35	0.49152	0.48114015	0.4837583	0.3965903
40	0.475493	0.46350169	0.4735709	0.3825875
Amplitude/weight				
25	0.00853	0.007853	0.007761	0.007448
30	0.008487	0.007762	0.007475	0.007563
35	0.008065	0.007516	0.006226	0.007042
40	0.007802	0.00724	0.006006	0.006893
Amplitude/diameter				
25	0.102097	0.097686	0.096933	0.097005
30	0.101583	0.096557	0.09337	0.098503
35	0.096528	0.093495	0.077763	0.091708
40	0.09338	0.09	0.075017	0.089776

4. CONCLUSION

This paper presented non-destructive measure VFSS and determination of mangosteen at low frequency. The texture property can be classifier into 4 group (good, translucent fresh order, translucent combination with yellow gummy latex and yellow gummy latex) vibration base on 25 Hz, there is the best amplitude and ratio of amplitude with diameter. Frequency bare vibration at 35 and 40 Hz can be classify yellow gummy latex, the amplitude is lowest than other frequency base on vibration.

ACKNOWLEDGE

The authors acknowledge the support by the graduation scholarship, Prince of Songkla University (PSU) and would like to thank Dr. Kittinan maliwan, lecturer in Mechanical Engineering, PSU for help technical in providing vibration set as well as Electrical Engineering(EE) department for their Kind technical help and use of laboratory.

REFERENCES

- [1] Boonrat, S., Tipakorn B., Chamnongthai., Kanyakanarat S., and Okuda, M., A nondestructive hardness inspection of mangosteen using Near Infrared(NR) Transmittance. National Conference on Kasetsart University Symopsiam, 1998, KU, Bangkok, Thailand.
- [2] B. Diezma Iglesias, M. Ruiz-Altisent and P. Jancsó. Vibrational analysis of seedless watermelons: use in the detection of internal hollows. Spanish Journal of Agricultural Research (2005) 3(1), 52-60
- [3] L. Lleó, P. Barreiro, A. Fernández, M. Bringas , B. Diezma and M. Ruiz-Altisent. Evaluation of the storability of Piel de Sapo melons with sensor fusion. Information and Technology for Sustainable Fruit and Vegetable Production FRUTIC 05, 12 . 16 September 2005, Montpellier France

- [4] Junichi Sugiyama, Muhammad Imran Al-Haq and Mizuki Tsuta. Application of Portable Acoustic Firmness Tester for Fruits. Information and Technology for Sustainable Fruit and Vegetable Production FRUTIC 05, 12 . 16 September 2005, Montpellier France
- [5] Kongrattanaprasert, W., Arunrungrusmi, S., Pungsiri, B., Chamnongthai, K., and Okuda, M., 2000, Nondestructive Maturity Determination of Durian by Force Vibration, International Conference on Intelligent Technologies (InTech'2000), ABAC, Bangkok, Thailand.
- [6] Muramatsu N., Sakura N., Yamamoto R., Nevins D.J., Takahara T., Ogata T., 1997. Comparison of non-destructive acoustic method with an intrusive method for firmness measurement of kiwifruit. *Postharvest Biol Tec* 12, 221-228.
- [7] Nourain Jamal, Ying Yi-bin, Wang Jian-ping, Rao Xiu-qin, Yu Chao-gang. Firmness evaluation of melon using its vibration characteristic and finite element analysis. *J Zhejiang Univ SCI* 2005 6B(6):483-490.
- [8] Pankasemsuk, T., O.Garner, J., B. Malta, F., and L. Silva, J. 1996. Translucent fresh disorder of mangosteen (*Garcinia mangostana* L.). *HortScience*. 31(1) : 112 -113.
- [9] Rittisak Jaritngam, Chusak Limsakul, Sayan Sdoodee, Saravut Jaritngam, Mareena Mani. 2001. To Detect Gumming Fruit of Mangosteen (*Garcinia mangostana* Linn.) by the Autoregressive Model Analysis Method. *Agricultural Science Journal*. Vol. 32 No.1-4 (Suppl.) January – August 2001. Thailand.
- [10] Sriyont Chaichumpan : “The Study on Neua Gaew a Physiological disorder of mangosteen (*Garcinia mangostana* Linn)”, Undergraduate Student, Department of Horticulture, Faculty of Agriculture, Kasetsan University, 1986.
- [11] Shoji Terasaki, Naoki Sakurai, Jacek Zebrowski c.g, Hideki Murayamad, Ryoichi Yamamotoe, Donald J. Nevins f. Laser Doppler vibrometer analysis of changes in elastic properties of ripening ‘La France’ pears after postharvest storage. *Postharvest Biology and Technology* 42 (2006) 198–207.
- [12] Somchai Amnngrusmi, Dejwoot Khawaparisuth, Kosin Chamnongthai : ‘Nondestructive 2D Cross-Sectional Visualization of A Mangosteen’, 1999, The fIAh International Symposium on Signal Processing and it’s Applications, August 22-25, Brisbane, Australia, pp. 443-445.
- [13] Sontisuk Teerachaichayut. 2007. Non-destructive prediction of translucent flesh disorder in intact mangosteen by short wavelength near infrared spectroscopy. *Postharvest Biology and Technology* 43 (2007) 202–206
- [14] Tawatchai Tongleam’, Nutthacha Jittiwanghl*, Pinit Kumhoml, Kosin Chamnongthai’. Non-Destructive Grading of Mangosteen by Using Microwave Moisture Sensing. International Symposium on Communications and Information Technologies 2004 (ISCIT 2004) Sapporo, Japan, October 26- 29, 2004.

[15] Voraphat Luckanatinvong. Effect of Water on Physiological Disorders of Mango Fruit (*Garcinia mangostana* Linn), Developmental Physiology, Master of Science (Agriculture), Department of Horticulture, Kasetsart University, 1996

[16] Voraphat Luckanatinvong. The Effect on Chemical Composition, Cell Viability and Influence of Water on Flesh Translucent Disorder in Mangosteen (*Garcinia mangostana* Linn), Master of Science (Agriculture), Major Field Horticulture, Department of Horticulture, Kasetsart University, 1996

[17] Yantarasri, T., C. Sivasomboon, J. Uthaibutra and J. Sornsrivichai. 1996. X-ray and NMR for nondestructive internal quality evaluation of durian and mangosteen fruits. *Acta Horticulturae*. 464: 97-101.

Paper II

Rittisak Jaritngam, Chusak Limsakul and Booncharoen Wongkittiserka, "The translucent and yellow gummy latex of mangosteen by using the VFSS Measurement," *Journal of Biology, Agriculture and Healthcare*, vol. 2, no. 1, pp 83-91, 2012.

The translucent and yellow gummy latex of mangosteen by using the VFSS Measurement

Rittisak Jaritngam*, Chusak Limsakul and Booncharoen Wongkittiserka

Department of Electrical Engineering, Prince of Songkla University

110/5, Kanchanavanid Road, Hat Yai, Songkhla 90112 Thailand

* E-mail of the corresponding author: rittisak.ja@chaiyo.com

Abstract

The vibration frequency base on strain gage sensor (VFSS) has proposed to predict an internal translucent and yellow gummy latex in mangosteen fruit, this measurement were used nondestructive method by vibrate on 25,30,35 and 40Hz. The VFSS were obtained an evaluation of feature extraction base on time and frequency domain, which can classify by two scatter plot. From the experimental results, the first day (day1), WAMP and RMS is the best feature comparing with the other feature, there have percentage accuracy higher than the other day. From this result, this method can obtain the high classification accuracy.

Keywords: Vibration Fruit base on Strain gage Sensor (VFSS), feature extraction, yellow gummy latex and translucent.

1. Introduction

The mangosteen is the queen of fruit and one of the high economical fruit. The problem and the quality to mangosteen is measured not only by external factors such as color, shape, size, skin blemishes, latex straining and insect damage, but also by internal factors such as translucent flesh and yellow gummy latex (Sontisuk, 2007). However, many methods used determine their qualities nondestructive measurement in the fruit. In recent year, the destructive technique use to study on translucent flesh of mangosteen. Sriyont (1986) study on Neua Geaw (thai for flesh translucent) physiological disorder of mangosteen using a destructive technique. Voraphat (1996) studied the effect of water to translucent flesh disorder using chemical technique. Moreover, the non-destructive measurement of mangosteen has invented in Thailand, Pankasemsuk (1996) used to the floating technique by using differences in specific gravity is non-destructive detection of translucent fresh disorder in mangosteen. Furthermore, the microwave technique used to classify the mangosteen with a translucent fresh disorder out from the good one finding of a threshold in term of magnitude of the reflect microwave signal through a mangosteen; the monopole probe is chosen (Tawatchai, 2004). Somchai(1999) had proposed the non-destructive 2D cross-sectional visualization a mangosteen. In addition to, the near infrared spectroscopy can be accurate mangosteen (Sontisuk, 2007). The X-ray and NMR used to nondestructive internal quality evaluation of durian and mangosteen fruits (Yantarasri, 1996). The resonance frequency measurement used to detect translucent fresh disorder and yellow gummy latex (Rittisak, 2001).

From the physiological disorder of mangosteen are reliable with the water and hollow in the fruit are shown in Table 1. In recent year, the nondestructive vibration used to determine the maturity levels of durian (Kongrattanasert, 2001), the acoustic measurement and a intrusive method for determining tissue firmness were compared to assess the textural properties of kiwifruit (Maramatsu, 1997), firmness measurement of muskmelons by acoustic impulse transmission (Junichi, 2005), the vibration element analysis to determine firmness evaluation of melon (Nourain, 2005). Moreover, the Laser Doppler Vibrometer (LDV) technique was monitor ripening behavior temperature (Shoji, 2006), the acoustic impulses were detected internal hollow in watermelon (B. Diezma, 2002), the acoustic response evaluation of the storability of Piel de Sapo melons (L Lleó, 2005). In table 1 shown the physiological texture property of mangosteen are reliable with water and hollow. Hence, many papers presents the nondestructive firmness

and differential texture property of fruit by using electrical measurement. In this paper, we propose a nondestructive technique by using VFSS measurement to detect flesh translucent and yellow gummy latex in mangosteen.

2. Material and Methods

2.1 Fruit sample and VFSS measurement

The mangosteen are purchased from a local fruit auction in Nakornsri Tummarat province, Thailand. The sample were delivered to laboratory of electrical engineering and experiment to record of signal data on the following by VFSS instrument as shown in Fig 1. About 100 sample Thai mangosteen were used to study the optimum condition of VFSS measurement and 26 intact mangosteen were used for evaluation the accuracy of translucent flesh disorder detection, 4 are translucent flesh disorder with yellow gummy latex and 20 are yellow gummy latex. The vibration signal were vibrated in medium sample at frequency was 25 to 40 Hz, amplitude input is 2.5 volt. After, the experiment was complete, the peel of each sample was slit with knife are take a photograph by digital camera, the sample were cut to record the internal as shown in Fig 2(a), 2(b),2(c)and2(d)

2.2 Instrument

The amplitude and frequency of vibration determine have many methods such as ultrasonic and accelerometer and Laser Doppler method can fix sensor with the fruit, there have response of vibration and accuracy. VFSS measurement has used in the vibration measurement of mangosteen.

The prototype system architecture for determination translucent fresh disorder and yellow gummy latex is shown in figure. The first, we put the mangosteen on the base of the prototype, base on vibration set, which can vibrate with frequency 0 – 50 Hz. The strain gauge sensor is adjusted by fix on the mangosteen. After that signals from this one sent to amplifier by instrument amplifier circuit (IC = INA 114) to A/D converter. Respectively, we can observe these signals on computer by labview programming and process them by matlab programming for classification of translucent fresh disorder and yellow gummy latex of mangosteen.

2.3. Data analysis

Feature from time domain are used in evaluation Time domain features are measured as a function of time, Because of their implementation and computation simplicity, time domain are popular in fruit analysis. All features in time domain can be implemented in real time. Nine features based on time domain are described as follows.

2.3.1 Mean Absolute Value (MAV):

MAV is similar to VFSS signal that normally used as an onset index to detect the unusual signal activity. MAV is the average of the absolute value of VFSS signal amplitude. It is defined as

$$MAV = \frac{1}{N} \sum_{i=1}^N |X_n| \quad (1)$$

2.3.2 Root Mean Square (RMS):

RMS is related to constant force and non-fatiguing contraction. Generally, it similar to SD, which can be expressed as

$$RMS = \sqrt{\frac{1}{N} \sum_{i=1}^N x_n^2} \quad (2)$$

2.3.3 Waveform length (WL):

WL is the cumulative length of waveform over time segment. WL is similar to waveform amplitude, frequency and time. The WL can be formulated as

$$WL = \sum_{n=1}^{N-1} |x_{n+1} - x_n| \quad (3)$$

2.3.4 Zero crossing (ZC):

ZC is the number of times that the amplitude values of VFSS signal crosses zero in x-axis. In VFSS feature, threshold condition is used to avoid from background noise. ZC provides an approximate estimation of frequency domain properties. The calculation is defined as

$$ZC = \sum_{n=1}^{N-1} \left[\text{sgn}(x_n \times x_{n+1}) \cap |x_n - x_{n+1}| \geq \text{threshold} \right];$$

$$\text{sgn}(x) = \begin{cases} 1, & \text{if } x \geq \text{threshold} \\ 0, & \text{otherwise.} \end{cases} \quad (4)$$

2.3.5 Slope Sign Change (SSC):

SSC is related to ZC. It is another method to represent the frequency domain properties of VFSS signal calculated in time domain. The number of changes between positive and negative slope among three sequential segments are performed with threshold function for avoiding background noise in VFSS signal. It is given by

$$SSC = \sum_{n=1}^{N-1} \left[f \left[(x_n - x_{n-1}) \times (x_n - x_{n+1}) \right] \right]; \quad (5)$$

$$f(x) = \begin{cases} 1, & \text{if } x \geq \text{threshold} \\ 0, & \text{otherwise.} \end{cases}$$

2.3.6 Willison amplitude (WAMP):

WAMP is the number of time resulting from the difference between VFSS signal amplitude of two adjoining segments that exceeds a predefined threshold, which is used to reduce background noises like in the calculation of ZC and SSC. It is given by

$$WAMP = \sum_{n=1}^{N-1} f(|x_n - x_{n-1}|); \quad (6)$$

$$f(x) = \begin{cases} 1, & \text{if } x \geq \text{threshold} \\ 0, & \text{otherwise.} \end{cases}$$

WAMP is related to the firing of motor unit action potentials and muscle contraction level. The suitable value of threshold parameter of features in ZC, SSC, and WAMP is normally chosen between 10 and 100 mV that is dependent on the setting of gain value of instrument. However, the optimal threshold suitable for VFSS analysis is discussed later.

2.3.7 Auto-regressive (AR) coefficients:

AR model described each sample of VFSS signals as a linear combination of previous VFSS samples (x_{n-i}) plus a white noise error term (w_n). In addition, p is the order of AR model. AR coefficients (α_i) are used as features in VFSS. The definition of AR model is given by

$$x_n = -\sum_{i=1}^p \alpha_i x_{n-i} + w_n \quad (7)$$

2.3.8 Mean Absolute Value Slope (MAVSLP):

MAVSLP is a modified version of MAV. The differences between the MAV of adjacent segments are determined. It can be defined as

$$MAVSLP_i = MAV_{i+1} - MAV_i; \quad i = 1, \dots, I - 1. \quad (8)$$

where I is the number of segments covering VFSS signal. When the number of segments increases, it may improve the representation of the original signal over the traditional MAV.

2.3.9 Histogram (HIST):

HIST is an estimate of the probability distribution of the VFSS signal. It is given by

$$HIST = \sum_{i=1}^j m_i \quad (9)$$

Where m_i is the counts the number and j be the total number

3. Results

To demonstrate the performance of classification, In this paper, the scatter plot can be separate the property of mangosteen. From the experimental results, in the first day, the RMS and WAMP are the best feature compared to the other VFSS features as we can observe from Fig4 (a). WAMP are less than 900, the RMS are less than 0.5. However, there are some translucent and yellow gummy latex of mangosteen in their group. But also, It's some good sample are concluded in the group unusual fruit sample. In addition to, the second day (day2), the MAVSLP and SSC are the best feature compared to the other VFSS features as we can observe from Fig4 (b). MAVSLP is less than 4, the SSC are less than 240. However, it's have some translucent and yellow gummy latex of mangosteen in their group. Not only, It's some good sample are concluded in the group unusual fruit sample. The lastly, in the third day (day3) the HIST and MAVSLP are

the best feature compared to the other VFSS features as we can observe from Fig4 (c). WAMP are higher than 0.008. In contrast, it's have some translucent and yellow gummy latex of mangosteen in their group. But also, some normal fruit are concluded in the group unusual fruit sample.

From the experiment results, the mangosteen from VFSS measurement on day1 of experimental is the best percentage classification is about 88.89 percentage classifier, on second day; (day 2), there is the percent in separating mangosteen well in order later and in the third day (day3), there give the percentage classification is the poor. However, in the first day and second day can be classify the translucent and yell gummy latex in the mangosteen are respectively similar with 66.67 and 69.23 percentage correct. Moreover, percentage classifier of mangosteen, we find on second day is the best is 81.82 percentage correct. But, there are not different with on day1 and day3. From the experiment, we need day1 is the best on classification, day2 is secondary and day3 is the poor. In overall analysis image, this measurement by classifier the sample on date of experiment can detect the unusual of mangosteen is correct 78.57 percentage accuracy shown in table2.

4. Conclusion

The VFSS of mangosteen fruit was sufficient to use for flesh translucent and yellow gummy latex detection in mangosteen The results of the propose methods that the percentage classify good sample and percentage correct the good sample on the first day has the highest, the second day are the secondary, and the third day is the poor. But, the first day has percentage classify unusual sample and percentage correct unusual sample is poor. Hence, the first day is the best because there is sum correct has the highest. However, the accuracy can be increase by rejection of other effects such as hardening pericap, fruit size and skin color before evaluation.

Acknowledge

The authors acknowledge the support by the graduation scholarship, Prince of Songkla University (PSU) and would like to thank Dr. Kittinan Maliwan, lecturer in Mechanical Engineering, PSU for help technical in providing vibration set as well as Electrical Engineering (EE) Department for their Kind technical help and use of laboratory. Moreover, I would like to thank the graduation school of PSU was supported in PH.D. Scholarship.

References

- Diezma B., Ruiz-Altisent M., Orihuel B.(2002), "Acoustic impulse response for detecting hollow heart in seedless watermelon", *Acta Horticulture* 599, 249-256.
- L. Lleó, P. Barreiro, A. Fernández, M. Bringas, B. Diezma and M. Ruiz-Altisent.(2005), "Evaluation of the storability of *Piel de Sapo* melons with sensor fusion", *The fifth International Conference on Information and Technology for Sustainable Fruit and Vegetable Production*, Montpellier, France, pp.523-531.
- Junichi Sugiyama, Muhammad Imran Al-Haq and Mizuki Tsuta.(2005), "Application of Portable Acoustic Firmness Tester for Fruits", *The fifth International Conference on Information and Technology for Sustainable Fruit and Vegetable Production*, Montpellier, France, pp.439-443.
- Kongrattanaprasert, S., Arunrungrusmi, S., Pungsiri, B., Chamnongthai, K., and Okuda, M. (2001), "Nondestructive Maturity Determination of Durian by Force Vibration", *The IEEE International Symposium on Circuits and System (ISCAS)*, Sydney, Australia, pp 441-444.
- Muramatsu N., Sakura N., Yamamoto R., Nevins D.J., Takahara T., Ogata T.(1997), "Comparison of non-destructive acoustic method with an intrusive method for firmness measurement of kiwifruit", *Postharvest Biology and Technology* 12, 221-228.

- Nourain Jamal, Ying Yi-bin, Wang Jian-ping, Rao Xiu-qin and Yu Chao-gang.(2005), “ Firmness evaluation of melon using its vibration characteristic and finite element analysis”, Journal of Zhejiang University 6B(6), 483-490.
- Pankasemsuk, T.,O.Garner, J., B. Malta,F., and L. Silva, J.(1996), “ Translucent fresh disorder of mangosteen(*Garcinia mangostana* L.) ”, HortScience 31(1), 112 -113.
- Rittisak jaritngam, Chusak Limsakul, Sayan Sdoodee, Saravut Jaritngam and Mareena Mani.(2001), “To Detect Gummy Fruit of Mangosteen (*Garcinia mangostana* Linn.) by the Autoregressive Model Analysis Method”, Journal of Agricultural Science 32, 1-4.
- Sriyont Chaichumpan.(1986), “The Study on Neua Gaew a Physiological disorder of mangosteen(*Garcinia mangostana* Linn) ”, Undergraduate Student, Department of Horticulture, Faculty of Agriculture, Kasetsart University, Thailand.
- Shoji Terasaki, Naoki Sakurai, Jacek Zebrowski c,g, Hideki Murayamad, Ryoichi Yamamotoe, Donald J. Nevins f.(2006), “Laser Doppler vibrometer analysis of changes in elastic properties of ripening ‘La France’ pears after postharvest storage”, Postharvest Biology and Technology 42, 198–207.
- Somchai Arunrungrusmi, Dejwoot Khawaparisuth, Kosin Chamnongthai.(1999), “Nondestructive 2D Cross-Sectional Visualization of A Mangosteen”, The fifth International Symposium on Signal Processing and its Applications, Brisbane, Australia, pp. 443-445.
- Sontisuk Teerachaichayut. (2007), “Non-destructive prediction of translucent flesh disorder in intact mangosteen by short wavelength near infrared spectroscopy”, Postharvest Biology and Technology 43 , 202–206.
- Tawatchai Tongleam, Nutthacha Jittiwaranghl, Pinit Kumhoml, Kosin Chamnongthai.(2004), “Non-Destructive Grading of Mangosteen by Using Microwave Moisture Sensing”, International Symposium on Communications and Information Technologies,Sapporo, Japan, pp 650-653.
- Voraphat Luckanatinvong.(1996), “Effect of Water on Physiological Disorders of Mangosteen Fruit (*Garcinia Mangostana* Linn) ”, Developmental Physiology, Master of Science(agriculture) Department of Horticulture, Kasetsart University, Thailand.
- Yantarasri, T., C. Sivasomboon, J. Uthaibutra and J. Sornsrivichai. (1996), “X- ray and NMR for nondestructive internal quality evaluation of durian and mangosteen fruits”, Acta Horticulture 464, 97-101.

Rittisak Jaritngam was born on February 1th, 1975. Ph.D. candidate of graduate school of Electrical Engineering, Prince of Songkla University, Thailand, he received the B.S. degree from Srinakharinrajavidyalaya University(SRU), Songkla, Thailand, in 1996, and the M.Eng degree from Prince of Songkla University(PSU), Songkla, Thailand, in 2000. His research interest are nondestructive measurement and postharvest technology in agriculture.

Chusak Limsakul was born on September 14th, 1956. Now, he is lecturer in electrical engineering, department of engineer, Prince of Songkla University(PSU), Songkla, Thailand and is Vice President for Research and Graduate Studies at the same; PSU. He received the B.S. degree from King Mongkut's Institute of Technology Ladkrabang, Thailand, in 1978, and the D.E.A. degree from INSAT France, in 1982, and Docteur Ingenieur from INSAT France, in 1985. His research interest are digital signal processing, sensors and instrumentations, and automation.

Booncharern Wongkittiserksa he is lecturer in electrical engineering ,department of engineer , Prince of Songkla University(PSU),Songkla, Thailand and Associate Dean for Graduate Study and International Relations in Engineering Faculty. He received the B.S. degree from King Mongkut's Institute of technology Ladkrabang, Thailand, in 1981, and the M.Eng degree from Mahidol University, Thailand, in 1986. His research interest are digital signal processing, sensors and biomedical instrumentation.

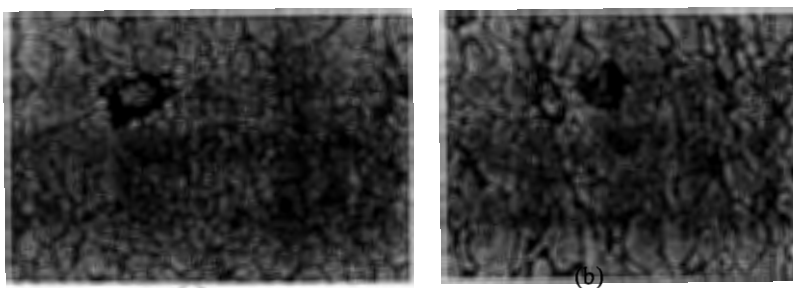


Fig 1 (a) normal of mangosteen, (b) translucent fresh disorder of mangosteen

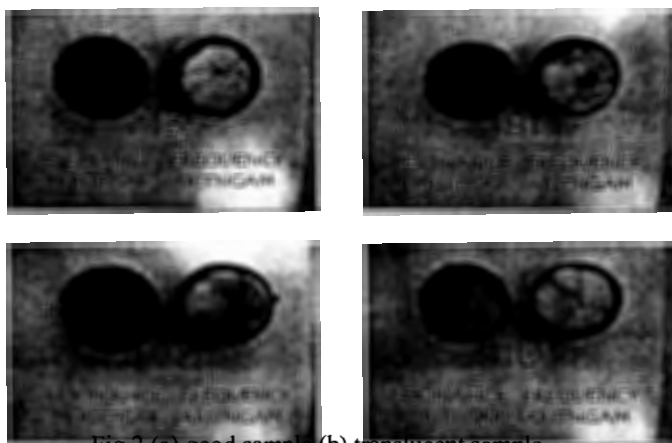
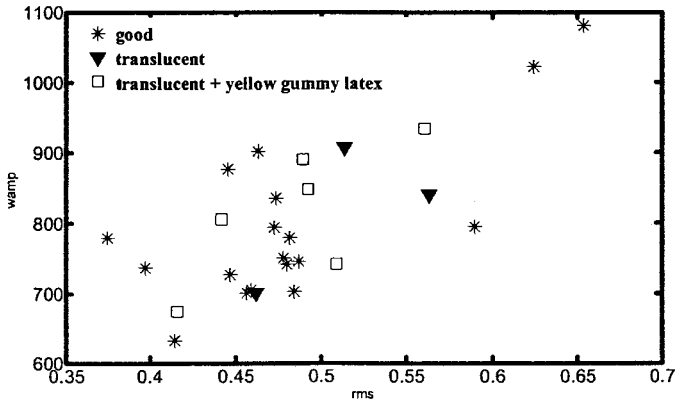
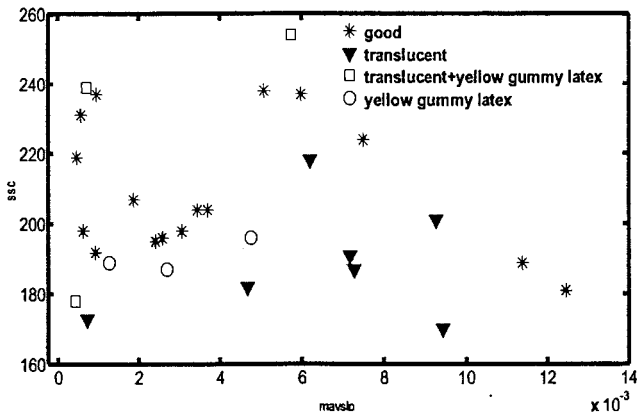


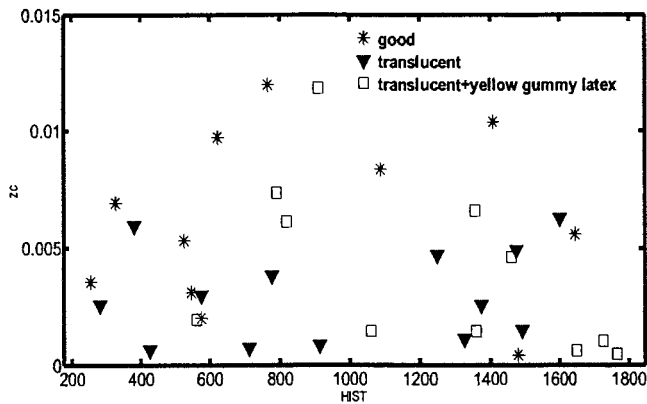
Fig 2 (a) good sample (b) translucent sample
(c) translucent fruit and yellow gummy latex (d) yellow gummy latex



(a)



(b)



(c)

(a) The first day of experiment, (b) the second day of experiment. and (c) the third day of experiment.

Fig 4 the scatter plots of three texture property of mangosteen

Table 1. The different of property in mangosteen

No.	Property	Translucent	Yellow Gummy latex	Normal	Reference
1	Opening of Cell	Solution	-	Air	(Sriyon,1986)
2	S.G.	Higher than 1	-	Lower than 1	(Vorapat,1996)
3	Water Volume		Higher than normal 1.21%		(Vorapat,1996)
4	Air Volume		Lower than normal 15		(Vorapat,1996)
5	Density		Higher than normal 3		(Vorapat,1996)

Table 2. The percentage correct of VFSS measurement

Method	Percentage correct				Sum correct
	Classify good sample	Correct good sample	Classify unusual sample	Correct unusual sample	
Group1;[Day1]	88.89	84.21	66.67	75	81.48
Group2;[Day2]	88.24	78.95	69.23	81.82	80
Group3;[Day3]	60	69.23	84.62	78.57	75.61
Total[Day1+Day2+Day3]			78.57		

Paper III

Rittisak Jaritngam, Chusak Limsakul and Booncharoen Wongkittiserka, " The translucent and yellow gummy latex of mangosteen by using autoregressive coefficient method ," Journal of Innovative Systems Design and Engineering, vol. 3, no. 5, pp 33-40, 2012.

The translucent and yellow gummy latex of mangosteen by using autoregressive coefficient method

Rittisak Jaritngam*, Chusak Limsakul and Boonchareem Wongkittiserksa

Department of Electrical Engineering, Prince of Songkla University, Songkhla, Thailand
110/5, Kanchanavanid Road, Hat Yai, Songkhla 90112 Thailand

* E-mail of the corresponding author: rittisak.ja@chaiyo.com

Abstract

A nondestructive measurement to predict an internal translucent disorder and yellow gummy latex in mangosteen fruit has proposed by using Vibration Frequency base on Strain gage Sensor (VFSS). This measurement were used vibrate with frequency 0 – 50 Hz The VFSS of 100 mangosteen samples were obtained an evaluation of various existed VFSS signal features base on time and frequency domains. From the experimental results, Auto-regressive (AR) coefficient was suggested to use as a feature for the VFSS measurement. We will be obtained the classification accuracy on good sample and device the sample into two groups.

Keywords: Vibration Fruit base on Strain gage Sensor (VFSS), Auto-regressive (AR) coefficient, feature extraction, yellow gummy latex and translucent.

1. Introduction

The mangosteen is the queen of fruit and one of the high economical fruit in Thailand. However, the problem and the quality of mangosteen is measured not only by external factors such as color, shape, size, skin blemishes, latex straining and insect damage, but also by internal factors such as translucent flesh disorder and yellow gummy latex which are also very importance for consumer acceptance Sontisuk (2007). Moreover, the high accuracy in section for a translucent fresh disorder is by opening the flesh up. Obviously, a nondestructive inspection is needed

In quality determination of mangosteen, Neua Gaew (the Thai for flesh translucent) Physiological disorder of mangosteen using a destructive technique. Voraphat (1996) studied the effect of water to flesh translucent disorder using a chemical technique.

From the literatures, there are many excited the non-destructive measurement of mangosteen in Thailand such as a floating technique (Pankasemsuk,1996), microwave technique Tongleam (2004), non-destructive 2D cross-sectional visualization (Arunrungrusmi,1999), near infrared spectroscopy (Sontisuk,2007), X-ray and NMR (Yantarasri et al,1996) and resonance frequency (Rittisak,2001). However, translucent fresh disorder and yellow gummy latex are relation with the different of hollow and water volume in mangosteen. So, the resonance frequency measurement was applied to detect the translucent fresh disorder and yellow gummy latex must be relation with the resonance frequency measurement to detect the different of hollow and water volume in mangosteen. In recent year, Kongrattanaprasert (2001) using to vibration in durian, acoustic measurement and a intrusive method in kiwifruit (Muramatsu,1997), acoustic impulse transmission in muskmelons (Sugiyama,2005), vibration in melon (Nourain,2005), Laser Doppler Vibrometer(LDV) in pear (Terasaki,2006), acoustic impulses in watermelon (B. Diezma Iglesias,2002), acoustic response in melons (L. Lleó,2005).

In this paper, we propose a nondestructive technique by using VFSS measurement combine with the AR coefficient to detect flesh translucent and yellow gummy latex in mangosteen.

2. Material and Methods

2.1 Fruit sample and VFSS Instrument

Mangosteens were purchased from a local fruit auction in Nakornsritummarat, Thailand. the samples were delivered to the laboratory of Electrical Engineering Laboratory, Prince of Songkla university and kept in a room, about 100 Thai mangosteens were used to study by VFSS measurement and 26 intact mangosteens were used for evaluating the accuracy of translucent flesh disorder detection, 20 intact mangosteen of translucent flesh disorder combine with gambol and 4 intact mangosteens of only yellow gummy latex to the recording of VFSS by a instrument. The vibration signal were vibrated in medium sample at frequency was 25 to 40 Hz, amplitude input is 2.5 volt. After, the experiment was complete, the peel of each sample was slit with knife are take a photograph by digital camera, the sample were cut to record the internal. After the VFSS measurement was complete, the peel of each sample was opened to investigate internal defects and were taken with a digital camera (Fujifilm, FinePix F700, Japan), then the samples were cut through and the fruit was record the internal features of measurement as shown in Fig. 1(a-d). The response of fruit to vibrations depends on their modulus of elasticity, their mass and their shape. Different types of vibrations can be used the most common being acoustic and mechanical. Using a microphone or a piezoelectric sensor, acoustic methods measure the signal have audible range: about 0-20,000 Hz (Peleg,1993). The acoustic signal captured is Fourier transformed and the main frequencies calculate. This paper, varieties of VFSS at 25, 30, 35 and 40 Hz are used as representative data in this study. Differential amplifiers were set gain are 500 time and sampling frequency was set at 1000 Hz using a 16 bit analog-to-digital converter board (NI, DAQCard-6024E). In the analysis, the window length of VFSS samples was set for 256 ms with the objective of real-time signal processing. In other words, the maximum permissible delay for VFSS sample should be 10 ms. Finally, we can observe these signal on computer by labview programming and process them by matlab programming for classification of translucent fresh disorder and yellow gummy latex of mangosteen (Rittisak, 2012)

2.2 Data analysis

2.2.1 The resonance frequency

In this case, the characteristic of mechanical vibration most parts of the energy radiated from the surface propagates as a transversal wave in the medium when the frequency of low frequency vibration is less than about 1 kHz, the velocity of transversal wave can be expressed as equation (1-4) in medium related to characteristic of medium are given by

$$V_i = \left(\frac{2(\mu_1^2 + \omega_b^2 \mu_2^2)}{\rho(\mu_1 + \sqrt{\mu_1^2 + \omega_b^2 \mu_2^2})} \right)^{1/2} \quad (1)$$

Where V_i is velocity of vibration. ρ is the density of the medium. ω_b is the angular frequency of vibration. μ_1 and μ_2 are the coefficients of shear elasticity and shear viscosity. Respectively, Velocity of vibration related to frequency and

wave propagation of vibration. So, property of shear elasticity can be found by velocity measurement of vibration and wave propagation at low frequency. In equation (1), if the shear elasticity is dominant compared with the shear viscosity so that $\mu_1 \gg \omega_b$, then μ_2 is satisfied. The velocity is written as

$$V_i = (\mu_i / \rho)^{1/2} \quad (2)$$

The signal of output vibration fruits, when reference voltage output vibration fruits from the prototype for determine velocity of vibration which can be obtained from

$$V_i = \frac{A}{\alpha T} \quad (3)$$

$$A = \frac{\alpha V_i}{F} \quad (4)$$

Where A is the voltage of the output vibration, T is the time of output vibration. α is voltage of output vibration from the prototype. F is the resonance frequency vibration.

The amplitude and frequency of vibration determining have many methods such as ultrasonic and accelerometer and LDV methods which can fix sensor on sample; there have response of vibration accuracy. In this paper, we used VFSS measurement that has been used in the vibration measuring of mangosteen. We choose the frequency vibration between 25 to 40 Hz and input signal is 2.5 Volt, for the mangosteen with different texture property when transfer input signal. Output signal has different amplitudes and frequency has related to internal air cavity, weight and diameter follow to texture property of mangosteen. In Fig 2(a-d), the good mangosteens have patterned signal difference with abnormal mangosteen, translucent flesh order and yellow gummy latex.

2.2.2 Auto-regressive (AR) coefficients

AR model described each sample of VFSS signals as a linear combination of previous VFSS samples (x_{n-i}) plus a white noise error term (w_n). In addition, p is the order of AR model. AR coefficients (α_i) are used as features in VFSS. The definition of AR model is given by

$$x_n = -\sum_{i=1}^p \alpha_i x_{n-i} + w_n \quad (5)$$

3. Results

From experiment result, the signal from time axis at 25,30,35,40 Hz on the vibration characteristics of the fruits is different when analyzed by AR coefficient. We found the vibration frequency at 25 Hz, coefficient order four was the most interesting that the fruit is divided into three groups. The first group has a coefficient less than -1, the secondary group has a coefficient more than 1, the last group has a coefficient between -1 to 1, respectively, some normal mangosteen have a coefficient between 1 and 1. In addition, the mangosteen in group2 has a coefficient between -0.05 to -0.1. As well as, the mangosteen in group3 have a coefficient between -0.05 to -0.1 the some normal mangosteen has the same range. In the other hand, in the coefficient order 5 to 10 was the cluster which was difficult

to separate.

The vibration frequency in 30 Hz, coefficient order 4 was the most interest because the normal mangosteen has ranged between 0 to -0.2. However, some abnormal mangosteen has the same range. Moreover, some normal mangosteen in the coefficient order 1 has a coefficient less than -0.6. The coefficient of translucent fresh disorder was separate from the most group. In the other hand, in the coefficient order 5 to 10 was the cluster which was difficult to separate.

The vibration frequency in 35 Hz, coefficient order 2 was the most interest the normal mangosteen has ranged between 0 to -0.1. Moreover, the coefficient order 4, the normal mangosteen has coefficient between -0.1 to -0.2. However, in the coefficient order 1,3,5,6,7,8,9 and 10 to 10 was the cluster which was difficult to separate.

The vibration frequency in 40 Hz, coefficient order 4 was the most interest the normal mangosteen has ranged between -0.1 to -0.2. Moreover, the coefficient order 5, the normal mangosteen has coefficient less than -0.1. In addition, the coefficient order 2, the normal mangosteen has coefficient between 0 to -0.1. As well as, the coefficient order 10, the normal mangosteen has coefficient less than 0. However, the coefficient of other mangosteen was the cluster which was difficult to separate.

4. Conclusion

From the experiment result, the vibration frequency in 25 Hz, coefficient order 4 was the most interest. Moreover, the vibration frequency in 30 Hz, the vibration frequency in 35 Hz, coefficient order 2,4,6 and 9 and the vibration frequency in 40 Hz, coefficient order 2,4,5 and 10 were the most interest the normal mangosteen were the most interest the normal mangosteen which can separate the good sample from the other sample. However, the coefficient of other mangosteen was the cluster which was difficult to separate.

Acknowledge

The authors acknowledge the support by the graduation scholarship, Prince of Songkla University (PSU) and would like to thank Dr. Kittinan Maliwan, lecturer in Mechanical Engineering, PSU for help technical in providing vibration set as well as Electrical Engineering (EE) Department for their kind technical help and use of laboratory. Moreover, I would like to thank the graduation school of PSU was supported in PH.D. Scholarship.

References

- Diezma B., Ruiz-Altisent M., Orihuel B.(2002), "Acoustic impulse response for detecting hollow heart in Seedless watermelon", *Acta Horticulture* 599, 249-256.
- L. Lleó, P. Barreiro, A. Fernández, M. Bringas, B. Diezma and M. Ruiz-Altisent.(2005), "Evaluation of the storability of *Piel de Sapo* melons with sensor fusion", *The fifth International Conference on Information and Technology for Sustainable Fruit and Vegetable Production*, Montpellier, France, pp.523-531.
- Junichi Sugiyama, Muhammad Imran Al-Haq and Mizuki Tsuta.(2005), "Application of Portable Acoustic Firmness Tester for Fruits", *The fifth International Conference on Information and Technology for Sustainable Fruit and Vegetable Production*, Montpellier, France, pp.439-443.
- Kongrattanaprasert, S., Arunrungrusmi, S., Pungsiri, B., Chamnongthai, K., and Okuda, M. (2001), "Nondestructive Maturity Determination of Durian by Force Vibration", *The IEEE International Symposium on Circuits and System (ISCAS)*, Sydney, Australia, pp 441-444.

Muramatsu N., Sakura N., Yamamoto R., Nevins D.J., Takahara T., Ogata T.(1997), "Comparison of non-destructive acoustic method with an intrusive method for firmness measurement of kiwifruit", *Postharvest Biology and Technology* 12, 221-228.

Nourain Jamal, Ying Yi-bin, Wang Jian-ping, Rao Xiu-qin and Yu Chao-gang.(2005), "Firmness evaluation of melon using its vibration characteristic and finite element analysis", *Journal of Zhejiang University* 6B(6), 483-490.

Pankasemsuk, T., O.Garner, J., B. Malta, F., and L. Silva, J.(1996), "Translucent fresh disorder of mangosteen (*Garcinia mangostana* L.)", *HortScience* 31(1), 112 -113.

Peleg K., (1993), "Comparison of non-destructive measurement of apple firmness", *J Agr Eng Res* 55(3), 227-238.

Rittisak Jaritngam, Chusak Limsakul, Sayan Sdoodee, Saravut Jaritngam and Mareena Mani.(2001), "To Detect Gumming Fruit of Mangosteen (*Garcinia mangostana* Linn.) by the Autoregressive Model Analysis Method", *Journal of Agricultural Science* 32, 1-4.

Rittisak Jaritngam, Chusak Limsakul and Booncharern Wongkittiserka (2012), "The translucent and yellow gummy latex of mangosteen by using the VFSS Measurement", *Journal of Biology, Agriculture and Healthcare* 2(1), 83-91.

Shoji Terasaki, Naoki Sakurai, Jacek Zebrowski, c.g, Hideki Murayamad, Ryoichi Yamamotoe, Donald J. Nevins f.(2006), "Laser Doppler vibrometer analysis of changes in elastic properties of ripening 'La France' pears after postharvest storage", *Postharvest Biology and Technology* 42, 198-207.

Somchai Arunrungrusmi, Dejwoot Khawaparisuth, Kosin Chamnongthai.(1999), "Nondestructive 2D Cross-Sectional Visualization of A Mangosteen", *The fifth International Symposium an Signal Processing and its Applications*, Brisbane, Australia, pp. 443-445.

Sontisuk Teerachaichayut. (2007), "Non-destructive prediction of translucent flesh disorder in intact mangosteen by short wavelength near infrared spectroscopy", *Postharvest Biology and Technology* 43 , 202-206.

Tawatchai Tongleam, Nutthacha Jittiwaranghl, Pinit Kumhoml, Kosin Chamnongthai.(2004), "Non-Destructive Grading of Mangosteen by Using Microwave Moisture Sensing", *International Symposium on Communications and Information Technologies*, Sapporo, Japan, pp 650-653.

Voraphat Luckanatinvong.(1996), "Effect of Water on Physiological Disorders of Mangosteen Fruit (*Garcinia Mangostana* Linn) ", *Developmental Physiology*, Master of Science(agriculture) Department of Horticulture, Kasetsart University, Thailand.

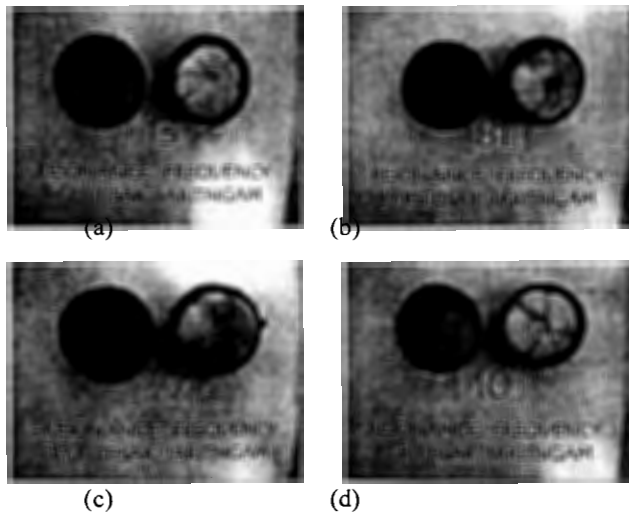
Yantarasri, T., C. Sivasomboon, J. Uthaibutra and J. Sornsrivichai. (1996), "X- ray and NMR for nondestructive internal quality evaluation of durian and mangosteen fruits", *Acta Horticulture* 464, 97-101.

Rittisak Jaritngam was born on Febuary 1th, 1975. Ph.D. candidate of graduate school of Electrical Engineering, Prince of Songkla University, Thailand, he received the B.S. degree from Srinakarintarawitrot University(SWU), Songkla, Thailand, in 1996, and the M.Eng degree from Prince of Songkla University(PSU), Songkla, Thailand, in 2000. His research interest are nondestructive measurement and postharvest technology in agriculture.

Chusak Limsakul was born on September 14th, 1956. Now, he is lecturer in electrical engineering, department of engineer, Prince of Songkla University(PSU), Songkla, Thailand and is Vice President for Research and Graduate Studies at the same; PSU. He received the B.S. degree from King Mongkut's Institute of technology Ladkrabang, Thailand, in 1978, and the D.E.A. degree from INSAT France, in 1982, and Docteur Ingenieur form INSAT France, in 1985. His research interest are digital signal processing, sensors and instrumentations, and automation.

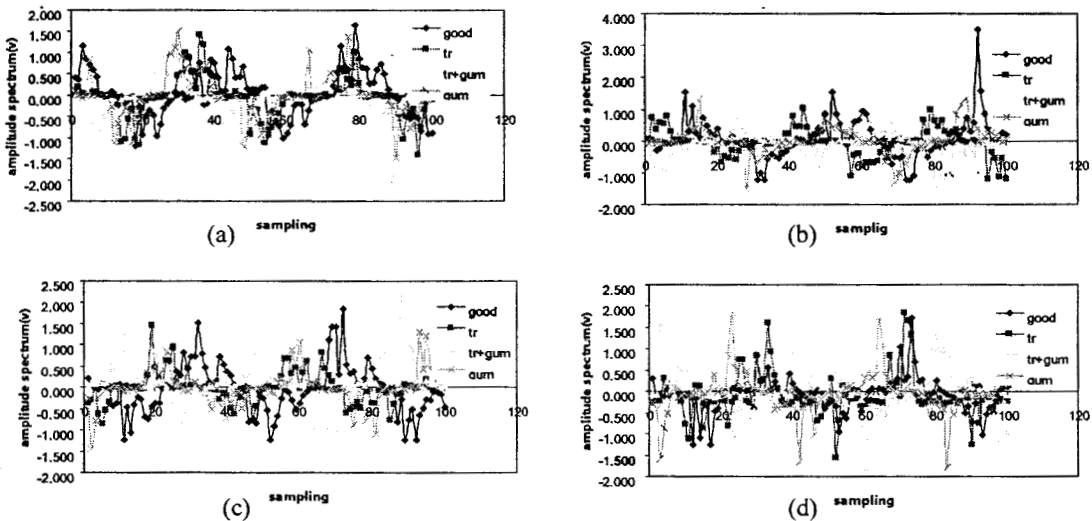
Booncharern Wongkittiserksa he is lecturer in electrical engineering ,department of engineer , Prince of Songkla University(PSU), Songkla, Thailand and Associate Dean for Graduate Study and International Relations in

Engineering Faculty. He received the B.S. degree from King Mongkut's Institute of technology Ladkrabang, Thailand, in 1981, and the M.Eng degree from Mahidol University, Thailand, in 1986. His research interest are digital signal processing, sensors and biomedical instrumentation.



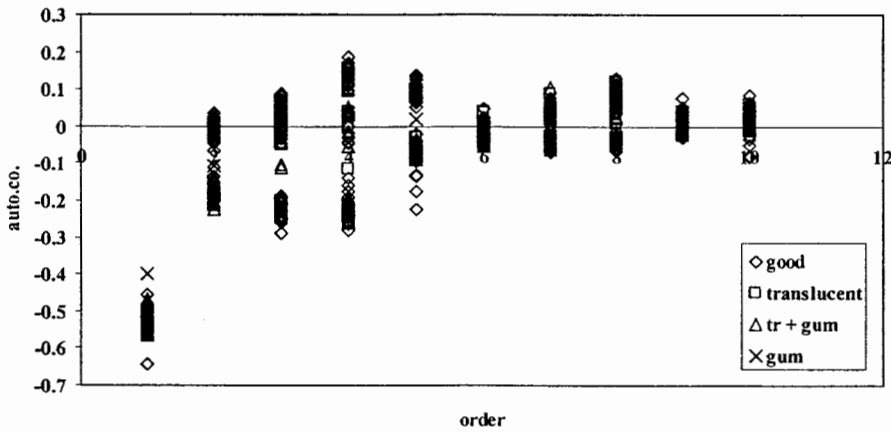
(a) good sample (b) translucent fresh disorder sample
 (c) translucent fresh disorder and yellow gummy latex (d) yellow gummy latex

Fig 1 the property of mangosteen



(a) time domain at 25 Hz vibration base, (b) time domain at 30 Hz vibration base
 (c) time domain at 35 Hz vibration base, (d) time domain at 40 Hz vibration base

Fig 2 the differential real time signal of texture property of mangosteen



(d)

- (a) AR coefficient at vibration frequency at 25 Hz (b) AR coefficient at vibration frequency at 30 Hz
(c) AR coefficient at vibration frequency at 35 Hz (d) AR coefficient at vibration frequency at 40 Hz

Fig 3 the AR coefficient from the vibration based on VFSS measurement

Paper IV

Rittisak Jaritngam, Chusak Limsakul and Booncharoen Wongkittiserka, "The relation between the texture properties of mangosteen (*Garcinia mangostana* Lim.) with the resonance frequency for detect the translucent and yellow gummy latex," *Emirates Journal of Food and Agriculture*, vol. 25, no. 2, 2013. (SCOPUS).

NUTRITION AND FOOD SCIENCE

The relation between the texture properties of mangosteen (*Garcinia mangostana* Linn.) and the resonance frequency in detection of the translucent and yellow gummy latex

Rittisak Jaritngam*, C. Limsakul and B. Wongkittiserksa

Department of Electrical Engineering, Faculty of Engineering, Prince of Songkla University, Thailand

Abstract

A nondestructive measurement to predict an internal translucent disorder and yellow gummy latex in mangosteen fruit has proposed by using Vibration Frequency based on Strain gage Sensor (VFSS). This measurement was used vibration with frequency 0 – 50 Hz. The VFSS of 100 mangosteen samples were obtained an evaluation of various existed VFSS signal features based on time and frequency domains. From the experimental results, mass is the best comparing with the other property. This measurement can detect the yellow gummy latex in mangosteen at 35 Hz and 40 Hz.

Key words: Vibration fruit based on Strain gage Sensor (VFSS), Feature extraction, Yellow gummy latex

Introduction

The mangosteen is the queen of fruit and one of the high economical fruit in Thailand. Moreover, it is also useful about an antioxidant for health (Migdalia et al., 2011). However, the problem and quality of mangosteen is measured not only by external factors such as color, shape, size, skin blemishes, latex training and insect damage and must not include the translucent and yellow gummy latex. Currently, by opening the flesh up was the high accuracy for checking the mangosteen. So, the non-destructive inspection is needed. In recent years, the quality determination of mangosteen, Voraphat (1996) studied the effect of water to translucent flesh disorder using a chemical technique. The non-destructive methods of mangosteen in Thailand, a floating technique using differences in specific gravity is currently undertaken for non-destructive detection of translucent flesh disorder in mangosteen. Similarly, Tawatchai et al. (2004) had been proposed the microwave technique to classify the translucent flesh disorder in term of magnitude of the reflection microwave signal.

However, it has been shown that the dielectric

of material changes accordingly to its moisture. By the time, the short wavelength infrared spectroscopy used to predict the translucent flesh disorder in intact mangosteen (Sontisuk, 2007). Somchai et al. (1999) had proposed the non-destructive 2D cross-sectional visualization of mangosteen. The X-ray and NMR techniques have been found as new potential tools for non-destructive internal quality evaluation of durian and mangosteen fruits (Yantarasri et al., 1996). The resonance frequency used to detect translucent flesh disorder and yellow gummy latex (Rittisak et al., 2001).

The Physiological disorder for mangosteen is reliable with the water and hollow in the fruit as shown in table 1. In resonance frequency to vibration measurement, Garcia-Romus et al. (2005) had proposed the response of fruit to vibration depends on their mass and shape. Moreover, De Belie et al. (2000) used this methodology to measure pear firmness while the fruits were still on the tree. These authors impacted each fruit near the stem and read the frequency at the opposite side using an accelerometer. Moreover, the non-destructive vibration used to determine the maturity levels of durian (Kongrattanaprasert et al., 2001), the acoustic measurement and an intrusive method for determining tissue firmness were compared to assess the textural properties of kiwifruit (Muramatsu et al., 1997), firmness measurement of muskmelons by acoustic impulse transmission (Junichi et al., 2005), the vibration element analysis to determine firmness evaluation of melon (Nourain

Received 20 March 2012; Revised 04 April 2012; Accepted 06 May 2012; Published Online 28 November 2012

*Corresponding Author

Rittisak Jaritngam
Department of Electrical Engineering, Faculty of Engineer,
Prince of Songkla University, Thailand

Email: rittisak.ja@gmail.com

et al., 2005). In addition, the Laser Doppler Vibrometer (LDV) technique was monitor ripening behavior temperature (Shoji et al., 2006), the acoustic impulses were detected internal hollow in watermelon (Diezma et al., 2002), the acoustic response evaluation of the storability of Piel de Sapo melons (Lleó et al., 2005).

In this paper, we propose a non-destructive technique by using VFSS measurement and analysis data by Fast Fourier Transform method (FFT) on frequency domain to detect translucent flesh disorder and yellow gummy latex in mangosteen.

Materials and Methods

Fruit sample and VFSS measurement

Mangosteens were purchased from a local fruit auction in Nakornsri Tummarat, Thailand. The sample was delivered to laboratory to record of signal data on the following by VFSS instrument. About 100 Thai mangosteens were used to study the optimum condition of VFSS measurement and 26 intact mangosteens were used for evaluation the accuracy of translucent flesh disorder detection. Four samples were appeared as translucent flesh disorder with yellow gummy latex while 20 samples were yellow gummy latex. The vibration

signal was vibrated in medium sample at frequency of 25 to 40 Hz while amplitude input was 2.5 volt. After, the experiment was completed; the peel of each sample was slit with knife and takes a photograph by digital camera. The samples were cut to record the internal morphology as shown in Figure 1(a), 1(b), 1(c) and 1(d).

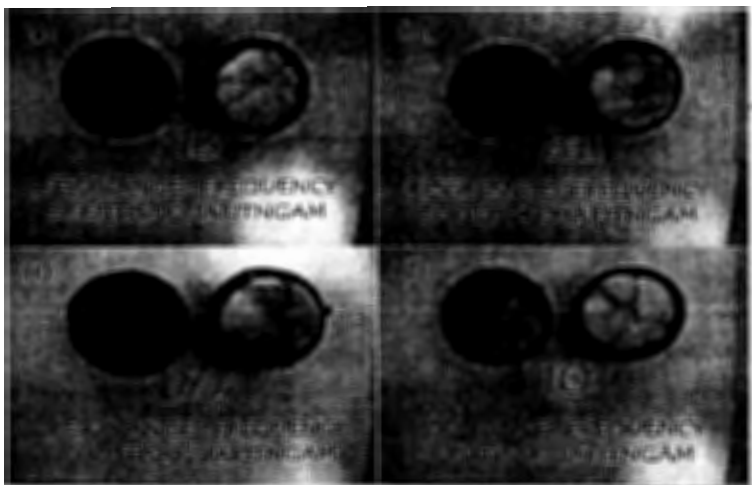
Instruments

The amplitude and frequency of vibration determine have many methods such as ultrasonic and accelerometer and Laser Doppler method can fix sensor with the fruit, there have response of vibration and accuracy. VFSS measurement has used in the vibration measurement of mangosteen.

The experimental device consists of the following steps. The first, we put the mangosteen on the base of the prototype, based on vibration set which can vibrate with frequency 0 - 50 Hz. Second, the strain gauge sensor is adjusted by fix on the mangosteen. After that signals from this one sent to amplifier by instrument amplifier circuit (IC = INA 114) to A/D converter. Respectively, we can observe these signals on computer by labview programming and process them by matlab programming for classification of translucent flesh disorder and yellow gummy latex of mangosteen.

Table 1. The different properties of mangosteen (Voraphat, 1996).

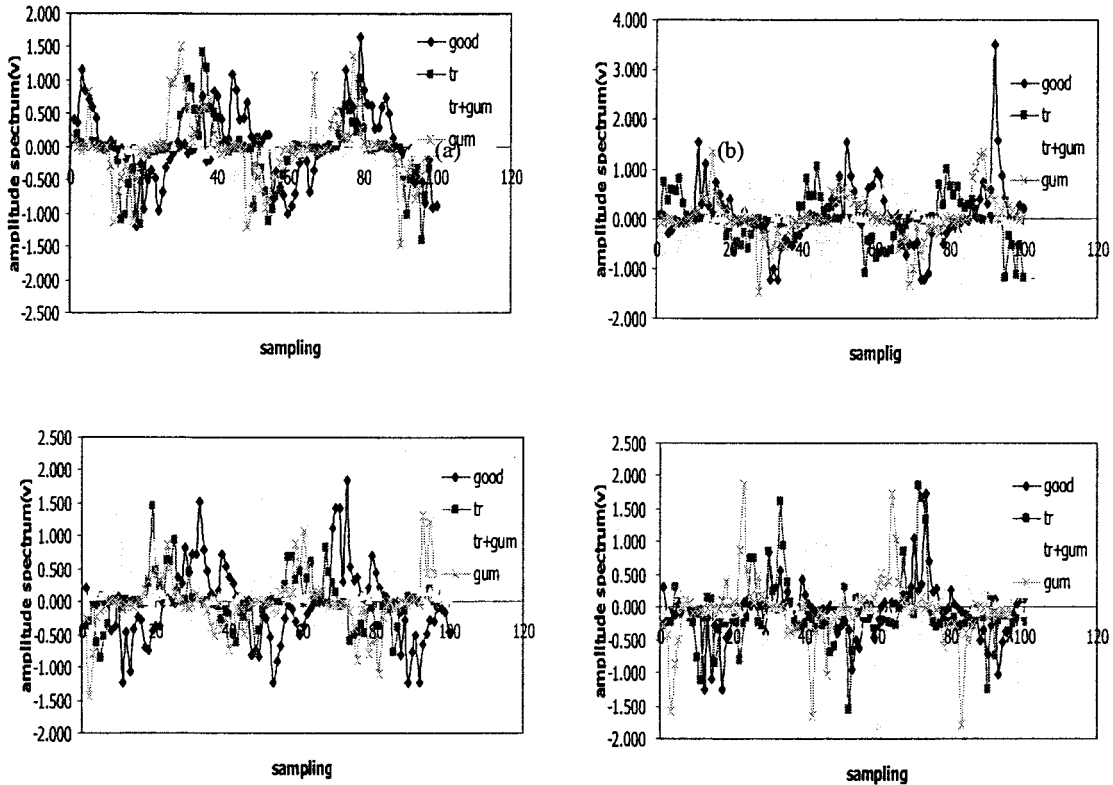
No.	Property	Translucent	Yellow Gummy latex	Normal
1	Specific Gravity	Higher than 1	-	Lower than 1
2	Water Volume	Higher than normal 1.21%		
3	Air Volume	Lower than normal 15 time		
4	Density	Higher than normal 3 time		



(a) good sample (b) translucent sample

(c) Translucent and yellow gummy latex (d) yellow gummy latex

Figure. 1 The texture property of mangosteen photograph by digital camera.



(2a) time domain at 25 Hz vibration base, (2b) time domain at 30 Hz vibration base
 (2c) time domain at 35 Hz vibration base, (2d) time domain at 40 Hz vibration base
 Figure. 2 The differential real time signal of texture property of mangosteen.

Results and Discussion

Data analysis

The resonance frequency in this case, the characteristic of mechanical vibration most parts of the energy radiated from the surface propagates as a transversal wave in the medium when the frequency of low frequency vibration is less than about 1 kHz, the velocity of transversal wave can be expressed as equation (1-4) in medium related to characteristic of medium are given by

$$V_i = \left(\frac{2(\mu_1^2 + \omega_b^2 \mu_2^2)}{\rho(\mu_1 + \sqrt{\mu_1^2 + \omega_b^2 \mu_2^2})} \right)^{1/2} \quad (1)$$

Where V_i is velocity of vibration. ρ is the density of the medium. ω_b is the angular frequency of vibration. μ_1 and μ_2 are the coefficients of shear elasticity and shear viscosity. Respectively, Velocity of vibration related to frequency and wave propagation of vibration. So, property of shear elasticity can be found by velocity measurement of

vibration and wave propagation at low frequency. In equation(1), if the shear elasticity is dominant compared with the shear viscosity so that $\mu_1 \gg \omega_b$ then μ_2 is satisfied. The velocity is written as

$$V_i = (\mu_1 / \rho)^{1/2} \quad (2)$$

The signal of output vibration fruits, when reference voltage output vibration fruits from the prototype for determine velocity of vibration which can be obtained from

$$V_i = \frac{A}{\alpha T} \quad (3)$$

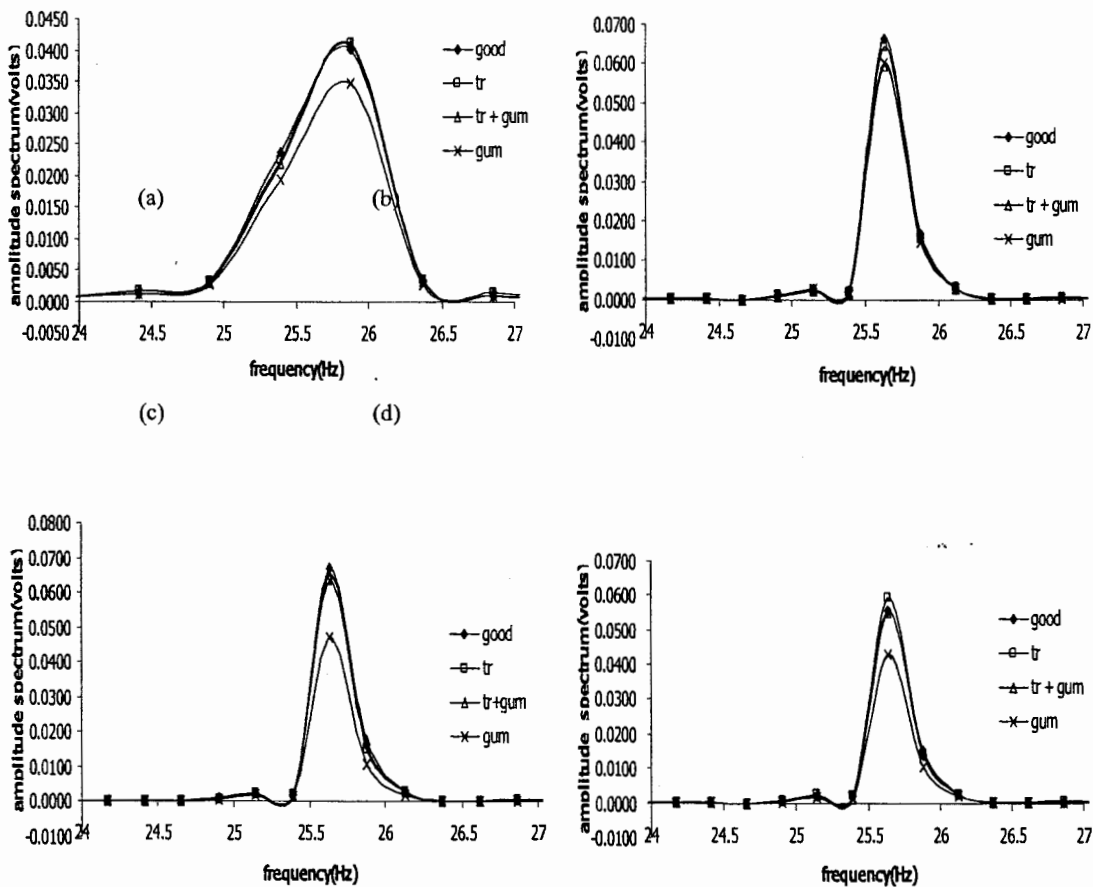
$$A = \frac{\alpha V_i}{F} \quad (4)$$

Where A is the voltage of output vibration. T is the time of output vibration. α is voltage of output vibration from the prototype. F is the resonance frequency vibration

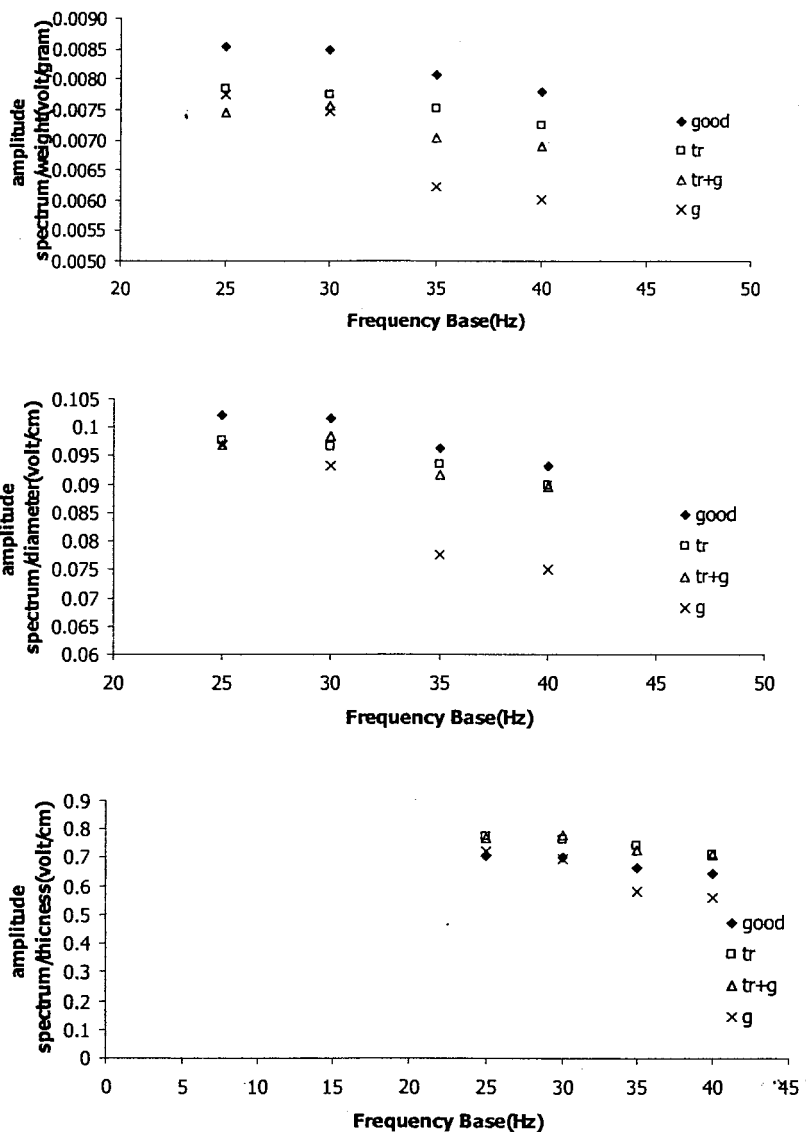
The amplitude and frequency of vibration determining have many methods such as ultrasonic and accelerometer and LDV methods which can fix sensor on sample; there have response of vibration accuracy. In this paper, we used VFSS measurement that has been used in the vibration measuring of mangosteen. We choose the frequency vibration between 25 to 40 Hz and input signal is 2.5 Volt, for the mangosteen with different texture property when transfer input signal. Output signal has different amplitudes and frequency has related to internal air cavity, weight and diameter follow to texture property of mangosteen. In Figure 2(a-d), the good mangosteen has patterned signal difference with unusual mangosteen, translucent flesh order and yellow gummy latex.

A Fast Fourier Transform (FFT) is converted from the time signal into a frequency spectrum with

frequency 0 to 500 Hz. The resonance frequency, there is usually a high peak, while the spectrum with good mangosteen shown usually one high peak at 26 Hz as we can observe from Figure 3(a-d). From the experiment result, weight and diameter have related with amplitude spectrum. Ratio of amplitude spectrum per weight in every frequency base is the best compared with the other as we can observe from Figure 4(a), there are obtains the ratio is higher than 0.008530 volt/g. There are higher than secondary base vibration about 0.000050 volt/g, the ratio of amplitude spectrum with diameter are the secondary. The lastly, amplitude spectrum per thickness peel are the poor shown in the Figures 4(b) and 4(c). However, this measurement can detect the yellow gummy latex in mangosteen at the 35 and 40 Hz, the amplitude is lowest compared with the other frequency.



(3a) frequency at 25 Hz vibration base, (3b) frequency at 30 Hz vibration base
 (3c) frequency at 35 Hz vibration base, (3d) frequency at 40 Hz vibration base
 Figure. 3 The typical spectrums for texture property.



(4a) ratio of amplitude spectrum/weight, (4b) ratio of amplitude spectrum/diameter
 (4c) ratio of amplitude spectrum/thickness peel.

Figure. 4 The frequency are the best by VFSS measurement comparison with the other vibration.

Table 2. Mean amplitude spectrum of the texture property in mangosteen.

Frequency(Hz)	Mean amplitude spectrum(Volt)			
	Good	Translucent	Translucent + Yellow gummy latex	Yellow gummy latex
Amplitude				
25	0.519877	0.502694	0.511703	0.494359
30	0.517261	0.496899	0.519601	0.476186
35	0.491520	0.481140	0.483758	0.396590
40	0.475493	0.463501	0.473570	0.382587

Table 3. Mean amplitude spectrum/weight of the texture property in mangosteen.

Frequency(Hz)	Mean amplitude spectrum/weight (Volt/g)			
	Good	Translucent	Translucent + Yellow gummy latex	Yellow gummy latex
Amplitude/weight				
25	0.008530	0.007853	0.007448	0.007761
30	0.008487	0.007762	0.007563	0.007475
35	0.008065	0.007516	0.007042	0.006226
40	0.007802	0.007240	0.006893	0.006006

Table 4. Mean amplitude spectrum/diameter of the texture property in mangosteen.

Frequency(Hz)	Mean amplitude spectrum/diameter (Volt/cm)			
	Good	Translucent	Translucent + Yellow gummy latex	Yellow gummy latex
Amplitude/diameter				
25	0.102097	0.097686	0.097005	0.096933
30	0.101583	0.096557	0.098503	0.093370
35	0.096528	0.093495	0.091708	0.077763
40	0.093380	0.090000	0.089776	0.075017

Table 5. Mean amplitude spectrum/thickness of the texture property in mangosteen.

Frequency(Hz)	Mean amplitude spectrum/thickness (Volt/cm)			
	Good	Translucent	Translucent + Yellow gummy latex	Yellow gummy latex
Amplitude/thickness				
25	0.705875	0.775671	0.769479	0.725665
30	0.702323	0.766728	0.781356	0.698989
35	0.667372	0.742412	0.727456	0.582151
40	0.645612	0.715195	0.712137	0.561596

From the experiment, the Table 2 presents the frequency based vibration within 25 and 30 Hz comparison with the amplitude spectrum. There are the best values about 0.476186 – 0.519877 volt and are higher than the frequency vibration based at 35 and 40 Hz which are valuable about 0.382587 – 0.491520 volt. Moreover, the amplitude spectrums of the good sample are higher than the other sample fruits. Hence, the yellow gummy latex sample can be detected at the frequency based vibration which has the value lowest than the other sample.

In Table 3, it is the value of amplitude spectrum per weight. From the experimental results, there are the same trend with the experiment from Table 2, the ratio of amplitude spectrum per weight in normal sample are higher than the other fruits are about 0.007802 – 0.00853 volt/g on the frequency based vibration. In addition, the frequency based vibration at the 25 Hz has the highest ratio in the 40 Hz frequency based vibration, the ratio has the poor. Moreover, the translucent flesh disorder and translucent flesh disorder combine with the yellow gummy latex are similar to 0.007240 – 0.007853 volt/g and 0.006893 – 0.007448 volt/g. In the part, the mangosteen has yellow gummy latex symptoms only will be the ratio valuable was poor in the same

vibration. From the experiment result, the trend of mangosteen can detect in the all frequency based vibration and sorts out mangosteen have yellow gummy latex in 35 and 40 Hz frequency based vibration.

Table 4, represents the value of amplitude spectrum per diameter. From the experimental results, there are the same trend with the experiment from Table 2 and 3, the ratio of amplitude spectrum per diameter in normal sample are higher than the other (about 0.093380 – 0.102097 volt/cm) on the frequency based vibration. In addition, the frequency based vibration at the 25 Hz has the highest and in the 40 Hz frequency based vibration, the ratio has the poor. Moreover, in the value of mangosteen are the translucent flesh disorder and translucent flesh disorder combine with yellow gummy latex are similar to 0.090000 – 0.097686 volt/cm and 0.089776 – 0.097005 volt/cm. Respectively, in the part, the ratio valuable of mangosteen having yellow gummy latex symptoms only was poor in the same vibration. From the experimental results, the trend of mangosteen can detect in the all frequency based vibration and sorts out mangosteen

group have yellow gummy latex in 35 and 40 Hz frequency based vibration.

Table 5 shows the value of amplitude spectrum per thickness peel. From the experiment result, the good mangosteen has ratio value of translucent flesh disorder and translucent flesh disorder combination with the yellow gummy latex between 0.645612 – 0.705875 volt/cm at the frequency based on 25, 30, 35 and 40 Hz. Moreover, the frequency based vibration is 25 Hz has highest and has lowest at the frequency base vibration about 40 Hz. However, the translucent flesh disorder and translucent flesh disorder combination with the yellow gummy will be the ratio valuable lowest which about 0.561596 – 0.725665 volt/cm in the same frequency based vibration.

Conclusion

The VFSS of mangosteen fruit was sufficient to use for translucent flesh disorder and yellow gummy latex detection in mangosteen. The texture property can be classified into 4 groups (good, translucent flesh disorder, translucent flesh disorder combination with yellow gummy latex and yellow gummy latex) vibration based on 25 Hz, where the best amplitude and ratio of amplitude with diameter are the same. Frequency based vibration at 35 and 40 Hz can be classify as yellow gummy latex, the amplitude is lowest than the other frequency based on vibration. However, the accuracy can be increased by rejection of other effects such as hardening pericarp, fruit size and skin color before evaluation.

Acknowledgement

The authors acknowledge the support by the graduation scholarship, Prince of Songkla University (PSU) and would like to thank Dr. Kittinan Maliwan, Lecturer in Mechanical Engineering, PSU for help technical in providing vibration set as well as Electrical Engineering (EE) department for their Kind technical help and use of laboratory.

References

- De Belie, N., S. Schotte Lammertyn, J. Nicolai, B. J. De Baerdemaeker. 2000. Firmness changes of pear fruit before and after harvest with acoustic impulse response technique. *J. Agric. Eng. Res.* 77(2):183-91.
- Diezma, B., M. Ruiz-Altisent and B. Orihuel. 2002. Acoustic impulse response for detecting hollow heart in seedless watermelon. *Acta Hort.* 599:249-256.
- Garcia-Ramos, F. J. C. Valero, I. Homer, J. Ortiz-Cañavate and M. Ruiz-Altisent. 2005. Non-destructive fruit firmness sensors: a review. *Spanish J. Agric. Res.* 3(1):61-73.
- Junichi, S., M. I. Al-Haq and M. Tsuta. 2005. Application of Portable Acoustic Firmness Tester for Fruits. The fifth International Conference on Information and Technology for Sustainable Fruit and Vegetable Production, Montpellier, France. p.439-443.
- Kongrattanaprasert, S., S. Arunrungrusmi, B. Pungsiri, K. Chamnongthai and M. Okuda. 2001. Nondestructive Maturity Determination of Durian by Force Vibration. The IEEE International Symposium on Circuits and System (ISCAS), Sydney, Australia. p.441-444.
- Lleó, L., P. Barreiro, A. Fernández, M. Bringas, B. Diezma and M. Ruiz-Altisent. 2005. Evaluation of the storability of *Piel de Sapo* melons with sensor fusion. The fifth International Conference on Information and Technology for Sustainable Fruit and Vegetable Production, Montpellier, France. p.523-531.
- Migdalia, A., A. Bello, L. Rastrelli, M. Montelieri, L. Delgado and C. Panfili. 2011. Antioxidant properties of pulp and peel of yellow mangosteen fruits. *Emir. J. Food Agric.* 23(6):517-524.
- Muramatsu, N., N. Sakurai, R. Yamamoto, D. J. Nevins, T. Takahara and T. Ogata. 1997. Comparison of non-destructive acoustic method with an intrusive method for firmness measurement of kiwifruit. *Postharvest Biol. Technol.* 12:221-228.
- Nourain, J., Y. Yi-Bin, W. Jian-Ping, R. Xiu-Qin and Y. Chao-Gang. 2005. Firmness evaluation of melon using its vibration characteristic and finite element analysis. *J. Zhejiang Univ. B.* (6):483-490.
- Rittisak, J., C. Limsakul, S. Sdoodee, S. Jaritngam and M. Mani. 2001. To detect gumming fruit of Mangosteen (*Garcinia mangostana* Linn.) by the autoregressive model analysis method. *J. Agric. Sci.* 32:1-4.
- Shoji, T., N. Sakurai, J. Zebrowski, H. Murayamad, R. Yamamotoe and D. J. Nevins. 2006. Laser Doppler vibrometer analysis of changes in elastic properties of ripening 'La France' pears after postharvest storage. *Postharvest Biol. Technol.* 42:198-207.

- Somchai, A., D. Khawaparisuth and K. Chamnongthai. 1999. Nondestructive 2D Cross-Sectional Visualization of A Mangosteen. The fifth International Symposium on Signal Processing and its Applications, Brisbane, Australia. p.443-445.
- Sontisuk, T. 2007. Non-destructive prediction of translucent flesh disorder in intact mangosteen by short wavelength near infrared spectroscopy. *Postharvest Biol. Technol.* 43:202-206.
- Tawatchai, T., N. Jittiwanghl, P. Kumhoml and K. Chamnongthai. 2004. Non-Destructive Grading of Mangosteen by Using Microwave Moisture Sensing. International Symposium on Communications and Information Technologies, Sapporo, Japan. p.650-653.
- Voraphat L. 1996. Effect of Water on **Physiological Disorders of Mangosteen Fruit (*Garcinia Mangostana* Linn).** **Developmental Physiology, Master of Science (Agriculture)** Department of Horticulture, Kasetsart University, Thailand.
- Yantarasri, T., C. Sivasomboon, J. Uthaibutra and J. Sornsrivichai. 1996. X- ray and NMR for nondestructive internal quality evaluation of durian and mangosteen fruits. *Acta Hort.* 464:97-101.

VITA

Name Rittisak Jaritngam

Student ID 5110130010

Educational Attainment

Degree	Name of Institution	Year of Graduation
B- Sci (Physic)	Srinakarinwirot University	1996
M-Eng (Electrical Engineering)	Prince of Songkla University	1999

Work-Position and Address

- non -

List of Publication and Proceedings

1. Rittisak Jaritngam, Chusak Limsakul and Booncharoen, " The Relation between the Resonance Frequency with the property For Detect the translucent and yellow gummy latex of mangosteens (*Garcinia mangostana* Linn.)," Proceedings of the International Conference on Arts, Social Sciences & Technology, Penang, Malaysia, pp.xxx-xxx, 2012.
2. Rittisak Jaritngam, Chusak Limsakul and Booncharoen Wongkittiserka, "The translucent and yellow gummy latex of mangosteen by using the VFSS Measurement," Journal of Biology. Agriculture and Healthcare, vol. 2, no. 1, pp 83-91, 2012.
3. Rittisak Jaritngam, Chusak Limsakul and Booncharoen Wongkittiserka, "The translucent and yellow gummy latex of mangosteen by using autoregressive coefficient method, " Journal of Innovative Systems Design and Engineering, Vol. 3, no. 5, pp 33-40, 2012.
4. Rittisak Jaritngam, Chusak Limsakul and Booncharoen Wongkittiserka, "The relation between the texture properties of mangosteen (*Garcinia mangostana* Linn.) with the resonance frequency for detect the translucent and yellow gummy latex," Emirates Journal of Food and Agriculture, Vol. 25, no. 2, pp 89-96, 2013.